Application of Radioisotope Imaging and Therapy in Patients with Breast Carcinomas that Express the Sodium Iodide Symporter Gene.

Vivienne MacLaren, MBChB, MRCP, FRCR

Submitted for Degree of MD
October 2008
Submitted to the University of Glasgow

Research conducted in the Division of Cancer Sciences and Molecular Pathology

Declaration

I declare that the work contained within this thesis is my own original work.

This work has not been previously submitted for a higher degree.

List of Contents

Chapter One – Introduction

Chapter Two – Materials and Methods

Section 7 – RNA Extraction and Analysis from Cell Lines

Section 8 – RNA Extraction and Analysis from Paraffin Embedded Tissue

Abstract

Aims

The Sodium Iodide Transporter (NIS), which is located in the basolateral membrane of the thyroid follicular cell, catalyses an active transport mechanism allowing Iodide, an essential component of the thyroid hormones Tri-iodothyronine (T3) and Thyroxine (T4), to accumulate in the thyroid gland. Differentiated thyroid cancers retain the appearance and function of normal thyroid cells, and can, therefore, trap iodine. Radioiodide scintigraphy and therapy are based on the uptake of radioiodide by NIS in thyroid tissue, which can concentrate all isotopes of iodine.

Breast cancer is the most common type of cancer in women in the UK, and is the second-most common cause of cancer-related death in women in the UK. This situation remains true in Scotland, with breast cancer representing 27.5% of all female cancers. Despite a reduction in mortality figures between 1994 and 2004 of 18%, five-year survival in Scotland remains only 80.2% for patients diagnosed between 1997 and 2001. When breast cancer recurs and becomes metastatic, it is treatable but not curable. Median overall survival of patients with metastatic disease remains poor, and is currently between one and two years. It is clear that metastatic breast cancer remains a challenging clinical issue and novel treatments are required.

Radionuclides play an important role in the management of malignancy, including prostate cancer, neural crest tumours and thyroid cancers. There is evidence that there may be a role for radionuclide therapy in breast cancer via the NIS mechanism. This was first suggested by Tazebay's landmark work in 2000, which demonstrated that a significant proportion (87%) of breast cancers contained detectable NIS protein by immunohistochemistry (IHC).

Experimental design

Tumour samples from patients with breast cancer were analysed by immunohistochemistry and ribonucleic acid (RNA) analysis, and this was correlated with functional activity of the NIS protein, by scintigraphic scanning of patients with metastatic breast cancer.

Results

Twenty-four patients had a Tc99m Pertechnetate scan; 20 patients had their RNA analysed; 22 patients had IHC performed on their tumour samples. NIS was detected only in the control Graves thyroid RNA and paraffin embedded cells extracted from a NIS expressing cell line. Breast tumour sample RNA did not demonstrate NIS. By IHC, 15 cases were defined as truly immunopositive, with the criteria for true positivity being a Histoscore of > 150, or demonstration of membrane staining. Seven cases were negative by the above criteria. Tc99m Pertechnetate uptake was observed in 11 of 24 patients who were scanned, i.e., 46%.

Of these 15 patients with positive expression of NIS in their breast cancer tissue sample, as measured by immunohistochemistry, 14 cases were also scanned. Of these, eight patients (57%) demonstrated uptake of Tc99m Pertechnetate on scintigraphy, i.e., were true positives; six did not, i.e., their screening test (IHC) had incorrectly predicted positive uptake on subsequent scanning (false positive screening). Therefore, a positive predictive value of 57% was observed when using IHC as a screening test for detecting those patients who would go on to have a positive scan. In contrast, six patients had negative NIS expression by IHC, and no uptake on scintigraphy, i.e., true negatives. Only one patient had a false negative screening IHC result. A negative predictive value of 86% was seen when using immunocytochemistry as a screening test for detecting those patients who would have a negative scan. Sensitivity was 88%, with a specificity of 50%.

Conclusions

This data has shown that the prevalence of patients with metastatic breast cancer expressing NIS on IHC is relatively high (68%), when compared with one other published study of similar patients[79]. Also, it has been demonstrated that a high proportion of NIS IHC positive patients who were scanned (57%) demonstrated uptake of Tc99m Pertechnetate in breast cancer primary or metastases.

It can be concluded that IHC does act as a useful screening test for those who may ultimately benefit from radioisotope treatment. The most appropriate radioisotope for therapy remains to be determined.

Chapter 1 – Introduction

Introduction

The thesis is that the known expression of the sodium iodide symporter (NIS) gene in human breast cancer tissue can be exploited as an imaging and therapeutic target. The ultimate purpose of this research is to develop novel radionuclide imaging and therapeutic strategies, in which radiohalides are administered to patients with breast carcinomas which express the NIS gene. Specific objectives of this research are:

(a) to quantify NIS RNA expression and NIS protein levels in archival specimens of breast carcinoma samples and axillary lymph node metastases.

(b) To evaluate [^{99m}Tc]-pertechnetate ($^{99m}TcO_4$) scintigraphy in patients with advanced NIS-positive breast carcinoma as a method of imaging metastatic deposits. The intensity of $^{99m}TcO_4$-generated images will be compared with the levels of NIS RNA and protein expression in the patients' archived material. The $^{99m}TcO_4$-generated images of metastatic deposits will be compared with standard imaging techniques.

In the introduction, the management of thyroid cancer and breast cancer is briefly reviewed, the role of targeted therapies and radionuclide therapies in cancer management is discussed and a strategy for exploiting NIS expression in the management of breast cancer is proposed.

Section 1 – Thyroid Cancer

Radioiodine has for many years been the mainstay of treatment in metastatic thyroid cancer. The wealth of experience accumulated in the radioisotope treatment of this tumour type is of potential use in evaluating radioisotope treatment strategies that may be applicable to patients with other types of cancer. One example of this is in the case of metastatic breast cancer, by exploiting knowledge of the biological pathways which may be common to the two cancers such as the sodium iodide symporter.

1.1 – Incidence, Survival and Aetiology of Thyroid Cancer

Thyroid cancer represents roughly 1% of all cancers, but is the most common malignant endocrine tumour. The peak age of incidence is in the third and fourth decade with females being more commonly affected in a ratio of 3:1. The Scottish annual incidence between 1997 and 2001 was reported to be 2.4 per 100,000 women and 0.9 per 100,000 men[1]. Standardised five-year survival rates for the period 1997-2001 were recorded as being 76% for men and 71% for women, aged between 15 and 74[1].

The aetiology of thyroid cancer is poorly understood. Irradiation of the neck during childhood, and exposure to ionizing radiation from nuclear fallout, as seen in the Chernobyl incident, have both been associated with an increased incidence[2][3]. Genetic abnormalities may have a key role in pathogenesis[4]**.** RET/PTC, NTRK and BRAF mutations are commonly seen in papillary thyroid cancer, while Ras, PTEN mutations and PPAR [gamma]–PAX8 rearrangement are recognised gene mutations for follicular thyroid cancer[5][6]**.**

1.2 – Pathophysiology of Normal and Malignant Thyroid

Iodide, which is an essential component of the thyroid hormones tri-iodothyronine (T3) and thyroxine (T4), accumulates in the thyroid gland via an active transport mechanism catalysed by the sodium iodide symporter, which is located in the basolateral membrane of the thyroid follicular cell (see figure one).

NIS-mediated iodide accumulation is under the control of pituitary-derived thyroid-stimulating hormone (TSH). A TSH responsive element (TRE) has been identified in the NIS promoter region, which is under cyclic-AMP control and is thyroid specific[7]. It has been shown that TSH stimulates NIS transcription and biosynthesis but is also involved in post-transcriptional regulation of NIS function[8]. This group also demonstrated that TSH was required for effective targeting of NIS to the plasma membrane.

Iodide is transported towards the colloid compartment of the thyroid cell by a process known as iodide efflux. This is generally thought to be mediated by a protein called pendrin[9]. Thereafter, iodide is organified, a complex process involving thyroid peroxidase, resulting in incorporation of iodide into tyrosyl residues in the thyroglobulin molecule (see figure two). Thus, iodide is stored in colloid, available to be secreted into the blood as thyroid hormones when required.

Papillary and follicular carcinomas account for up to 90% of all cases of thyroid cancer and are collectively referred to as differentiated thyroid cancer. The remainder comprises anaplastic and medullary carcinoma, lymphomas and, rarely, sarcomas. The differentiated cancers retain the appearance and function (albeit at a lower level) of normal thyroid cells, and can, therefore, trap iodine. Radioiodide scintigraphy and therapy are based on the uptake of radioiodide by NIS in thyroid tissue, which can concentrate all isotopes of iodine.

1.3 – Standard Treatment of Thyroid Cancer

Management of differentiated thyroid cancer is well protocolised in most departments. For an example of this, see figure three.

Total or near total thyroidectomy is the mainstay of differentiated thyroid cancer management[10], [11]. In addition to this, radioiodine has been a crucial component in the treatment of differentiated thyroid cancer for many years[12]. Most differentiated thyroid cancers retain the ability to trap iodine, so radioactive Iodine-131 (^{131}I) is initially used diagnostically to acquire a whole-body scan, for dual purposes: to screen for any residual

thyroid tissue; and to identify metastatic sites. This practice has become controversial, however, in view of thyroid stunning (see page five).

Debate also exists as to whether post-thyroidectomy ablation therapy of the thyroid remnant by radioiodine is necessary in all patients. The argument in favour of this course of management states that ablation makes patient follow-up by thyroglobulin (a tumour marker secreted into the bloodstream) assessment more sensitive, allows early detection of metastatic disease by radioiodine scans, and reduces the theoretical risk of anaplastic transformation of any residual thyroid tissue in the neck. A study of 1355 patients[13][14] showed that patients who had thyroid tumours greater than 1.5cm had a distinct survival advantage at 30 years if near total thyroidectomy followed by ^{131}I ablation and lifelong thyroid hormone therapy was employed.

The majority of clinicians and consensus guidelines now favour near total or total thyroidectomy followed by routine radioiodine thyroid ablation for anything other than very low risk patients, in view of the above data suggesting reduction in local recurrence and improvement in survival.

By this practice, sensitivity of both scanning and therapy can be optimised, as uptake of radioiodide is based on the inherent ability of thyroid cancer cells to trap iodine. This ability is enhanced by a high level of the physiological stimulus thyroid stimulating hormone (TSH). Therefore, standard preparation for radioiodine scans and therapy is to induce hypothyroidism by cessation of thyroxine therapy for at least four weeks [15][16].

Administered activities of ^{131}I for thyroid ablation vary between 30 and 220mCi (1.1 and 7.4GBq)[10]. Post-treatment scans are performed a few days later to confirm uptake of the radioiodine and identify any additional lesions not seen on the diagnostic scan.

Radioiodine also plays a valuable role in the treatment of recurrent or metastatic thyroid cancer. Following diagnosis of metastatic thyroid cancer, repeated therapeutic doses of radioiodine may be administered at four to six-monthly intervals, with activities ranging

between 5.5 and 11.1 GBq. While not curative therapy, this treatment strategy can be used repeatedly with relatively little toxicity.

Immediate adverse effects of radioiodide therapy are of nausea and mild bone marrow suppression, and are common but generally mild and self-limiting. Sialadenitis and xerostomia may also occur.

Thyroid stunning is a relatively recently appreciated phenomenon. A temporary reduction occurs in the ability of normal or metastatic malignant thyroid tissue to trap or retain ^{131}I, following prior administration of a diagnostic level of ^{131}I. If that ability recovers to its initial level, the effect is transient and can be called 'stunning'. If it never fully recovers, the effect is permanent and may be viewed as 'partial ablation'[17]. It appears that any scintigraphically sufficient amount of diagnostic ^{131}I activity will induce thyroid stunning, even if therapeutic administration of ^{131}I occurs within the following two to three days[18].

Thyroid stunning is important as it may cause a failure of radioiodine therapy, with all the attendant consequences. In the great majority of thyroid cancer patients, diagnostic ^{131}I scintigraphy performed before ^{131}I therapy reveals no unexpected pathological findings and does not change the course of treatment. The main justification for ^{131}I diagnostic studies is for dosimetric purposes. Some believe that, in view of stunning, diagnostic administration of ^{131}I prior to radioiodine therapy is counter-productive and unnecessary, and if administered should be limited to a maximum of 4Gy absorbed dose by thyroid[18]. It is not clear whether similar stunning phenomena would occur with the use of radioiodide therapy in malignancies other than thyroid.

In conclusion, radioiodine therapy of thyroid cancer is extremely well established and, it is now recognised, exploits an endogenously expressed receptor, (NIS). There is a wealth of safety data regarding long-term use of radioiodine in the adjuvant setting, and also regarding repeated use in the metastatic setting. The thyroid experience can be extrapolated to some degree for potential use in other malignancies such as metastatic breast cancer.

Section 2 – Breast Cancer

2.1 – Incidence, Aetiology and Survival of Patients with Metastatic Breast Cancer

Breast cancer is the most common type of cancer in women in the UK, and is the second-most common cause of cancer-related death in women in the UK. Incidence rates vary considerably geographically, with the highest rates occurring in the developed world, and the lowest rates in Africa and Asia. In the year 2000, there were more than one million new cases and approximately 373,000 deaths from breast cancer worldwide, with an age standardised death rate (ASR) of 12.51 (per 100,000). An ASR of 26.81 was recorded in the UK in 2000[19].

This situation remains true in Scotland, with breast cancer representing 27.5% of all female cancers. This accounted for 3,646 new diagnoses of breast cancer in 2002, and 1,082 deaths due to breast cancer in 2004[1]. The peak age of incidence is 63, and the majority of cancers occur in women aged between 50 and 70 years old, hence the screening programme encompasses this age range.

Risk factors for breast cancer include early menarche and late menopause, nulliparity, late age at birth of first child, obesity, strong family history, BRCA1 and 2 carriage, diet rich in fat, meat and alcohol, prolonged use of hormone replacement therapy (HRT), and exposure to ionizing radiation. Protective factors include prolonged breast feeding, intake of fibre, fruits, vegetables and antioxidant vitamins, and physical activity.

Despite a reduction in mortality figures between 1994 and 2004 of 18%, five-year survival in Scotland remains only 80.2% for patients diagnosed between 1997 and 2001[1]. When breast cancer recurs and becomes metastatic, it is treatable but not curable. Average survival is currently between one and two years, although some women may live with the disease for many years, particularly when they have hormone responsive disease, and/or skeletal metastases only. It is clear that metastatic breast cancer remains a challenging clinical issue and novel treatments are required.

2.2 – Molecular Biology of Breast Cancer: An Overview

There are a great number of molecular aberrations recognised in breast cancer cells, however, only a small number have become clinically relevant. These include overexpression of Her2/neu[20][21][22], and oestrogen and progesterone receptor expression[23][24].

There is compelling evidence that breast cancers can develop in a multistep process, passing through a number of intermediate hyperplastic and neoplastic forms, each having a greater chance of transforming to a malignant state than the one before. The reliable recognition of these stages is of great value in learning more about the pathogenesis of breast cancer[25].

Oncogenes are recognised to play an important role in the development of breast cancer. These are genes whose activation and overexpression can contribute to the development of cancer. A striking example is the protooncogene c-erb-B-2 (Her2/neu), which encodes a transmembrane tyrosine kinase receptor. It has been shown that Her2/neu is amplified in approximately 20-30% of invasive breast cancers[21], resulting in more of the protein encoded by the gene being present; hence function of the protein is enhanced. The resulting phosphorylation of tyrosine residues initiates complex signaling pathways that ultimately lead to cell division.

2.3 – Standard Treatment of Metastatic Breast Cancer

Prior to treatment for metastatic breast cancer, confirmation of cytological diagnosis is indicated, followed by staging investigations to assess extent of disease. Once a diagnosis of recurrent or metastatic breast cancer has been made, an analysis of Her2/neu, oestrogen receptor (ER) and progesterone receptor (PR) expression in the primary breast cancer or metastases should be made. Thereafter, a patient's therapy is "tailored" to correlate with the molecular expression of their malignant cells.

In hormone receptor positive disease, treatment may safely begin with endocrine therapy in the majority of cases[26], but ultimately most reasonably fit women with metastatic breast

cancer will receive chemotherapy, either because they have hormone receptor negative disease or because their disease has become refractory to endocrine therapy[27].

Despite the availability of a great number of chemotherapeutic agents and combinations thereof, most women will ultimately require to cease treatment with these agents due to toxicity, or due to treatment failure consequent to acquired drug resistance. First line treatment in metastatic breast cancer is dependent on a number of factors, including fitness for aggressive chemotherapeutic regimens, previous exposure to agents now used increasingly in the adjuvant setting, such as anthracyclines and taxanes, and hormonal status. In a fit patient with oestrogen receptor positive disease, hormonal therapy will typically be used. If a patient is ER negative, or requires a response to therapy more quickly than can be expected with hormonal therapy (weeks to months), then chemotherapy will be employed as first-line treatment. The choice of agent will depend on whether the patient has been exposed to chemotherapy as treatment for early breast cancer. This is increasingly the case. Anthracycline-based chemotherapy is preferred over non-anthracycline-based chemotherapy in the advanced disease setting[28]**.** Taxanes are also considered for first-line use[29]. For less fit patients, treatment with agents such as capecitabine or vinorelbine is frequently used[30][31].

Bisphosphonates reduce skeletal complications, delay progression of existing bone metastases and reduce the development of new lesions in patients with metastatic breast cancer. They act by interfering with osteoblast and osteoclast activity. In breast cancer patients, bisphosphonate therapy is currently recommended for patients with radiographic evidence of bone destruction[32][33][34].

Radiotherapy, although standard treatment in early breast cancer, has little role to play in the management of metastatic breast cancer, other than to provide local control for a breast tumour, or to palliate brain or bone metastases. Radiotherapy is used frequently for localised bone pain with 60-70% of patients responding to treatment and about one-third achieving a complete response to pain[35]. There is no place currently for radioisotopes in the routine management of metastatic breast cancer.

2.4 – Targeted Therapy of Metastatic Breast Cancer

"Targeted therapy" has become a frequently used expression in recent years, with numerous potential novel therapeutic targets being identified through our increasing understanding of the biology of breast cancer development and progression.

The degree of media attention and clinical success witnessed in the management of chronic myeloid leukaemia (CML) and gastrointestinal stromal tumour (GIST) treatment with Imatinib (Glivec), has encouraged interest in a similar "magic" bullet for breast cancer[36]. Imatinib is a small molecule signal transduction inhibitor that specifically targets protein tyrosine kinases Abl, Arg (*Abl*-related gene), KIT, platelet-derived growth-factor receptor (PDGF-R)—and the *bcr-abl* fusion gene present in CML. Therapy with this agent induces dramatic and often durable clinical responses in most patients. In patients with CML, rates of complete response approach 100%[37]. However, solid tumours display more complex genetic changes and heterogeneity as compared with haematologic malignancies, so this clinical scenario is not likely to be replicated as easily in breast cancer.

The earliest example of targeted therapy in breast cancer is hormonal manipulation, which includes ovarian ablation by surgery, radiotherapy or more recently drug therapy[38], and the anti-oestrogen drug Tamoxifen[24]. Although it is a widely held perception that hormonal therapy is a "static" therapy and induces slow responses, this class of drugs actually accounts for the largest impact of all systemic therapies for breast cancer and leads to greater relative reductions in recurrence for early-stage disease than chemotherapy[39]. More recently, a new class of hormonal agents in breast cancer has been developed and are now in regular clinical use in postmenopausal women. Of these aromatase inhibitors, Letrozole has shown advantage in disease-free survival in postmenopausal women when given adjuvantly following tamoxifen treatment[40].

Chemotherapy also represents a form of targeted therapy in that the disruption of DNA (deoxyribonucleic acid) replication and cell division preferentially affects tumor cells over non- malignant tissue.

Several biologic pathways have emerged over the past few decades which appear to be critical to carcinogenesis and can be exploited, or "targeted" for therapeutic purposes[41]. A member of the Her gene family, encoding the epidermal growth factor receptor (EGFR) is recognised as being expressed in some cases of breast cancer. Its expression may be associated with a worse clinical outcome as well as estrogen-receptor (ER) negativity[42]. Antibodies to EGFR are being assessed in clinical trials, although no activity has yet been reported in breast cancer.

An example of a targeted therapy is Rapamycin. This inhibits the phosphorylation of mTOR (a pivotal downstream kinase that links stimuli from receptors to regulation of the cell cycle), thus blocking the downstream activation of various kinases and disrupting the cell cycle[43]. CCI-779 is a rapamycin analogue which in a phase II trial involving chemotherapy refractory breast cancer patients showed some activity[44].

Cyclin-dependent kinases (CDKs) are proteins involved in various phases of the cell cycle that allow the cell to pass from a resting state, G_0, into active cycling and mitosis. Flavopiridol is a nonspecific CDK inhibitor, trials of which in combination with several chemotherapeutic agents are ongoing in breast cancer.

The c-myc oncogene encodes a nuclear protein that acts as a transcriptional regulator involved in cellular proliferation, differentiation, and apoptosis. It is overexpressed in up to 25% of breast tumors[45] and, in some series, has been associated with a worse prognosis or more aggressive clinical features[46]. There also appears to be a role for myc in hormone responsiveness and chemotherapy resistance[47]. Antisense trials targeting c-myc are in progress.

However, more clinically relevant than any of these examples, as outlined previously, Her2/neu is overexpressed in 20-30% of breast cancers, usually as a result of gene amplification. This oncogene has received interest due to its recognised association with lymph node metastases, short relapse time, poor survival, and decreased response to endocrine therapy and chemotherapy. Her2/neu represents an excellent example of the

translation of basic science to clinical practice. In addition to the prognostic information that Her2/neu status affords, the availability of the humanised monoclonal antibody Trastuzumab (Herceptin) has been proven in a number of clinical studies to improve outcome in patients whose metastatic breast cancers overexpress Her2/neu, both when used as a single agent first line, with objective response rates of 26%[48], and when used in combination with chemotherapy, where superior response rates (50% versus 32%), time to progression (seven months versus five months), and median survival of 25 months versus 20 months were demonstrated[49]. Also, there is early evidence of a role for Herceptin in the adjuvant setting. The HERA trial[50] demonstrated a reduction in breast cancer events with a hazard ratio of 0.54. Cardiac toxicity was noted in 0.5% of women treated with Trastuzumab however, and there are concerns regarding the possible medium to long-term cardiotoxic effects of this treatment.

It may never be possible to find a genuinely specific breast cancer-targeted therapy. Any drug developed that targets a specific genetic abnormality is likely to be practically useful in only a limited number of patients, and resistance will almost certainly develop over time. However, such therapies can play a valuable role in tackling breast cancer, and it is likely that drugs such as Trastuzumab will increasingly be used in combination therapies.

Thus, it can be seen that any effective novel approach to metastatic breast cancer therapy is to be welcomed.

Secion 3 – Radionuclides

3.1 – General Use

Nuclear medicine involves the use of unsealed radioactive sources to deliver radiation to tumours or target organs selectively. The exact mechanism of action is poorly understood, but involves delivery of low dose rate radiation, usually involving emission of alpha or beta particles, or an Auger electron. The basis for successful radionuclide therapy is sufficient uptake and prolonged retention of the radiopharmaceutical in the target tissues.

For benign diseases such as thyrotoxicosis and arthritis, radionuclide therapy provides a valuable alternative to surgery or medical therapy. In cancer treatment, it may be used as part of a therapeutic strategy with curative intent, such as in thyroid cancer therapy, or for disease control and palliation, for example in prostate cancer. Toxicity is generally limited to the haemopoietic tissues and few, mild side-effects are observed. It is generally accepted that long-term consequences are no greater than those associated with chemotherapy or external beam radiotherapy.

3.2 – Applications of Radionuclides in Benign Disease

One of the oldest and still most widely used applications of radionuclide therapy is Iodine-131 (^{131}I) for thyrotoxicosis. Long-term follow-up studies have confirmed the safety of this treatment. The treatment is safe and cost effective, but causes permanent hypothyroidism in almost all patients treated for hyperthyroidism, most markedly those with Graves' disease[51][52]. In general, thyroid function returns to normal within two to six months after treatment, and hypothyroidism can develop within four to 12 months.

The intra-articular administration of radiolabelled colloids such as the pure β emitter Yttrium-90 (^{90}Y) citrate and Rhenium-186 are effective in more than 60% of patients with rheumatoid arthritis and other arthritic disease[52][53][54].

3.3 – Applications of Radionuclides in Malignancy

Radioactive phosphorus, in the form of ^{32}P orthophosphate (^{32}P), has been in use since

the 1930s for the treatment of myeloproliferative disorders such as polycythaemia vera and essential thrombocythaemia. ^{32}P is a pure ß-emitting radionuclide with a physical half-life of 14.3 days. Acting by incorporation of radiophosphorus into the DNA of rapidly proliferating cells, leading to DNA damage, ^{32}P therapy may induce remission and prolong survival in these diseases[52][55]. Because of its strong incorporation into various phosphate-containing intracellular constituents, including DNA and RNA, and the potential long-term consequences of this, it is no longer in widespread use. However, as ^{32}P is the only radionuclide that can be administered orally, it is extremely useful in many underdeveloped countries.

^{31}I-m-iodobenzylguanidine (MIBG) is used in the treatment of neural crest tumours. Structurally similar to norepinephrine, MIBG is taken up by cells of neural crest origin, via the cell membrane and neurosecretory storage granules in the cytoplasm. Active uptake leads to retention of ^{131}I-MIBG in neural crest tumours, resulting in high tumour/non-tumour ratios. Radioactively labeled MIBG was first used in the early 1980s to image these tumors. More than 90% of phaeochromocytomas and neuroblastomas, around 35% of medullary thyroid carcinomas, and 70% of carcinoid tumours concentrate MIBG, are susceptible to treatment of this type[52].

Strontium is an element that behaves biologically like calcium. It localises in bone, mainly in areas of osteoblastic activity[56]. ^{89}Sr has a relatively long physical half-life of 50.5 days and emits only a ß-particle. After intravenous administration, ^{89}Sr is concentrated in bone in proportion to local osteoblastic activity. Its use was revived in the 1980s after a long period of redundancy for treatment of painful bony metastases in prostate cancer. Multicentre-controlled studies in metastatic prostate cancer have shown that ^{89}Sr is as effective as radiotherapy and that it may delay the onset of pain at new sites[57].

Samarium-153 (^{153}Sm), a nuclide with a physical half-life of 1.9 days, is a beta emitter. A phosphonate-samarium complex concentrates in the skeleton, in proportion to osteoblastic activity. About 65% of the dose remains in the skeleton[56]. ^{153}Sm is the most widely used pain palliation radiopharmaceutical agent in the United States, mainly due to its ease of use.

Rhenium-186 (^{186}Re) has a physical half-life of 3.7 days and emits a ß-particle. A study by Sciuto et al. with ^{186}Re showed overall pain palliation of 92% in breast cancer patients[58]. The tumour-to-bone marrow absorbed dose ratio was 14:1, suggesting its clinical relevance in patients with compromised bone marrow reserve. Several studies reported the safety and efficacy of use of ^{186}Re in bone pain palliation. The maximum tolerated administered activity of ^{186}Re in patients with metastatic breast cancer was found to be 2,405 MegaBequerels (MBq) with thrombocytopenia as dose-limiting toxicity[59] and a response rate of 77% has been reported[60].

Although external beam radiotherapy is the mainstay in the management of malignant bone pain, its overall efficacy for pain control is from 60-90%[61][62][63], no better than radionuclides. Interestingly, a recent Cochrane review showed that there is no difference between the degree of palliation achieved by external radiation therapy treatment versus radionuclide-based therapy[64]. Also, if multiple lesions require external beam radiotherapy, the side effects, in particular myelosuppression, limit the dose that can be delivered. It is well recognised that the pain in patients with multiple bony metastases has a tendency to move site on an almost daily basis, rendering external beam radiotherapy a somewhat impotent treatment modality. Hemibody radiation therapy has been used in patients with widespread painful lesions, but can lead to significant toxicity. In contrast, radionuclides can ablate both symptomatic and asymptomatic lesions, with minimal toxicity.

Radionuclides also offer other advantages in comparison with external radiotherapy. Radionuclide therapy such as strontium does not require special or costly equipment and thus is suitable for most hospitals with outpatient-based clinics, adequate laboratories, and basic radioactive shielding facilities. In addition, some studies in prostate cancer reveal an economic advantage to the addition of radionuclides to standard management with external beam radiotherapy[65][66].

3.4 – ^{131}I-iodine

Most radionuclide therapy in clinical practice today is with ^{131}I. Its physical half-life is eight days and the majority of its energy is emitted as non-therapeutic gamma rays. This

requires that patients are isolated in shielded rooms for several days. Only one-third of the energy is emitted as beta rays, contributing directly to the therapeutic effect[52].

3.5 – Pertechnetate

Pertechnetate ($^{99m}TcO_4$) has ionic characteristics in common with iodide. Pertechnetate behaves similarly following intravenous administration, but has a practically advantageous shorter half-life of six hours. In addition, it is relatively inexpensive and readily available. It is therefore widely used in standard diagnostic imaging procedures. Pertechnetate is trapped, but not organified in the thyroid, and is frequently used as an alternative to iodide in thyroid diagnostic studies.

3.6 – Use of Radionuclides Diagnostically in Breast Cancer

Bone scintigraphy using Tc99m Methylene disphosphonate has for many years been a widely used screening method for diagnosis and monitoring of bone metastases in most types of malignancy. The uptake depends on both local blood flow and osteoblastic activity. Osteoblastic response is secondary to osteoclastic bone resorption induced by the metastatic tumour itself. It is this osteoblastic response that is necessary for metastases to show increased activity on bone scan, but this is a relatively slow process and may require several weeks before a lesion can be visualised on bone scan.

Other than in this diagnostic capacity, however, radioisotopes have thus far had only a minor role in the routine management of metastatic breast cancer.

3.7 – Use of Radionuclides Therapeutically in Breast Cancer

The majority of patients with metastatic breast cancer affecting bones have more than one involved bony site. The administration of a radiopharmaceutical systemically has the potential to treat multiple metastases simultaneously.

In comparison to prostate cancer, the body of evidence regarding therapeutic use of radioisotopes in breast cancer is scarce. Theoretically, pain palliation in breast cancer could show unique features, as the microenvironment of bone metastases is quite different,

with prostate cancer having a prevalently osteoblastic structure and breast cancer a lytic or mixed pattern. There may be a difference in how well radioisotopes localise in these areas.

Radioactive isotopes of strontium and phosphorus have been most extensively used in treating breast cancer, as it was recognised that these elements were preferentially incorporated into the sites of all bone metastases at rates up to 25 times greater than they were in normal bone[67].

Sciuto et al performed a randomised study in patients with metastatic breast cancer, comparing treatment with Rhenium-186 and Strontium-89[58]. The results demonstrated that both ^{89}Sr and ^{186}Re are effective in palliation of painful breast bone metastases without significant differences in the overall response rate and in the degree of response.

In summary, radioisotopes are extensively used in the management of benign and malignant disease. There is currently no place for use of radioisotopes in the standard management of metastatic breast cancer, although there are theoretical advantages of this type of therapy over external beam radiotherapy and chemotherapy. Radioisotope treatment of metastatic breast cancer, if feasible, would be a valuable addition to the armamentarium of therapies against metastatic breast cancer.

Section 4 - Sodium Importer Symporter (NIS)

4.1 Characterisation and function of NIS

THE Na^+/I^- symporter (NIS) is an integral plasma membrane glycoprotein, first identified in the thyroid gland, where NIS mediates the active transport of I^- into the thyroid follicular cells. This is a preliminary step in the biosynthesis of thyroid hormones T_3 and T_4 (tri-iodothyronine and thyroxine respectively). These hormones play a vital role in metabolism and growth, most significantly of the nervous system. NIS cotransports one iodide ion against its electrochemical gradient, using the inwardly directed Na^+ gradient generated by the Na^+/K^+ adenosinetriphosphatase (ATPase). The NIS receptor is blocked by the Na+ K+ ATPase inhibitor ouabain, in addition to competitive inhibitors, such as thiocyanate (SCN^-) and perchlorate (ClO_4^-)[68].

NIS is also expressed endogenously in a number of tissues, which include salivary glands, gastric mucosa, and lactating mammary gland. The functional significance of NIS in the gastric mucosa and salivary glands is unknown. However, it is postulated to be related to antimicrobial activity. Conversely, in the lactating mammary gland, it is clear that NIS functions to mediate the translocation of I^- into the milk, making this available for the newborn to synthesize his own thyroid hormones[69][70].

4.2 - Isolation of the NIS gene

cRNAs synthesized in vitro from a rat thyroid-derived cell line (FRTL-5) complimentary deoxyribonucleic acid (cDNA) library were microinjected into Xenopus laevis oocytes and assayed for NIS activity. A single positive clone was identified, allowing isolation of the (cDNA) encoding rat NIS[71]. The subsequently cloned human NIS gene[72] was found to be 87% homologous to the rat gene, although human NIS contains 20 additional amino acids in the C-terminal region. The human NIS (hNIS) gene is located on chromosome 19p12-13.2 encoding a glycoprotein of 643 amino acids, with a molecular mass of approximately 70-90 kDa. The coding region of hNIS contains 15 exons interrupted by 14 introns and codes for a 3.9kb mRNA[73].

4.3 Development of NIS Antibodies

Antibodies were first generated by Levy et al in 1997[74] using the defined sequence of the C-terminal peptide (amino acids 603-618). These antibodies have allowed for development of immunohistochemical techniques, to detect NIS protein in a wide variety of tissues.

4.4 Application of NIS-based Research in Breast Cancer

The seminal paper in clinical NIS based research was published in Nature Medicine in 2000[75]. This group examined NIS expression in both animal and human tissue. Firstly, it was shown that lactating mice took up radioiodide into their mammary tissue. The radioisotope was concentrated more than 6000% in milk compared with its level in blood, with saturation occurring at about two hours. Also, membrane immunostaining for NIS protein was seen in rat thyroid, stomach and lactating mammary tissue. Hormonal regulation experiments showed that in the lactating rat, a complex interplay of hormones controlled NIS expression. In addition, *in vivo* scintigraphic imaging of experimental mammary adenocarcinomas in nongestational, nonlactating female transgenic mice carrying either an activated Ras oncogene or overexpressing the Neu oncogene demonstrated pronounced, active, specific NIS activity that was inhibited competitively by perchlorate.

Tissue specimens were examined by immunohistochemical (IHC) analysis using two polyclonal antibodies (Ct-1 and Ct-2) and one monoclonal NIS-specific antibody. By immunohistochemistry, Tazebay and co-workers showed further that 87% of 23 human invasive breast cancers and 83% of 6 ductal carcinomas in situ expressed NIS, compared with only 23% of 13 extratumoural samples from the surrounding non-malignant breast tissues. Even more significantly, none of the eight “normal” breast samples from reductive mammoplasties examined expressed NIS. The same group examined the immunohistochemical profile of NIS in thyroid, breast, and other carcinomas using high-density tissue microarrays and conventional sections[76]. Validating the use of microarrays, they analysed 371 breast specimens, and the results were in concordance with findings stated previously: NIS expression was observed in whole tissue sections in 76% of invasive breast carcinoma and 88% of ductal carcinoma in situ samples. The majority of

normal breast cores were negative (87%), as were 70% of normal/nonproliferative samples analysed. Plasma membrane immunoreactivity was observed in gestational breast tissues, and in some in situ ductal carcinomas and invasive ductal carcinomas.

These studies demonstrate the presence of NIS protein in breast cancer cells, but provide no functional information. Moon demonstrated that the postulated correlation between NIS expression and uptake of radioiodide did hold true in primary human breast cancers: 25 breast cancer patients were examined by scintigraphy and active uptake by the tumours was seen in those four patients whose tumours had comparatively higher levels of NIS mRNA[77]. Min et al showed that 80% (eight out of 10) of patients with positive NIS immunostaining in a thyroid malignancy responded to radioiodine therapy with ^{131}I for metastatic disease[78], whereas those with negative immunostaining responded poorly.

The above literature suggested that selective targeting of NIS positive breast cancer cells might be feasible. In 2004, Wapnir et al published data on 27 patients with metastatic breast cancer who were recruited into a clinical study designed to test this theory[79]. Twenty-three of these women had their samples analysed by immunohistochemistry. All patients also had scintigraphy performed. The first seven patients had imaging performed using pertechnetate; thereafter patients were scanned with iodide to allow dosimetry studies to be done. An attempt was made to suppress background thyroid activity using Tri-iodothyronine orally in about half of the patients. Of the 23 samples analysed for NIS protein expression, eight demonstrated NIS significantly (34.8%). Of these eight women, two had positive uptake on their scans. This suggests that the number of patients who have NIS positive breast cancers that actively uptake may be less than previously thought. Thyroid dosimetry was performed in three patients. By extrapolation, it was estimated that the potential dose to a NIS avid lung metastasis in one patient would be 30Gy with tolerable doses to thyroid and whole body.

Arturi demonstrated hormonal regulation of expression of NIS in an ER positive human mammary adenocarcinoma cell line MCF-7, where uptake of iodide was affected by insulin, IGF1/11 and prolactin[80].

Kogai and colleagues reported an increase in NIS messenger ribonucleic acid (mRNA), NIS protein, and I^- uptake activity by ninefold, in MCF-7 in response to all trans-retinoic acid (ATRA) treatment[81]. Trans-retinoic acid is a well-recognised differentiation agent. This suggests that expression of NIS in breast cancer has the potential to be manipulated to improve therapeutic outcome, in much the same way thyroid cancer patients have their thyroid uptake maximised by TSH stimulation.

Helguera showed that while I^- uptake is governed by NIS in breast cancer cells, I^2 uptake can be seen to be independent of NIS expression[82]. It is suggested that I^2 uptake may be mediated by a common transporter in mammary and non-mammary cells.

Knostman has recently shown that the discrepancy seen between NIS expression at IHC, and functional uptake of radioiodide may be explained by the presence of activation of the phosphatidylinositol-3 kinase (PI3K) protein in breast cancer cells[83]. This protein seems to interfere with NIS cell surface trafficking leading to localisation of NIS in the cell rather than at the cell surface, perhaps explaining why NIS positive breast cancer may not always take up radioiodide.

In addition, Tazebay showed that suckling hormones could positively influence NIS expression and functional activity in ovariectomised, lactating mice[75], albeit in a fairly complex manner. Oestrogen, prolactin and oxytocin in combination seemed to produce the maximal degree of NIS expression.

The previously mentioned data suggests that NIS positivity and uptake in breast cancers may not be as high as initially thought in the Tazebay study. However, a level of 34.8% NIS expression compares well with the level of Her2/neu expression seen in breast cancer of 20-30%. In addition, as demonstrated above, there may exist methods for maximising expression and/or uptake by manipulation of hormonal levels, or administration of agents capable of stimulating NIS expression, such as All-trans-retinoic acid.

4.5 Application of NIS based research in other cancers

Human and rat NIS have been introduced into several different tumour cell lines under

the control of various promoters using different transfer methodologies.

Shimura's group reported transfection of the rat NIS cDNA into a malignant rat thyroid cell line (FRTL-Tc) that ordinarily does not show I^- transport activity[84]. The cell line that resulted from the transfection (Tc-rNIS), demonstrated a 60-fold increase in $^{125}I^-$ accumulation in vitro. Tumours formed with Tc-rNIS cells accumulated up to 27.3% of the total administered $^{125}I^-$, showing an 11-fold to 27-fold increase in $^{125}I^-$ concentration, compared with non-transfected cells.

Mandell and colleagues imaged rat NIS-transduced A375 human melanoma tumours, which accumulated significantly more $^{123}I^-$ than non-transduced tumours[85].

Kang and colleagues showed radioiodine uptake in a hepatoma cell line SK-Hep1 in vitro and in vivo after transfer of the human NIS gene[86].

Haberkorn used NIS-transduced prostate carcinoma cells to study in vivo biodistribution. In rat, the human NIS-expressing tumours accumulated up to 22 times more I^- than contralateral transplanted wild-type tumours[87].

Boland used the AdNIS vector to transfect human SiHa cervix cancer cells and MCF-7 breast cancer cells, in nude mice[88]. Uptake in AdNIS-injected tumours was four to 25 times higher than in non-treated tumours. On average, 11% of the total amount of injected $^{125}I^-$ was recovered per gram of AdNIS-treated tumour tissue.

Nakamoto and co-workers established a novel breast cancer cell line, MCF3B, by stably transfecting NIS into the MCF-7 cell line[89]. In a biodistribution study using MCF3B-xenografted mice, high $^{125}I^-$ uptake (16.7%) was observed in the tumors one hour after injection. In addition, high tumour-to-normal tissue ratios were also observed.

Although it has been demonstrated by the above groups that successful NIS gene transfer can occur to non-NIS expressing tumours, it was generally not possible to detect tumour shrinkage with radioiodide treatment, probably secondary to the rapid efflux of ^{131}I observed. As the retention time of $^{131}I^-$ in these tumours was, at best, only a few

hours, this was not enough to deliver a radiation dose necessary to have any discernible therapeutic effect.

Boland proposed to increase the retention time of radioiodine in tumour cells by coupling the transfection of the NIS gene with thyroid peroxidase (TPO) – a gene involved in I^- organification[90]. As previously stated, the organification process causes radioiodine to be retained within the thyroid for several days. This long retention time, similar to the physical half-life of ^{131}I (i.e., eight days), allows a significant radiation dose to be delivered to tumour. In practice, the simultaneous transfection of both these genes can be hard to achieve. This group constructed a recombinant adenovirus encoding the human TPO gene under the control of the cytomegalovirus early promoter (AdTPO). A significant increase in I^- organification was observed in SiHa human cervix tumour cells coinfected with AdNIS and AdTPO. The levels of I^- organification obtained, however, were too low to increase significantly the I^- retention time in the target cells. However, Huang showed that the transfection of non-small cell lung cancer (NSCLC) cells with both NIS and TPO genes did lead to increased radioiodide uptake and retention, as well as to enhanced tumour cell kill[91].

It may be the case that organification is not required in all tissues to allow retention of radioisotope in cells. This could explain the encouraging therapeutic results reported in various NIS-transduced tumours that do not organify I^-. For example, Spitzweg stably transfected the human prostatic adenocarcinoma cell line LNCaP with NIS cDNA under the control of the prostate-specific antigen promoter[92]. Xenografts in mice were treated with a single 3 mCi dose of ^{131}I, and an average of 80-90% tumour volume reduction was seen in comparison with untreated controls. Following this, in vivo NIS gene transfer into LNCaP cell tumours was performed using a replication-deficient human adenovirus carrying the human NIS gene linked to the CMV promoter (Ad5-CMV-NIS). LNCaP xenografts showed a clear therapeutic response to ^{131}I, with an average volume reduction in tumour size of 84%.

Dingli's group recently reported $^{131}I^-$ therapy of NIS-transfected myeloma in SCID

mice[93]. They developed a self-inactivating lentivector controlled by an immunoglobulin promoter that resulted in efficacious and specific expression of a NIS transgene in myeloma cells. A single dose of therapeutic ^{131}I led to complete and durable remission. The result was impressive – all tumours in which 50-100% of the cells expressed NIS completely regressed two weeks after a single dose of 1 mCi ^{131}I. Noting that treatment was successful even though hNIS was not transduced into every myeloma cell, the investigators postulated that non-transduced cells could be killed by electrons emitted by $^{131}I^{-}$ from distant cells. Such emitted electrons can travel several cell diameters in vivo. This is a classical example of "cross-fire" radiation damage by β-emitters, known as the "bystander effect".

Carlin's group demonstrated radioiodide uptake in a number of cell lines transfected with human NIS including glioma, neuroblastoma, and ovarian carcinoma. Iodide accumulation was enhanced by factors of 10 to 41. It was also shown that spheroids of NIS expressing glioma cells were significantly more susceptible to lethal effects of I^{131} than monolayers. The multicellular three-dimensional spheroids are used to model avascular micrometastases. It was postulated that the increased cell kill seen was due to enhanced efficiency of absorption of decay energy in three-dimensional cultures[94].

The above results provide strong evidence that radioiodide therapy may be effective in cancer cells that functionally express NIS. In addition, the ability to organify iodide does not seem to be an absolute requirement for these malignant cells. Many strategies have emerged to optimise NIS expression and uptake in cancer cells. It is recognised that a proportion of breast cancer cells express NIS endogenously, and this provides a sound basis to further explore the feasibility of radioiodide therapy in this disease.

Section 5 – Conclusion of Introduction

The Sodium Iodide Symporter represents a novel target in metastatic breast cancer. This receptor appears to be expressed endogenously in a high percentage of cases, allowing the prospect that patients could be treated with a radiohalide. There is a great wealth of experience regarding use of radioiodine in thyroid cancer, and this can be used to guide management of radionuclides in breast cancer.

The aim of this study was to assess the feasibility of radionuclide therapy in a group of patients with metastatic breast cancer, by analysing tissue samples for NIS expression and correlating this with uptake of radioiodine in their sites of metastatic breast cancer.

Chapter 2 – Material and methods

Section 6 – Immunohistochemistry

6.1 – Materials

6.1.1 – General Equipment

DAKO Autostainer (Carpinteria, California, USA), slide racks (Azlon), ph tester sticks (Merck), pressure cooker (Vision biosystems), microwave (Proline), DAKO wax pen, magnetic stirrer (Flatspin 2), humidified chamber (Biogenics), slides (Mcquilkin, UK), coverslips (VWR, UK), Pertex permanent mounting medium glue (Cellpath,UK).

6.1.2 General Plastic and Glassware

Standard pipettes and droppers, glass dishes.

6.1.3 Chemicals and Reagents

Xylene, ethanol, Tris buffered saline (TBS), normal goat serum (NGS, 1ml in 19mls of TRIS, DAKO Cytomation kit), Diaminobenzidine (DAB, DAKO Cytomation kit), peroxidase blocking agent (ChP, DAKO Cytomation kit), Antibody diluent (DAKO Cytomation kit), haematoxylin, Scott's tap water substitute (STWS), 0.5% copper sulphate in 0.9% N Saline, Tween (Sigma, UK), Antibody diluent (DAKO Cytomation kit).

6.1.4 – Buffers

Citrate pH6 buffer was made up as follows: 2.1g citric acid was dissolved in 1000mls double-distilled (dd) H20, and 2 Molar (M) sodium hydroxide (NaOH) was added until the solution was pH6.

Ethylenediamine tetra-acetic acid (EDTA) pH8 buffer was made up as follows: H20, EDTA (Sigma, UK) and Trisma base (Sigma, UK).

Autostainer buffer made up of 3L Tris saline and 0.5mls/L Tween.

For rabbit anti-NIS polyclonal antibody from Prof Jhiang, Ohio: solution of 40mls 3%

Hydrogen peroxide (Sigma, UK) was made up in 360mls methanol, Citric acid buffer: as above, Tris buffered saline (TBS) and 1% bovine serum albumin (Sigma, UK)

6.1.5 – Tissue Samples and Antibodies

6.1.5.1 – Tissue and Cell Samples – Thyroid, Breast and Cultured Cell Sample

Archival tissue was obtained from patients with thyroid cancers, Graves disease and breast cancer. A cell block from UVW-NIS cells grown in culture (as described in section 7.1.2) and spun down, was also prepared.

6.1.5.2 – Primary Antibodies

Mouse anti-NIS monoclonal antibody was purchased from Chemicon, USA. The epitope is in the region 625-643 amino acids of human NIS.

Rabbit anti-NIS polyclonal antibody was a gift from Prof Jhiang, Ohio.

6.1.5.3 – Secondary antibody

DAKO Envision Secondary antibody (DAKO, USA).

6.2 – Methods

6.2.1 – Preparation of Tissue Samples

A protocol for the study was approved by the local ethical committee (LREC), and in accordance with this, written consent was obtained from all patients participating in the imaging study, to allow release of tissue blocks from the relevant pathology departments.

For those outwith the imaging study, specimens were anonymised and therefore did not require specific consent from patients.

Tissue blocks of the original operative sample were obtained and 4μm sections were cut using a microtome and mounted on glass slides.

6.2.2 – Deparaffination of Tissue Samples

Slides were placed in racks and paraffin removed by immersion in xylene for 4 minutes (performed twice), and then three immersions in 100% ethanol for 1 minute each, followed by an immersion in methanol. The slides were thereafter kept moist in tap water at room temperature.

6.2.3 – Antigen Retrieval Procedure

The techniques generally involved the application of heat for varying lengths of time to formalin-fixed, paraffin-embedded (FFPE) tissue sections in an aqueous solution. Citrate buffer of pH6.0 and Tris-EDTA pH8.0 are the most commonly used retrieval solutions and are suitable for most antibodies. Preliminary experiments to optimise the methodology demonstrated Tris-EDTA antigen retrieval provided superior staining to that using citrate.

1.5L of Tris-EDTA antigen retrieval mix was prepared using 1.5 litres of distilled water, 0.555g of EDTA and 0.825g of Trisma base. It was confirmed that pH was 8.0 using disposable pH tester sticks. The solution was placed in a pressure cooker and heated in the microwave for 20 minutes. Once heated, slide racks were placed in the pressure cooker and the weighted lid put in place. Slides were heated for five minutes at full pressure. Thereafter slides were allowed to cool at room temperature for 20 minutes. Following this, cold tap water was placed inside the pressure cooker to further cool the slides and prevent drying and slide racks were transferred (with care not to allow drying) into a glass dish containing TBS.

1.5L of Citrate antigen retrieval mix was prepared using 1.5 litres of distilled water, 2.1g citric acid in 1000mls ddH_20. 2M NaOH was added to reach pH6.

6.2.4 – Loading of Reagents onto DAKO Autostainer

The DAKO Autostainer is an automated slide processing system (DAKO, California, USA) which was used to process samples.

Non-specific background staining due to non-immunological binding of specific sera to

specific sites within tissue by hydrophobic forces was blocked by normal goat serum (NGS) 200µL per sample for 20 minutes. Slides were then rinsed.

Primary antibody incubation was then performed at one in 1000 dilution with antibody diluent for 60 minutes, and then slides were rinsed.

Some tissues contain endogenous peroxidases which can lead to non-specific staining. Endogenous endoperoxidase staining was blocked with hydrogen peroxide 3% solution 200µL (DAKO) for five minutes and slides were rinsed.

Secondary antibody was applied with 200 µL per sample for 30 minutes, and rinsed.

Diaminobenzidine chromogenic substrate was used- 200 µL per sample for five minutes, then repeated once more. Upon oxidation, DAB forms a stable, brown, end-product at the site of the target antigen. Slides were rinsed and kept moist.

6.2.5 – Slide Counterstaining, Fixing and Mounting

Slides were placed in haematoxylin solution to counterstain nuclei for an appropriate amount of time (Haematoxylin stains nuclei dependent on the age of the solution, which degenerates with time, therefore there is a relationship between age of solution and length of time required to adequately counterstain), then washed in tap water. Slides were then blued using Scott's tap water substitute as follows: immersion in STWS for 2 minutes, or until slides were coloured blue. Slides were then rinsed in tap water and placed in 0.5% copper sulphate solution for 5 minutes. A final rinse in tap water was followed by dehydration in methanol for 1 minute, followed by 100% ethanol for 1 minute, four times. Slides were immersed in 100% xylene for 10 seconds three times. Finally, slides were mounted with coverslips manually with mounting medium.

6.2.6 Assessment of Staining by Light Microscopy

Slides were viewed on a Leica microscope under x10, x20 and x40 magnification. First, the control slide was viewed to ensure adequate staining. Then each slide was viewed with the corresponding negative control to assess staining.

6.2.7 – Manual Methods

The deparaffination and antigen retrieval steps were performed as described above. Excess fluid was wiped from slides, and the tissue section drawn around with wax pen.

Normal Goat Serum was added dropwise. Slides were incubated for 10 minutes at room temperature. Then, primary antibody (200µl) was dropped on sample slides and the same volume of antibody diluent on the negative slides. The slides were incubated overnight at 2-8°C. The slides were washed in TBS using a magnetic stirrer for 5 minutes (changing TBS midway).

The slides were blotted with absorbent paper, then peroxidase blocking agent was added dropwise, and slides were incubated for 5 minutes. The slides were washed twice in TBS solution for a total of 5 minutes using a magnetic stirrer. The slides were blotted with absorbent paper, then DAKO Envision Secondary Antibody was added dropwise onto the slides. Slides were incubated for 30 minutes. The slides were washed in TBS using a magnetic stirrer twice for a total of 5 minutes.

Slides were counterstained, fixed and mounted as described in section 6.2.5.

6.2.8 – Antibodies

6.2.8.1 – Anti-NIS monoclonal antibody staining

Mouse anti-NIS monoclonal antibody was purchased from Chemicon, USA initially in 2004. The epitope is in the region 625-643 amino acids of human NIS. This was used with the DAKO Autostainer and manual methods as described in section 6.2.

6.2.8.2 Anti-NIS Polyclonal Antibody Staining

Rabbit anti-NIS polyclonal antibody was a gift from Professor Jhiang, Ohio, received in March 2006.

The suggested protocol supplied by Professor Jhiang's group was followed.

Briefly, citric acid buffer 1L was heated in a pressure cooker in the microwave for 15 minutes.

Deparaffination and rehydration were performed as described in section 6.2.2.

Endogenous peroxidase activity was blocked as follows: slides were soaked in 3% Hydrogen peroxide in methanol for 5 minutes, and rinsed in distilled H_20 for 1 minute twice.

Antigen retrieval was performed: slides were dipped in heated distilled H_20 in a jar 10 times gently and placed in citric acid buffer in a pressure cooker in microwave for 8 minutes. The heated jar was removed and cooled. Tissue was blocked as described in section 6.2.4.

Slides were transferred into TBS and washed for 1 minute twice in magnetic stirrer. 2% Bovine serum albumin (BSA)-TBS was applied to the slides and they were incubated in a humidified chamber for 1 hour at room temperature.

Primary antibody incubation was as follows: the primary antibody was diluted in 1% BSA-TBS, 1 in 1000. Excess blocking solution was blotted with paper. Dilute antibody was applied to slides, and they were incubated in humidified chamber for 1 hour at room temperature.

Secondary antibody incubation was as follows: Envision secondary antibody was used. Excess primary antibody was drained, and slides were washed in TBS in magnetic stirrer for 1 minute three times. Excess TBS was blotted off with paper. The secondary antibody was applied to slides and incubated in humidified chamber for 20 minutes at room temperature.

Signal detection was performed as follows: excess secondary antibody was drained, and washed in TBS in magnetic stirrer for 1 minute three times. Excess TBS was blotted with paper. DAB was applied and slides incubated in humidified chamber for 10 minutes.

Slides were washed in distilled H_20 three times for 1 minute.

Haematoxylin staining and clarifying, dehydration and mounting were performed as described in section 6.2.5.

Initial staining was poor in terms of intensity, using differentiated thyroid cancer specimens as a positive control. The technique was optimised further by using a Graves thyroid specimen as a positive control. The suggested protocol was further improved by substitution of the manual process of antibody incubation outlined above with the standard DAKO protocol for antibody incubation, outlined in section 6.2.4.

In the experiments using patient samples, the polyclonal antibody with standard EDTA protocol as described above using the DAKO Autostainer was used, as this produced less background staining and better staining of the positive control than the suggested protocol.

Section 7 – RNA Extraction and Analysis from Cell Lines

7.1 – Materials

7.1.1 – General Equipment

5% CO_2 from cylinder supply (Air Products PLC, Walton-on-Thames), Surrey Microscope (Olympus, model CK2).

PCR machine - ABI 7700 Sequence Detection system (Perkin-Elmer Applied Biosystems, Foster City, USA).

7.1.2 – Media and Chemicals

RPMI -1640 (Sigma-Aldrich, UK) and Minimal Essential Medium (MEM, Sigma-Aldrich, UK). L-Glutamine (Gibco, Paisley, UK), Foetal bovine serum (Autogen Bioclear), Fungizone (Gibco), Penicillin- Streptomycin (Gibco), Trypsin 0.5% Stock (Gibco), Phosphate Buffered Saline (PBS).

Beta-mercapto-ethanol (Fisons Scientific Equipment, Loughborough).

7.1.3 – Reagents and Kits

GAPDH (glyceraldehyde-3-phosphate dehydrogenase) primers and probe, Oswel, UK.

NIS primers and probe, TAGN, UK.

RT-PCR reagents: (Roche, UK) 5mM MgCl, 5µl 10X PCR buffer, dNTP mix (1mM each nucleotide), 1 unit of RNAse inibitor, 2.5µM random hexamers and 2.5 units of MuLV Reverse Transcriptase.

Qiagen RNeasy RNA extraction kit, Cat Number 74104, Qiagen Ltd, West Sussex, UK.

7.1.4 – Agarose Gel Electrophoresis Equipment

Agarose (Medford Ltd, Chesworth, UK), Tris-acetate-EDTA buffer (TAE) 40X stock solution diluted to 1X using distilled H20, Ethidium bromide (Sigma, UK), loading

dye, DNA 1KB ladder (Gibco -Cat.no. 1565-016, UK), electrophoresis tank (Anachem Bioscience), Gene Genius Bio Imaging system (Synegene Ltd., Beacon House, Nuffield Rd, Cambridge).

7.1.5 – Plasticware and Glassware

T75 flasks (Iwaki Ltd), pipettes, 30 ml universal containers (Sterlin Ltd), Olympus slides and coverslips, BDH Haemocytometer (Weber Scientific International, Marlborough Rd, West Sussex).

7.1.6 – Cell Lines

UVW-NIS, a glioma cell line expressing NIS was designed by a member of the group and was used extensively as a positive control. It was made as follows: UVW human glioma cells were transfected with cDNA encoding the human NIS gene to create the NIS-6 line[93]. Cells were maintained in Minimal Essential Medium, supplemented with 10% foetal bovine serum, fungizone, and penicillin/streptomycin. Cells were cultured at 37°C, in a T75 flask in 5% CO_2.

MCF7, a well recognised ER/PR positive human breast cancer cell line, derived from a pleural effusion, known to express NIS only at low levels[80] was obtained from the Department of Medical Oncology, University of Glasgow. Cells were maintained in RPMI Medium, supplemented with 10% foetal bovine serum, fungizone, and penicillin/ streptomycin. Cells were cultured at 37°C, in a T75 flask in 5% CO2.

T47D, an ER negative human breast cancer cell line, derived from a pleural effusion and not known to express NIS was obtained from the Department of Medical Oncology, University of Glasgow. Cells were maintained in RPMI Medium, supplemented with 10% foetal bovine serum, fungizone, and penicillin/streptomycin. Cells were cultured at 37°C, in a T75 flask in 5% CO_2.

7.2 – Methods

7.2.1 – RNA Extraction and Analysis from Cell Lines

7.2.1.1 – Cell Culture and RNA Extraction

Cells were incubated at 37°C in 5% CO_2 in culture media as described above. Media was changed after 24-72 hours.

Cells were trypsinised every three to five days once confluent, depending on rate of cell growth as follows:

Stock trypsin was diluted one in eight in PBS. Media was removed in the tissue culture hood. 10mls PBS was added to each flask, to wash off media. This was shaken gently and discarded. 2mls of trypsin was added to the bottom of each flask, and shaken gently. Flask was placed in an incubator at 37°C for 5 minutes. Once cells had detached, 8mls of media was added to inactivate the trypsin. The 10mls solution was transferred to a universal tube. This was made into a cell suspension with a 10 ml syringe and an 18 gauge needle. This was passed through the needle three times, and placed back in the universal tube.

Cells were counted using a haemocytometer placed under a microscope using X10 magnification.

2.5×10^5 cells were then placed in 2 T75 flasks, 20mls media and a few mls 5% $C0_2$ added to each flask. Flasks were kept at a temperature of 37ºC.

Total RNA was extracted from cell lines using the Qiagen RNeasy kit according to the manufacturer's instructions and evaluated by RT-PCR. Once cells were confluent, they were trypsinised as described above, counted and centrifuged at 1500rpm for 4 minutes. Supernatant was discarded, and tissue was re-suspended in Buffer RLT (™Qiagen inc), from kit, but requiring addition of beta-mercapto-ethanol. The samples were vortexed and homogenised in a syringe with an 18 gauge needle. 70% ethanol was added to lysate and mixed by pipetting.

Samples were applied to RNeasy mini-columns (™Qiagen inc) in 2ml collection tubes. Then, samples were centrifuged at 10,000rpm for 15 seconds. Thereafter, flow-through was discarded.

700µl Buffer RW1 (™Qiagen inc) was added to each column, and the columns centrifuged at 10,000rpm for 15 seconds. The tubes with flow-through were discarded.

Columns were transferred into new 2ml collection tubes, and 500µl Buffer RPE (™Qiagen inc) pipetted onto columns. The columns were centrifuged at 10,000rpm for 15 seconds. Flow-through was discarded.

Thereafter, 500µl Buffer RPE was added, and samples centrifuged for 2 minutes to dry off silica-gel membrane. Then, columns were transferred to new 1.5ml collection tubes.

30-50µl RNase free H_20 was pipetted onto the gel membrane of the collection tubes, and centrifuged for 1 minute to elute RNA. Samples were labelled and frozen at -70°C.

7.2.1.2 – Analysis of RNA using RT-PCR

RNA obtained was used in a 2-step RT-PCR (Roche, UK) reaction using NIS primers to amplify any NIS present.

Standard RT-PCR was carried out under the following conditions. 1µg of total RNA was reverse transcribed in a 50µl reaction volume, containing 5mM MgCl, 5µl 10X PCR buffer, dNTP mix (1mM each nucleotide), 1 unit of RNAse inibitor, 2.5µM random hexamers and 2.5 units of MuLV Reverse Transcriptase.

The RT thermal cycling conditions were as follows: 42ºC for 15 minutes, 99ºC for 5 minutes and 4ºC for 5 minutes.

10µl of the resulting solution containing cDNA template was added to an amplification reaction containing a final volume of 50µl with 1µl 50mm MgCl, 4µL 10X PCR buffer, 32.75µl ddH_2O, 2ng each of Forward and Reverse NIS primers, and 0.25ul Taq polymerase (2.5U/100ul).

The PCR thermal cycling conditions were as follows: 94ºC for 3 minutes, then 35 cycles of 94ºC for 1 minute, 60ºC for 1 minute and 72ºC for 1 minute. Primer sequences were designed from the published sequence for the human sodium iodide symporter (hNIS). The sense primer corresponded to bases 630-649 (5'-CTTCTGAACTCGGTCCTCAC-3') of the human NIS sequence. The antisense primer was complementary to bases 1064-1083 of the human NIS sequence (5'-TCCAGAATGTATAGCGGCTC-3'). These primers generated a PCR product of 454 base pairs.

In later experiments, a NIS sense primer corresponding to bases 696-715 (5'-ACCTACGAGTACCTGGAGAT-3') was used, with an antisense primer complementary to bases 814-832(AGCCCGGTCACTTGGTTCA-3'). These primers generated a NIS PCR product of 137 base pairs. This primer set was utilised as the use of potentially partially degraded RNA samples necessitated the amplification of a small target sequence.

A separate amplification reaction was performed as an internal standard using the housekeeping gene glyceraldehyde-3-phosphate dehydrogenase (GAPDH). Primer sequences were designed from the published sequence of human GAPDH. The sense primer corresponded to bases 77-95 (5'-GCATTGCTGATGATCTTGAGGC-3') of the human GAPDH sequence. The antisense primer was complementary to bases 487-509 (5'-TCGGAGTCAACGGATTTGG-3'). These primers generated a PCR product of 432 base pairs.

The resulting PCR products were run on a 1% agarose gel. This was made by dissolving 2g of agar in 200mls TAE 1 X Buffer consisting of 0.04M Tris-Acetate and 0.001M EDTA at pH 8.3, and heating in the microwave for 2 minutes. When cooled, 10µl ethidium bromide was added with care and mixed. This mixture was poured into a gel mould and allowed to set with a comb in place. When set the comb was removed. The gel was placed in an electrophoresis tank and covered with TAE 1 X Buffer. 10µl DNA 1kb ladder was placed in the 1st well. 2µl loading dye was added to the 20µl PCR product, and 10µl placed in each well. The machine was turned to 100V and run for 30-45 minutes. The gel was viewed under ultraviolet light and photographed using Gene Genius Bio Imaging system.

Section 8 – RNA Extraction and Analysis from Paraffin Embedded Tissue

8.1 – Materials

8.1.1 – Equipment

8.1.1.1 – General Equipment

Microtome (Leica), Heating block (Techne), waterbath (Thermo Shandon), rotating oven (Hybaid), microcentrifuge, cold centrifuge, large centrifuge, vortex (Jencons), PCR machine, Gilsons P1, P10, P200, P1000 (Gilsons, UK).

8.1.1.2 – General Plasticware

Pipettes, eppendorffs, 30 ml universal containers (as before).

8.1.1.3 – Chemicals

Xylene, 100% ethanol, 70% ethanol, 50% ethanol, 20% ethanol, Trizol (Invitrogen, Paisley), chloroform, isopropanol.

8.1.1.4 – Buffers

50 mM TrisHydroChloride (TrisHCL) (pH8) - made up of 0.444g Tris HCl (Sigma, UK) and 0.265g Trisma Base (Sigma, UK) in 100mls DEPC H_20.

10% SDS: 5g Sodium Deca Sulphate in 50 mls DEPC H_20 (BDH, UK).

10mg/ml proteinase K (Sigma, UK).

8.1.1.5 – RNA extraction kits

Qiagen RNeasy kit (Qiagen Ltd, West Sussex, UK).

ZYMO Pinpoint kit (California, USA).

Purescript kit (Flowgen, Nottingham, UK).

Ambion kit (Recover All Nucleic Acid Total Isolation, catalogue no 1975, Ambion, Austin, Texas, USA).

8.1.1.6 – RT-PCR kits and components

GAPDH primers and probe, ABI, UK.

NIS primers and probe, TAGN, UK.

Porphobilinogen deaminase Primers, Eurogentec Ltd, Winchester Hill, Romsey, UK.

Minelute PCR Purification kit (Qiagen, UK).

GAPDH 1 Step method- ABI Multiscribe, ABI Probe/Primers GAPDH mix, ABI Universal mix, nuclease- free H20 (all Ambion), 2X Taqman mastermix (ABI)

NIS and GAPDH 2 Step: 5 X RT buffer (Invitrogen, Paisley, UK), 0.1M DTT (dithiothreitol) (Invitrogen, Paisley, UK), 25mM dNTPs (Invitrogen, Paisley, UK), Random hexamers (Invitrogen, Paisley, UK), RTase (X10) (Invitrogen, Paisley, UK), 10µl Rnasin (Invitrogen, Paisley, UK), Murine Moloney virus (M-MLV) (Invitrogen, Paisley, UK).

PCR core kit for two-step method (Roche Applied Science, UK).

Rnase sprays (RNase zap, Ambion, UK)

Photospectrometer (Eppendorff Biophotometer)

PCR machine - ABI 7700 Sequence Detection system (Perkin-Elmer Applied Biosystems, Foster City, USA).

8.1.1.7 – Agarose Gel Electrophoresis Equipment

Agarose (Medford Ltd, Chesworth, UK), Tris-acetate-EDTA buffer (TAE) 100X stock solution diluted to 1X using distilled H20, Ethidium bromide (Sigma, UK), loading dye, DNA 1Kilobase ladder (Gibco –Catalogue number 1565-016, UK), electrophoresis tank (Anachem Bioscience), Gene Genius Bio Imaging system (Synegene Ltd., Beacon House, Nuffield Rd Cambridge).

8.1.1.8 – Nanodrop Equipment

Nanodrop ND-1000 (Ambion, UK).

8.1.1.9 – Taqman PCR Equipment

ABI Taqman 7900HT, ABI one step RT-PCR kit.

8.1.2 – Tissue Samples

Archival paraffin-embedded thyroid and breast tissue 10-20µm thick, cut using a microtome and stored in eppendorff tubes at room temperature.

8.2 – Methods

8.2.1 – Collection and Preparation of Tissue and Cell Samples

A protocol for the study was approved by the local ethical committee, and in accordance with this, written consent was obtained from all patients participating in the imaging study, to allow release of tissue blocks from the relevant pathology departments.

For those outwith the imaging study, specimens were anonymised and therefore did not require specific consent from patients.

Sections were cut using a microtome designated for PCR work, ranging from 1 x 10µm section to 4 x 20µm sections depending on the RNA extraction kit specifications.

8.2.2 – Maintenance of RNAse Free Working Environment

Anti-RNAse sprays were used to clean the workbench and pipettes prior to their use. Pipettes were treated with UV light prior to use. A designated area was used for RNA work only to avoid contamination.

8.2.3 – Extraction of RNA

8.2.3.1 – Extraction of RNA using Qiagen RNeasy kit

First, paraffin embedded thyroid samples were deparaffinated as follows. Each sample was immersed in 1000µl of 100% xylene in a 1.5ml microfuge tube, and incubated at room temperature for 30 minutes. The xylene was removed by pipetting and the step was repeated. The samples were centrifuged at 3000rpm for 5 minutes at room temperature. Each sample was immersed in 1000µl of 100% ethanol and incubated at room temperature for 2 minutes. The samples were centrifuged at 3000rpm at room temperature and the ethanol removed by pipetting. This step was repeated with 70%, 50% and 20% ethanol. Finally, 1ml double distilled H_20 was added for 2 minutes, and samples were centrifuged at 13, 4000 rpm for 10 minutes, then H_20 removed by pipetting. Samples were left at 37°C for 40 minutes to air-dry. Thereafter, instructions were followed as described in section 7.2.1.2.

8.2.3.2 – Extraction of RNA using ZYMO kit

Thyroid samples were deparaffinated as described above.

20µl of RNA digestion buffer and 5µl proteinase K were added to tubes containing recovered tissue, mixed gently and incubated at 55°C for 4 hours. Tubes were centrifuged for 30 seconds. Then, 50µl of RNA extraction buffer was added to each tube and mixed by pipetting. Then, 75µl 100% ethanol was added to each tube and vortexed. The tubes were transferred to ZYMO spin columns and these columns placed in 2ml collection tubes. The columns and tubes were centrifuged at full speed for 1 minute. 200µl RNA wash buffer was added to each spin column and centrifuged at full speed for 1 minute. Another 200µl of RNA wash buffer was added to each column and centrifuged. The columns were transferred into new 1.5ml tubes, and 10µl of RNA elution buffer, prewarmed to 60°C was added. Samples were labelled and frozen at -70°C.

8.2.3.3 – Extraction of RNA using Trizol method

Fresh 20µm sections of NIS pellet, thyroid, reactive node and breast cancer were deparaffinated as follows. Samples were incubated with 1ml xylene and vortexed for a few seconds. Then samples were centrifuged at 13,000 rpm for 5 minutes. Supernatant was removed and discarded. 1ml 100% ethanol was added and this step repeated. Nescofilm (a clear film) was placed over the top of the tubes and pierced. Samples were vacuum dessicated dry for 5 minutes. The following solutions were made up: -50 mM Tris HCl solution (pH8), made with 0.444g Tris HCl, 0.265g Trisma Base, 100mls DEPC H_20 and 10% SDS solution, made with 5g SDS in 50mls DEPC H_20.

4.5mls TrisHCL mix was added to 0.5mls SDS mix in a universal container. 1ml of this mixture was added to 50µl Proteinase K (10µg/mL). Thereafter, 100µl of this mixture was added to each Eppendorf tube. Samples were incubated overnight at 37°C in a waterbath.

Samples were centrifuged at 13,000rpm for 6 minutes at 4°C. Supernatant was removed and samples transferred to RNase free Eppendorfs. Samples were mixed by pipetting.

800µl Trizol was added to each sample and pipetted. Samples were incubated at room temperature for 5 minutes.

160µl chloroform was added to each sample and shaken vigorously for 15 seconds, and then samples were incubated at room temperature for 3 minutes. Thereafter, samples were centrifuged at -4°C at 13,000rpm for 15 minutes.

The aqueous phase was removed with care, and transferred to RNase free tubes.

RNA was precipitated with 500µl isopropanol and mixed. Samples were incubated at -20°C for 1 hour.

Following this, samples were centrifuged at -4°C at 13,000rpm for 20 minutes.

Supernatant was removed and discarded. The visible pellet was washed twice with 0.5-1ml 100% ethanol, by inversion three times.

Samples were centrifuged at -4°C at 13,000rpm for 5 minutes.

All supernatant was removed. The pellet was air-dried for 1 hour.

Then samples were re-suspended in 20µl DEPC H_20, vortexed for a few seconds, and then centrifuged for 15 seconds at 13,000rpm. Samples were placed in heating block at 55°C for 5 minutes. Finally, samples were centrifuged for 15 seconds at 13,000rpm, and then stored at -20°C.

8.2.3.4 – Extraction of RNA using Purescript Kit.

Fresh 10µm sections of NIS pellet, thyroid, reactive node and breast cancer were cut using a microtome. Sections were then deparaffinated as follows. 500µl 100% xylene was added to each tube. Tubes were then incubated for 5 minutes at room temperature mixing constantly. Samples were then centrifuged at room temperature at 13,400 rpm for 3 minutes. The xylene was removed by pipetting. This step was repeated twice. Thereafter, 500µL 100% ethanol was added to each tube. Tubes were incubated for 5 minutes at room temperature with constant mixing. Samples were centrifuged at room temperature at 13,400 rpm for 3 minutes. The ethanol was removed and discarded. This step was repeated once.

Then, 300µl cell lysis solution was added to each tube, and the samples were homogenised with a tube pestle 20 times. 1.5µl fresh proteinase K (20mg/ml) was added to each tube, and the tubes inverted 25 times. Samples were incubated whilst constantly mixing at 55°C in a rotary hybridization oven overnight.

Thereafter, samples were cooled to room temperature.

100µl protein-DNA precipitation solution was added to lysate in each tube, and inverted 10 times. Samples were placed on ice for 5 minutes. Then, samples were centrifuged at 13,400 rpm at room temperature for 3 minutes. The tissue was thus tightly pelleted.

The supernatant from each tube was pipetted into clean 1.5ml eppendorff tubes with 300µl isopropanol and 0.5µl glycogen (20mg/ml). Samples were mixed by inverting 50 times.

Then, samples were incubated at -20°C for 1 hour. Samples were centrifuged at 13,400 rpm at 4°C for 3 minutes.

Supernatant was removed and discarded, and tubes were drained on absorbent paper. 300µl of 70% ethanol was added to each tube, and inverted 5 times.

Samples were centrifuged at 13,400 rpm for 1 minute at 4°C. Ethanol was removed and discarded. This step was repeated once.

Then tubes were inverted and drained on absorbent paper, and air-dried for 15 minutes.

25µl of RNA hydration solution was added to each tube, and incubated on ice for 1 hour.

Samples were labelled and stored at -70°C.

8.2.3.5 – Extraction of RNA using Ambion Kit

The Ambion (Austin, Texas) kit was used. 4 x 20µm sections were cut using a microtome.

First, sections were deparaffinated. Each sample was immersed in 1000µl of xylene in a 1.5ml microfuge tube, vortexed for a few seconds and then centrifuged at 13,400rpm for 3 minutes.

Then xylene was removed by pipetting with care.

Samples were washed twice with 100% ethanol. This involved adding 1 ml ethanol and vortexing and centrifuging as with xylene.

Following this, all ethanol was removed by pipetting, and left to air-dry for 15 minutes on tissue paper with top open. Digestion was performed by adding 400µl digestion buffer and

40µl proteinase, placing in rotor oven for 3 hours at 50°C. Once digestion was complete, samples were stored at -20°C.

Nucleic acid isolation was then performed. 480µl Isolation Additive was added to each sample and vortexed to mix. Then 1.1ml 100% ethanol was added to each sample and mixed by pipetting. A filter cartridge was placed in each collection tube, and 700µl of the sample/ethanol mixture was pipetted onto the filter cartridge. Samples were centrifuged at 10,000rpm for 60 seconds to pass the mixture through the filter. The flow-through was discarded, and the filter cartridge re-inserted into the same collection tube. This process was repeated until all the sample had passed through (three passes).

700µl of Wash 1 was added to each Filter Cartridge, and centrifuged for 60 seconds at 10,000rpm. The flow-through was discarded, and the filter cartridge re-inserted.

500µl of Wash 2/3 was added to the filter cartridge, and centrifuged for 60 seconds at 10,000rpm. The flow-through was discarded and the filter cartridge re-inserted into the same collection tube. The assembly was centrifuged for 30 seconds to remove residual fluid from the filter.

6µl of 10x DNase buffer, 4µl of DNase and 50µl of nuclease-free water were added to each filter cartridge, as a master mix. The tubes were capped and incubated for 30 minutes at room temperature.

700µl of Wash 1 was added to each filter cartridge and incubated for 60 seconds at room temperature. Samples were centrifuged at 10,000rpm for 30 seconds. The flow-through was discarded and the filter cartridge re-inserted into the same collection tube.

500µl of Wash 2/3 was added to each filter cartridge. Samples were centrifuged at 10,000rpm for 30 seconds. The flow-through was discarded and the filter cartridge re-inserted into the same collection tube. This process was repeated once.

The cartridges were transferred to fresh collection tubes. 30µl of pre-warmed nuclease free water, heated to 95° C was applied to the centre of each filter. Samples were incubated

at room temperature for 1 minute, and then were centrifuged for 1 minute at 13,000 rpm. This process was repeated with a second 30µl of water to increase the eluate to 60µl.

Samples were stored at -80 ° C.

8.2.4 – Analysis of RNA by RT-PCR

In the case of the Qiagen and ZYMO methods, RT-PCR was performed as described in section 7.2.1.2.

In the case of the Trizol and Purescript methods, an internal housekeeping gene found in all human cells and involved in haem biosynthesis - Porphobilinogen deaminase was used. This was the standard housekeeping gene used at that time at the GRI lab where this work was done. Primers were obtained from Eurogentec. Details were as follows:

The forward primer was PBDG F4, which had a sequence as follows: 5'GACCATGCAGGCTACCATCC 3'. The location of the base pair was 906-925 (inclusive), exon 13.

The reverse primer was PBDG R1 with a sequence as follows: 5'AACTGTGGGTCATCCTCAGG 3'. The location of the base pair was 952-971(inclusive), exon 14.

The amplimer size of the F4/R1 product was 65 base pairs.

An additional forward primer F3 with a sequence as follows: 5'AAGGACCAGGACATCTTGGA3' was used which detected an amplimer size of 265 base pairs. A NIS positive transfectant UVW-NIS was used as a positive control in all described reactions.

8.2.5 – Assessment of RNA Quality

8.2.5.1 – Assessment of RNA Quality by Agarose Gel Electrophoresis

The resulting PCR products in the case of the Qiagen and ZYMO methods were run on a 1% agarose gel. This was made by dissolving 2g of agar in 200mls TAE 1 X Buffer consisting of 0.04M Tris-Acetate and 0.001M EDTA at pH 8.3, and heating in the microwave for 2 minutes. When cooled, 10µl ethidium bromide was added with care and mixed. This mixture was poured into a gel mould and allowed to set with a comb in place. When set the comb was removed. The gel was placed in an electrophoresis tank and covered with TAE 1 X Buffer. 10µl DNA 1kb ladder was placed in the first well. 2µl loading dye was added to the 20µl PCR product, and 10µl placed in each well. The machine was turned to 100V and run for 30-45 minutes. The gel was viewed under UV light and photographed using Gene Genius Bio Imaging system.

8.2.5.2 – Assessment of RNA Quality by Nanodrop

Quality of samples was checked using the Nanodrop ND-1000 (Ambion, UK), a spectrophotometer designed to analyse small amounts of RNA or DNA, by the following method. The Nanodrop was calibrated to zero using distilled water. 1µl of each sample was placed in the nanodrop machine and a photospectometry reading of RNA concentration and of A260/280 to assess purity was obtained. Quick assessment of nucleic acid purity is performed by determining the ratios of spectrophotometric absorbance of a sample at a wavelength of 260/280.This procedure was first described by Warburg and Christian as a means to measure protein purity in the presence of nucleic acid contamination, it is most commonly used today to assess purity of nucleic acid samples[95]. For a summary of methods used in RNA extraction, see table two.

8.2.5.3 – Assessment of RNA Quality by Taqman PCR

In conjunction with the Ambion method of RNA extraction, the Real Time Taqman PCR method was developed, to analyse samples for presence of GAPDH (internal house-keeping gene) and NIS sequences. The methods used for analysis for both GAPDH and NIS are described:

8.2.5.3.1 – NIS

Briefly, RT was performed as follows. A mastermix was made up, containing 80µl of 5X RT mix, 40µl 0.1M DTT, 20µl 25mM deoxy Nucleotide Triphosphates (dNTPs), 20µl random hexamers and 20µl H_20.

To this 180µl mastermix was added 20µl M-MLV and 10µl RNAse inhibitor. The RNA was heated to 65°C for 5 minutes, then centrifuged at a maximum speed and placed on ice. 21µl of the master mix was added to 19µl of RNA and incubated at room temperature for 10 minutes. Then samples were placed in an incubator at 37°C for 2 hours.

Following this step, samples were heated to 65°C in a heating block for 10 minutes and stored at -20°C.

Initially NIS specific probe and primers (TAGN, Newcastle, UK, as before) were used in the following mastermix (sufficient for 10 reactions) – 12.5µL 2X Taqman mastermix, 0.125 µl of probe, 0.25µl of forward and reverse primers and 9.375µl of H20. 22.5 µl mastermix was added to 2.5µl cDNA within each well of a 96 well plate. Then, the plate was briefly centrifuged.

Thereafter the 96 well plate was loaded on the Taqman machine.

The plate was heated to 50°C for 2 min, 95°C for 10 min then 40 cycles of 95°C for 15 sec, followed by 60°C for 1 min.

Samples were run in duplicate with nuclease-free H_20 as a negative control in both RT and PCR steps, and NIS standards as a positive control.

Standards were made up as follows: RNA was extracted from NIS-6, which is a cell line known to express NIS. cDNA was made by reverse transcription as described in section 7.2.12. 400µl dsDNA was made from cDNA in a standard PCR reaction as described in section 7.2.1.2 using NIS primers.

10µl of double stranded DNA was run on a gel to check that NIS signal was detected.

The NIS cDNA was then purified using the Minelute PCR Purification kit as follows. The cDNA was placed in spin columns, and 400µl Buffer HC was added per 100µl dsDNA. The protocol was followed and 200µl eluted volume was obtained. The ds DNA was placed in a photospectrometer. The concentration, as quantified at A260, was 0.28 µg/µl.

The following equation was used:

No of molecules ds NIS per µl volume = A260/13.2 X S X Avogadro's Number/10^{12},

Where S is size of NIS fragment (0.137) in base pairs.

So, 0.28/ (13.2 x 0.137) X 6.02 x $10^{23}/10^{12}$

= 0.28/1.8084 X (6.02 x 10^{11})

= 0.1548 X (6.02 x 10^{11})

= 0.932 X 10^{11}

= 9.32 x 10^{10} molecules NIS /µL.

1/9.32 = 0.107, so 10.73µl double stranded DNA was added to 89.27µl H20 to make up 100µl of 10^{10} molecules /µl solution.

Serial dilutions were made from this solution in order to obtain standards containing 10^1 to 10^8 copies of NIS-PCR product per reaction.

8.2.5.3.2 – GAPDH

8.2.5.3.2.1 – One-step Method

In initial experiments at GRI laboratory, sample integrity was established by analysis of the expression of the housekeeping gene GAPDH using a one-step RT-PCR protocol, as was standard there. It was felt that a one-step process was less prone to error than two-step processes, and should be used when initially attempting to analyse whether RNA had been successfully extracted from paraffin embedded tissue.

Briefly, the one-step method to detect GAPDH only was as follows: GAPDH signal was detected using standard ABI (Applied Biosystems, Warrington, UK) primers and probe. For each GAPDH reaction, 0.625µl ABI Multiscribe, 1.25µl ABI Probe/Primers mix, 12.5µl ABI Universal mix and 8.625µl nuclease- free H20 (Ambion) were added. 2µl of sample RNA was added to 23µl of this master mix.

Sample and mastermix were added to wells in a 96 well plate. Thereafter the 96-well plate was loaded on the Taqman machine. PCR conditions were as follows: 48°C for 30 minutes, 95°C for 10 minutes, then forty cycles of 95°C for 15 seconds followed by 60°C for 1 minute**.**

8.2.5.3.2.2 – Two-step Method

As good quality RNA was not reliably detected using the one-step method, a more familiar two-step method, as used in analysing RNA extracted from cell lines was used. It was felt it may be easier to determine problems with the NIS reaction, if the steps were separated. two-step Taqman RT-PCR allowed exact quantitation of starting number of copies of each target sequence under identical reaction conditions. Initial copy number was established using a standard curve.

Briefly, RT was performed as follows. A mastermix was made up (sufficient for 10 reactions), containing 80µl of 5X RT mix, 40µl 0.1M DTT, 20µl 25mM deoxy Nucleotide Triphosphates (dNTPs**)**, 20µl random hexamers and 20µl $H_2$0.

To this 180µl mastermix was added 20µl M-MLV and 10µl RNAse inhibitor. The RNA was heated to 65°C for 5 minutes, then centrifuged at a pulse spin and placed on ice. 21µl of the master mix was added to 19µl of RNA and incubated at room temperature for 10 minutes. Then samples were placed in an incubator at 37°C for 2 hours.

Following this step, samples were heated to 65°C in a heating block for 10 minutes and stored at -20°C.

Taqman PCR step was then performed as follows: A mastermix was made up using 2x Mastermix (ABI) – 12.5µl per sample, Probe/primer mix (ABI) – 1.25µL per sample and Nuclease free H_20 - 8.75µl per sample. 22.5 µl mastermix was added to 2.5µl cDNA within each well of a 96 well plate. Then, the plate was briefly centrifuged.

Thereafter the 96 well plate was loaded on the Taqman machine.

The plate was heated to 50°C for 2 min, 95°C for 10 min then 40 cycles of 95°C for 15 sec, followed by 60°C for 1 min.

Samples were run in duplicate.

ABI 7700 sequence detection software determined the initial amounts of target sequence present in samples by direct comparison of their Threshold cycle (Ct) value with the Ct values of known standards (see section 10.2.2.1.1 for explanation of Ct value), which were used as positive controls. Nuclease- free H_20 was used as a negative control in both RT and PCR steps. GAPDH Standards were made up as described in NIS section 8.2.6.1. RNA was extracted as described from NIS-6 cell line. The size of GAPDH product was 432 base pairs.

Section 9 – Radioisotope Imaging

9.1 – Materials

9.1.1 – General Equipment

A whole body gamma camera scanner (Philips Prism 2000XP) fitted with a low energy general purpose collimator was employed and a 15% window, centred on the 140keV photopeak, was selected to image whole body distribution.

Tc99m Pertechnetate was obtained from the radiopharmaceutical department on site at the Western Infirmary, Glasgow.

9.2 – Methods

An ideal radioisotope has a half life similar to the length of the test, and is available at the site of the test. As outlined before, Tc99m Pertechnetate has these qualities and is relatively cheap. It is widely used in nuclear medicine departments already, in bone scanning protocols. It is generated on site from decay of its parent compound molybdenum-99. Tc99m Pertechnetate decays by electron capture and emits gamma rays with an energy of 140 keV.

Imaging of the distribution of a radioisotope is by a gamma camera. This consists of a large detector in front of which the patient is positioned. This camera is computer controlled, to allow variation in scan acquisition time, and from which copy images can be generated. Gamma rays are emitted in all directions and require to be "focused" via a collimator. Following this the gamma camera acquires an image of the radioisotope's distribution, by detection of the collimated gamma rays emitted by the radioisotope, which are transformed into flashes of light by the scintillation crystal. This light is then converted into electronic signals by photomultiplier tubes. These signals contain information on the spatial localisation of the source of the emitted gamma rays, and their magnitude.

A low energy collimator was used, in order to obtain the best imaging of Tc99m Pertechnetate decay. Maximal image resolution was achieved by placing the collimator close to the organ of interest.

Patients were recruited from the Beatson oncology centre metastatic breast cancer clinic. They were screened for eligibility by reading of the case notes. If agreeable to receiving information in the study, they were given a consent form and counselled. Standard inclusion and exclusion criteria applied (see figures four and five).

A protocol amendment was made, with 2 changes to the original Study Protocol.

These were as follows:

1) An amendment to the length of time prior to radio-isotope imaging in which screening procedures can take place.

2) An amendment to allow patients on regular bisphosphonates to be recruited into this study.

The rationale for this was as follows: patients who are currently recruited into this study are seen at breast clinics and their eligibility confirmed. However, because of waiting times in the nuclear medicine imaging department, scans are often not performed within 14 days. Consequently patients will require a further visit for a repeat blood profile adding to an unnecessary visit for the patient. As these patients are not on any specific anti cancer therapy it is not expected there be any change in either their blood screen or their clinical condition between screening and the imaging and the plan is therefore to allow more flexibility in the time from screening investigations up to 28 days.

Increasingly patients with advanced disease, who are the target population for this study, are on bisphosphonates. It is not anticipated that bisphosphonates would change the expression of the NIS gene, while theoretically this may be the case for hormonal therapy. The exclusion criteria where therefore changed to allow patients who are on regular bisphosphonates but no other therapy to be recruited into this study.

The eligibility criteria were later modified during the study to allow patients who were

receiving chemotherapy to be included in the study. Other published studies had not excluded patients on the basis of any treatment, and there was felt to be no convincing evidence that chemotherapy should interact with NIS expression.

All patients were scanned according to the protocol which had been agreed upon by the investigators prior to commencement of the first phase of the study. This was as follows: Imaging was undertaken at 4 hours and 24 hours after intravenous administration of 600MBq Tc99m Pertechnetate. At 4 hours after injection, a scanning whole body acquisition was performed for 20 minutes duration into a 256 x 1024 matrix. Additional static images of the axilla were acquired into a 512 x 512 matrix for 400s duration. A further whole body scan was acquired 24 hours after injection for a total scanning time of 45 minutes.

There were three phases of the study in total. In phase one, the scanning protocol involved intravenous injection of 600MBq of Tc99m Pertechnetate with no blocking agent.

In phase two of the study perchlorate, a blocking agent, was administered intravenously at the same time as the Tc99m Pertechnetate. The aim of this agent was to decrease endogenous uptake as per published evidence[96].

In the third phase of the study, blocking of endogenous uptake was attempted via use of potassium iodate – 170mg potassium iodate was given orally 30 minutes before the Tc99m Pertechnetate. This is a well recognised agent used to block thyroid uptake in nuclear incidents, and also clinically[97][98].

Section 10 – Results

10.1 – Pathology Details

Thirty-three patients in total were recruited into the clinical study, and gave consent for their tissue to be obtained and to be scanned. The median age of the patients in the study was 57 years old. The median time which had elapsed since the original breast cancer diagnosis in those patients scanned was 4.4 years. Patients who were recruited into the study had a range of metastatic disease which included bone, visceral, soft tissue and nodal disease, and a combination of these. Sites of metastatic disease in the patients who underwent radio-isotope imaging for NIS uptake are shown in table six. One patient (patient 11) had two breast primaries treated simultaneously. In this case pathology blocks were obtained from the left breast only, as this was most clinically relevant.

Tumour tissue blocks were only requested for the 24 patients who ultimately entered the NIS imaging trial. Nine patients withdrew consent for the scanning trial. Reasons for withdrawal were not pursued, but in general patients felt unwilling or unable to attend. No sample was received from patient nine.

The total number of patients whose tissue samples were obtained for NIS expression studies was 23. ER status was available for 22 of these 24 patients. Twelve patients in the study were oestrogen receptor (ER) positive, 10 were ER negative. In all cases where results were available, ER status was assessed by IHC.

With regard to Her-2 status, five patient samples were positive by IHC (1 was 1+, 4 were 3+), and 12 were negative. Results were unavailable in seven patients. Progesterone receptor status (PR) was available in 10 patients, and was positive in four, negative in six. Grade was available in 15 cases, and was Grade 1 in one patient, Grade 2 in four patients, and Grade 3 in 10 patients.

Pathological type was available in 21 patients and was ductal in the majority – 18 – and lobular in three. Pathological type was unavailable for three patients, in one case as records of reports were not held back as far as 1995, in one patient who had a core

biopsy only, and in one where only nodes and lymphatics were involved, with no obvious primary tumour to allow further analysis.

Fifteen patients were node positive (10 patients were TNM stage N1, two were N2 and three were N3).

Of the 15 patients who were NIS positive by IHC, ER results were available in 14. Seven patients were ER positive according to pathology records (50%). Of these seven patients, four demonstrated Tc99m Pertechnetate uptake (57%).

Of those 11 patients who demonstrated positive uptake on scintigraphy, five were ER positive also. Only one patient with positive scintigraphy was Her 2 positive, however this was only analysed in six of these cases.

For pathological information on the study patients, please see table nine**.**

It should be noted that these results were obtained from patient's pathology records.

For details of current therapy of the patients who were scanned in this study please see table 10. Three patients were about to start chemotherapy, but had no previous exposure to treatment for metastatic disease. One patient was receiving neoadjuvant chemotherapy for non-metastatic disease. Twenty patients were receiving between their first and seventh line of treatment for metastatic disease. Six patients were either receiving or had completed first-line treatment for metastatic disease, three were on second-line treatment, five on third line, one patient was on fourth- line therapy, one on fifth-line, two on sixth-line and two on seventh-line treatment.

10.2 – Immunohistochemistry

Immunohistochemistry is scored by assessing the number of cells which stain for the protein in question, and the intensity of this staining, usually graded 0-3. The Histoscore has been developed, particularly in breast cancer, as a single measure of positivity, attained by combining these two parameters, to a maximum score of 300[99].

See figures six to eight for examples of immunostaining that can be seen with NIS in malignant breast and thyroid tissue, and Graves's thyroid tissue. See table three for a summary of immunocytochemical methods used by other groups, who have looked at NIS IHC expression.

In this study, 4µm sections of thyroid tissue, both malignant and Graves's disease, were cut using a microtome and mounted on glass slides. All parameters described in Section 6.2 were optimised: Antigen retrieval methods (EDTA and citrate), varying concentrations of antibody dilution, manual and DAKO automated staining. Optimisation was performed by comparison of thyroid positive control tissue using all these different methods, by examination under the microscope. In addition both the rabbit anti-NIS polyclonal antibody, which was a kind gift from Professor Jhiang, and the monoclonal antibody (Chemicon, MAB3564) were compared.

Using the polyclonal rabbit anti-NIS antibody with EDTA antigen retrieval, staining with one in 1000 dilution, for 60 minutes using the DAKO Autostainer demonstrated the most consistently strong staining of thyroid Graves control slides.

Malignant tissue removed at the time of original surgery or diagnosis was available for analysis in 22 of the study patients (patients 1-8, 10-12, 14-23 and patient X). The tissue had been stored at room temperature, and paraffin embedded. The sample from patient 13 was a core biopsy only and too degraded to be informative at immunohistochemistry. The sample from patient nine was never received from the pathology department and therefore there is no IHC for this patient.

Patient X, had IHC performed on her pathology sample, but withdrew consent to be

scanned.

In two patients (patients 15 and 17), nodal and/or lymphatic tissue was assessed only, rather than the breast tissue, as this was the sample which when assessed on standard Haematoxylin and Eosin (H and E) staining was felt to be least degraded, and therefore most likely to be informative. In patient 15, nodal and lymphatic tissues were assessed, and in patient 17, a jugular node was assessed.

For each breast tissue sample, 2 x 4μ sections were cut using a microtome and mounted on glass slides, one with no primary antibody as a negative control. Graves thyroid tissue was used as a positive control in every case.

Therefore 22 breast cancer tissue samples were evaluable for NIS expression by IHC (please see table four).

Staining intensity was graded visually, from 0-3 + by 2 observers, with 3+ being represented by the positive control of a Graves disease sample.

The number of cells was assessed using a semiquantitative scoring method that evaluates the number of positive tumour cells over total tumour cells, ie the percentage of positive tumour cells. This method, as compared to a categorical scoring system (eg simply classed as positive if, for example >10% positive), showed substantial agreement between observers [100]. Interobserver agreement between the two observers in this study was excellent, with agreement on intensity of staining in all cases, with a third observer scoring a proportion of samples and who was in agreement. Percentage of cells which were staining was agreed within 10% in all cases.

No samples showed 0 grade staining. A typical example of NIS protein expression in a Graves thyroid control as demonstrated by 3+ staining by IHC is shown for reference (see figure nine). Staining was not as intense in differentiated thyroid cancer, an example of which is seen in figure 10.

NIS protein expression was detected in all 22 cancer samples. In patient 15, two samples

were analysed -a4 which was nodal tissue, and a7 which was lymphatic tissue. In both of these cases 100% of cells demonstrated staining, but in a4 the intensity was described as 2+ and in a7 as 3+. Therefore both samples demonstrated positive IHC, albeit with slightly different Histoscores (200 and 300).

In the other 21 patient samples, 3+ staining occurred in two samples, 2+ in 11 samples, and 1+ in eight samples.

A mean of 85 % of cells stained, with a range of 20-100%, and a median of 80%. The mean Histoscore was 154, with a range from 20-300, and a median value of 160.

Cytoplasmic NIS protein expression, as defined by IHC, was detected in all 22 breast cancer tissue samples, in four of which membranous NIS staining was also observed. Of these, two of four demonstrated positive staining in 100% of cells, and two of four demonstrated positive staining in 80% of cells.

Fifteen cases were defined as truly immunopositive, with the criteria for true positivity being a Histoscore of > 150, or demonstration of membrane staining. Seven cases were negative by the above criteria. See table four for immunocytochemistry results, and figures 11 and 12 for examples of immunostaining from study patients.

In addition, breast cancer tissue removed at the time of original surgery was available for analysis in 25 patients who were randomly selected from the pathology department archive. These samples were analysed by immunocytochemistry using the Chemicon anti-NIS monoclonal antibody as described above in section 6.2. Reaction conditions were optimised using differentiated thyroid cancer blocks as a positive control, as described in section 6.2. These showed consistently poor staining, with no sample demonstrating membranous staining or scored as having cytoplasmic staining >20%.

Eleven blocks were randomly selected from these 25 samples and re-analysed with the polyclonal anti-NIS antibody from Professor Jhiang, when this became available. Due to time constraints, all of the randomly selected samples could not be re-analysed. None

of 11 blocks demonstrated positive immunostaining, as assessed by the afore-mentioned criteria (see table five). The mean percentage of cells staining was 32%, with a median of 30. The mean Histoscore was 38%, with a median of 30%.

Of note, in this study, samples were analysed independently by two observers, with a third observer reviewing a proportion of samples, ensuring reliability of results.

10.3 – RNA Extraction and Analysis of NIS RNA Expression

Most archival tissue in pathology departments is formalin fixed and paraffin embedded. Whilst DNA can be extracted reliably, these samples are challenging in terms of RNA extraction, as there is a great propensity for extensive RNA degradation before completion of the formalin fixation process. In addition, formalin fixation can cause cross-linkage between nucleic acids and proteins and can also covalently modify RNA by the addition of mono-methylol groups to the bases, making subsequent RNA extraction, reverse transcription and quantitation analysis problematic [101].

Traditionally, RNA extraction techniques have involved the use of hazardous organic solvents in the guanidinium thiocyanate method to remove paraffin and purify nucleic acids. Several researchers have demonstrated that RNA extraction can be achieved reliably from formalin-fixed paraffin-embedded tissue, using traditional acid guanidinium thiocyanate-phenol techniques[102][103]. These methods are time consuming, however and a number of column based kits have been developed. Generally, FFPE samples are deparaffinated using a series of xylene and ethanol washes. Following this, samples are subjected to a protease digestion step with an incubation time tailored for recovery of RNA. The nucleic acids are purified using a rapid glass-filter methodology that includes an on-filter nuclease treatment and are eluted into either water or the low salt buffer provided. In addition, newer methods of extracting RNA have been developed, for example with the use of laser capture microdissection[104]. This is a method which allows for isolation of pure cell populations from histologic sections.

When analysing potentially degraded tissue, which is likely to contain small fragments of RNA, an approach utilizing quantitative PCR (Taqman PCR) seems to be particularly suitable, as it allows for quantitative determination of gene transcript levels even in tissue extracts containing partially fragmented RNA. As this experimental strategy requires only minute amounts of RNA it should be applicable to formalin-fixed, paraffin-embedded tissue sections. Furthermore, the ability of Taqman PCR to assay very small fragments of mRNAs makes this technique amenable to studies where the RNA is moderately or even highly degraded, as in the case of RNA from archived tissues[105].

10.3.1 – RNA Extraction and Analysis of NIS Expression from Cell Lines In Vitro

RNA was extracted from the cell lines UVW-NIS, MCF7, and T47D, using the Qiagen RNeasy kit as described in section 7.2.1. RT-PCR to isolate NIS RNA was performed as described previously in section 7.2.1 2. Gel electrophoresis of the PCR products demonstrated that UVW-NIS was positive for NIS gene expression. However, neither T47D nor MCF7 expressed NIS in detectable amounts (see figure 13).

10.3.2 – RNA Extraction and Analysis of NIS Expression from Paraffin Embedded Tissue

With the methods described in Section 8, consistently good signals were obtained with the GAPDH reactions, but very little signal was detected from the NIS reaction. It was considered possible that NIS primers and/or probe may have degraded with time and/or exposure to light. Therefore, in an attempt to optimise the reaction, new NIS forward and reverse primers and probe were designed and obtained from ABI. These had the same sequence as described in section 7.2.1.2, corresponding to a 137 base pairs amplicon. These were supplied as a pellet and required to be reconstituted. This was performed using 1Mm Tris-hydrochloride ph 8 / 0.01Mm EDTA, to a 100µM working concentration.

Initially, reactions were performed as in section 8.2.6.1, using 0.25µl probe and primers in a 25µl reaction volume (ie 10µM). The method was optimized using 5µM and 20µM probe concentration. Improved results were seen with 5µM. A further attempt was made to optimise results by using 45 PCR cycles. However, best results for NIS were seen using

5µM probe concentration, 10µM primer concentration and 40 PCR cycles (see appendix 1, slide 1).

Tissue blocks were requested for 24 patients. In four cases (patients nine, 22, 23 and 24) samples could not be obtained, or were not analysed due to time constraints. Of note, RNA was extracted and analysed from the core biopsy for patient 13, as there was adequate tissue, but there was not adequate tissue to perform IHC. The sample was run for IHC, but on review was felt to be too poor to analyse in terms of quality. Therefore 20 samples were available for analysis for RNA extraction and RT-PCR to analyse NIS expression.

Extensive attempts were made to extract RNA from formalin fixed paraffin embedded tissue (FFPE) using a number of kits. Details are found in section 8.2.3.

Briefly, when the Qiagen kit, which had been used successfully to extract RNA from cell lines as described previously, was used, no bands were seen consistently on agarose gel electrophoresis, suggesting no good quality RNA had been obtained (see figure 14**).**

Thereafter, similar attempts with the ZYMO kit, suggested that the quality of the RNA was poor.

The Trizol method, which is established for extracting RNA from fresh tissue at GRI pathology department was then used, again with similar results. RNA quality was analysed by agarose gel electrophoresis, and revealed no good quality RNA.

The Purescript kit revealed little RNA as assessed by detection of GAPDH by Taqman PCR. The Ambion kit consistently revealed good RNA as assessed by detection of GAPDH by Taqman PCR.

10.3.2.1 – Assessment of RNA quality

Nanodrop and Taqman PCR were used to analyse RNA quality.

10.3.2.1.1 – Assessment of RNA quality by Nanodrop

Samples were assessed using the Nanodrop machine as described in section 8.2.5.2.

Results were not available for patient nine, but all other results are presented in table one, and purity was good in the majority of samples, as was concentration.

10.3.2.1.2 – Assessment of RNA Quality by Taqman PCR

Real-time PCR is a method that determines the presence of a specific DNA sequence. A fluorescent reporter is released during the amplification cycle. This reporter is covalently linked to the 5'end of a probe specific to the sequence of interest, and a fluorescent quencher is linked to the 3' end. When the probe is intact, the proximity of the reporter to the quencher suppresses reporter fluorescence.

During PCR, the probe anneals to the target sequence, and the polymerase has activity which cleaves the probe. The increase in fluorescence from the reporter is quantified. Quantification is performed by assessing the Threshold cycle (Ct), which is the point where the PCR reaction enters the exponential phase, and the total amount of free reporter rises above the background level. The quantity for each sample is derived from the Ct value. The machine compares the Ct value for every sample to the Ct values from the standards for the target sequence in question *eg* NIS or GAPDH. As samples are run in duplicate, the machine calculates the mean quantity.

RNA extraction using the Ambion method was performed as described in section 8.2.3.5. The RT step was performed as described in section 8.2.3.5. RNA was extracted from the 20 available study patient breast cancer samples reliably using the Ambion kit, and analysed using the Taqman 7900HT machine, as per the described protocol in section 8.2.6. To confirm RNA was of good quality, it was analysed by the Nanodrop as described in section 8.2.5.2 (see table one**).** Taqman PCR was performed as described in section 8.2.6. The housekeeping gene GAPDH was consistently detected in patient samples. (See table seven). All samples were run in duplicate.

Threshold cycle (Ct) numbers for the GAP reaction were between 24 and 39. Mean quantity varied between 3130 and 4.67×10^7.

NIS was detected only in the Graves thyroid RNA and paraffin embedded NIS expressing

cells (see table seven for results and appendix one for examples**).** NIS was not detected by this method in the breast tumour samples.

10.4 – Radioisotope Imaging

Patients were recruited from the Beatson oncology centre metastatic breast cancer clinic, as described in section 9.2.1. In all patients who underwent scintigraphy, the nuclear medicine scan was correlated with standard imaging. The timescale of imaging and imaging modality are summarized in table six. Computed tomography (CT), bone scan and chest x-ray (cxr) were all used as well recognized standard staging investigations.

10.4.1 – Phase One

Ten patients were recruited and eight patients were scanned in this phase of the study. Two patients declined to be scanned. The protocol as described in section 9.2.1 was adhered to in all cases. One additional patient who was recruited into the second phase will be included as she was mistakenly given no blocking agent (patient 18).

Of the nine patients in total (numbers one to eight, and 18), a mixture of findings were demonstrated on conventional imaging. Please see table six for details. In summary, patients one, four and 18 demonstrated visceral, bone and nodal metastases on conventional imaging, patients two, three and six had visceral and bone metastases, patients five and seven had visceral and soft tissue disease, and patient eight visceral and nodal disease.

All images were reviewed by a panel of five investigators (myself, Professor of Nuclear Medicine, Consultant Medical Oncologist, Scientific group leader, and nuclear medicine scientist) with the investigators "blinded" for the clinical details, and corresponding conventional imaging findings, and a consensus reached on the NIS scan findings. Positive uptake of Tc99m Pertechnetate was observed in two patients (patient numbers three and six) in both cases in bone metastases. Both of these patients had known visceral and bone disease but only demonstrated bony uptake, i.e., differential uptake was seen at different disease sites. Patient three demonstrated uptake only in the pelvis, lumbar spine and left shoulder, whereas on conventional imaging had shown disease in almost whole skeleton

including skull base, spine, pelvis, rib cage, shoulders, humeri and femora (isotope bone scan), and liver and lung on liver Ultrasound scan(Uss) and chest x-ray (cxr). It should be noted that conventional imaging had been performed three to four months before the Tc99m Pertechnetate scan, and the patient had been receiving treatment with a bisphophonate, perhaps altering the activity of her bone disease. She had also recently completed treatment with FEC chemotherapy, perhaps altering uptake in visceral lesions, although a cxr during chemotherapy showed responding but present lung metastases, and a liver Uss showed worsening liver metastases.

In patient six, uptake was seen in only the left femoral head and mediastinum, thought to be either left pleural disease or a thoracic spine lesion by the panel. No uptake was seen in T4 or L3 vertebrae, or right pleural effusion, pericardial effusion or small lung nodules (see appendix two, figures one and two). This patient had a seven-month gap between conventional and study imaging, and had again been receiving regular bisphosphonate. The lung nodules on CT were not absolutely diagnostic of metastases, and should be viewed as inconclusive.

Marked physiological uptake was seen in this phase of the study which impeded interpretation of images. This was most marked in the stomach, salivary glands and thyroid gland at 4 hours, and in the bowel at 24 hours (see appendix two, figures three and four). Some improvement followed software masking of images (see appendix two, figure five). This involved masking of sites of physiological uptake of Tc99m Pertechnetate, using Link Medical MAPS 10000 software. Regions of interest were drawn manually around sites of physiological uptake on images in the anterior and posterior projections. Counts within these regions of interest were then set to zero.

Of note, the 20-minute image did not provide any additional information to the 4-hour image.

10.4.2 – Phase Two

Twelve patients were recruited into this phase of the study and 10 were scanned. Two patients withdrew consent to participate in the scanning study.

As stated previously, one patient did not receive perchlorate so has been included for analysis on phase one. One patient from phase three received perchlorate, rather than potassium iodate and will be included in this phase. Other than this, the agreed protocol as described in section 9.2.1 was followed. Briefly, in this phase, an attempt was made to block physiological uptake with escalating doses of perchlorate. Doses of 100 to 300 mg were administered, with two patients receiving 100mg, three receiving 200mg, and five receiving 300mg perchlorate.

In terms of conventional imaging, the ten patient's characteristics were as follows (numbers 9-17 and 23): two patients had bone only disease, two had nodal disease, three had a combination of visceral and bone disease, one had breast and nodal disease, one had visceral and nodal disease, and one had visceral and soft tissue disease.

All images were reviewed by a panel of five investigators (myself, Professor of Nuclear Medicine, Consultant Medical Oncologist, Scientific group leader, and nuclear medicine scientist) with the investigators "blinded" for the clinical details, and corresponding conventional imaging findings, and a consensus reached on the NIS scan findings. Five patients demonstrated positive uptake (10, 13, 14, 16 and 23). Patient 10 had received 100mg, patient 13 had received 200mg, and patients 14, 16 and 23 had received 300 mg of perchlorate. Patient 10 revealed Tc99m Pertechnetate uptake in only one site of disease – supraclavicular nodes, which was the only disease noted on conventional imaging, i.e., she had uptake in all her known metastatic disease. Patient 13 was known from conventional imaging (CT) to have a large breast primary, and also small axillary nodes. These were also palpable clinically. She went on to have neoadjuvant chemotherapy, and at the time of mastectomy and axillary node clearance, was found to have had a complete pathological response, with no evidence of malignancy in her breast or axillary nodes (10

removed). Therefore, the axillary nodes seen on CT, but not on the Tc99m Pertechnetate scan may have been reactive only.

Patient 14 was seen on CT to have multiple bilateral lung metastases, and a large chest wall mass. Uptake with Tc99m Pertechnetate was seen only in the large chest wall mass, not the small lung metastases. However, this may have been related to size as these metastases were subcentimetre in size.

Patient 16 had disease on conventional imaging in liver, bone and a pleural effusion. Tc99m Pertechnetate uptake was demonstrated in the pleural effusion only.

Patient 23 had MRI and CT performed which revealed small bowel disease (this was biopsy proven), and whole vertebral column disease on MRI. Her imaging had not been updated during her six cycles of FEC chemotherapy, as MRI spine was static over a period of years, and CT was not felt to be helpful. This was the reason that there was a long interval between her conventional imaging and Tc99m Pertechnetate scan. However, this patient did have a CT at the end of her course of chemotherapy, which was one month after her Tc99m Pertechnetate scan, and this suggested peritoneal disease, and possible porta hepatis nodes. Of note, later CT imaging did not confirm findings of nodes at porta hepatis, and therefore this was not likely to be of significance. Also of interest, this patient had vertebral disease seen repeatedly on MRI, but isotope bone scanning was normal. Tc99m Pertechnetate uptake was seen only in the vertebral column, and not convincingly in the small bowel. However, this is a difficult area to visualise on Tc99m Pertechnetate scanning due to general physiological uptake, which was seen despite administration of 300mg perchlorate.

Therefore, of the five patients who demonstrated uptake on Tc99m Pertechnetate scanning, differential uptake was seen in at least four of these, with only one patient showing uptake in all the known sites of soft tissue disease, although there was only one site of known disease within this patient (patient 10). It should be noted that patient 13 may have only had actual malignancy in her breast lesion and not in the axillary nodes seen on CT.

One patient demonstrated uptake in only their known soft tissue lesion (patient 14), and one patient in only one of two sites of visceral disease and not at all in bone metastases (patient 16). One patient with disease in spine and small bowel mesentery demonstrated uptake in spine only (patient 23).

For Tc99m Pertechnetate images of these patients please see appendix two, figures six to 10.

Perchlorate appeared to qualitatively reduce physiological uptake most markedly in the bowel, with no obvious response to increasing dose from 100mg to 300mg. A temporal effect was noted between the 4 hour and 24 hour scans, i.e. a difference in intensity of uptake was seen at these two different time points, in some cases with blocking seeming to be impaired at 24 hours. For example, in patient 16, thyroid activity seemed to be evident at 24 hours, and not seen at 4 hours, indicating that thyroid uptake was blocked at least initially (see appendix two, figure 11).

10.4.3 – Phase Three

Ten patients were recruited, and six were scanned. Four patients withdrew consent for the scanning study.

One patient with disease in the spine and in the small bowel mesentery demonstrated uptake in the spine only (patient 23). This patient received 300 mg perchlorate, and therefore will be included in phase two for analysis.

Five patients were therefore analysed (numbers 19-22 and 24).

In terms of conventional imaging, the five patient's characteristics were as follows: one patient had disease in soft tissue only, one in nodal areas only, one in viscera and bone, and two had visceral, bone and nodal disease.

All images were reviewed by a panel of five investigators (myself, Professor of Nuclear Medicine, Consultant Medical Oncologist, Scientific group leader, and nuclear medicine scientist) with the investigators "blinded" for the clinical details, and corresponding

conventional imaging findings, and a consensus reached on the NIS scan findings. Four patients demonstrated positive uptake. One patient demonstrated uptake in her only site of disease which was a soft tissue mass (patient 19). Patient 20 demonstrated uptake in a sternal lesion only, with no uptake in liver, pleural effusion or rib and spine metastases. It should be noted that the pleural effusion was pleurodesed three years previously, which may have rendered it sterile.

One patient with extensive bone, nodal and liver metastases demonstrated uptake in the large liver lesion and lower vertebral metastases only (patient 22).

One patient with disease in neck and axillary nodes showed uptake in neck nodes only (patient 24). However, it should be noted that the neck nodes (right supraclavicular) were noted clinically 18 months prior to the Tc99m Pertechnetate scan, and these and axillary nodes were confirmed on CT at that time. In the interim, the patient received two lines of chemotherapy, with some response in the neck node and 6 months prior to the Tc99m Pertechnetate scan the patient received palliative radiotherapy to this area. The CT closest in time to the Tc99m Pertechnetate scan (three months prior) revealed new right axillary nodes, but right supraclavicular nodes were not seen. The Tc99m Pertechnetate scan detected uptake in the right supraclavicular area only, suggesting continuing activity in this area.

Please see appendix two, figures 12 to 15.

Potassium iodate 170mg was used as an agent to block physiologic uptake in this phase of the study. In three of the five patients who received potassium iodate, there was no discernable thyroid uptake i.e., blocking was complete. In patients 20 and 24, however, there seemed to be incomplete blocking of thyroid activity i.e., minimal thyroid uptake was seen (see appendix two, figure 16 for example). Please see table eight for details.

In summary, radio-isotope uptake was observed in 11 of 24 patients in total i.e., 46%. It should be noted that assessment of uptake was made in a qualitative, rather than quantitative manner.

It was noted that two patients controlled on Thyroxine therapy (patients 11 and 15) showed no change in thyroid uptake, as compared with those not on Thyroxine.

10.5 – Correlation Between Positive Scans and Positive IHC

Twenty-four patients were scanned in the imaging study. In two cases (patients nine and 24), the breast cancer tumour samples were not obtained, as they could not be found in the relevant hospital archives. In one case (patient 13), the sample was too degraded to allow informative analysis. Of note, with respect to these three cases for which tumour samples were unavailable, one patient (patient nine) demonstrated no uptake on scintigraphy, and two (patients 13 and 24) showed Tc99m Pertechnetate uptake.

In one case, the patient had immunostaining performed on their breast cancer sample, but declined to be scanned due to ill health (patient X –see table four).

Therefore, there were 21 patients with informative breast cancer samples in which NIS expression by IHC was performed and who underwent Tc99m Pertechnetate imaging. Comments can be made regarding the correlation of NIS expression by IHC and scintigraphy in these 21 patients only.

Positive predictive value is defined as the number of true positives/number of true positives and false positives. Negative predictive value is defined as the number of true negatives/ number of true and false negatives.

Of the 14 patients (this excluding patient X) with positive expression of NIS in their breast cancer tissue sample, as measured by immunohistochemistry, eight patients (57%) demonstrated uptake of Tc99m Pertechnetate on scintigraphy i.e., were true positives, six did not, i.e., their screening test (IHC) had incorrectly predicted positive uptake on subsequent scanning (false positive screening). Therefore a positive predictive value of 57% was observed when using immunocytochemistry as a screening test for detecting those patients who would go on to have a positive scan. In contrast, six patients had negative NIS expression by IHC, and no uptake on scintigraphy, i.e., true negatives. Only one patient had a false negative screening IHC result (patient 14). A negative predictive

value of 86% was seen when using immunocytochemistry as a screening test for detecting those patients who would have a negative scan.

Sensitivity is defined as the number of true positive cases/ number of true positives and false negatives. Specificity is defined as the number of true negatives/ number of true negatives and false positives. Sensitivity was 88%, with a specificity of 50%.

Section 11 – Discussion

11.1 – Background

Breast cancer remains the most common cause of cancer in women in the UK. In 2006, breast cancer accounted for 17% of female deaths from cancer in the UK and was the most common cause of death from cancer in women until 1998; since then there have been more deaths from lung cancer[106].

Although survival has improved in recent years, novel and effective, non-toxic approaches to therapy in patients with metastatic or relapsed breast cancer remain elusive.

A seminal publication in breast cancer research was published in Nature Medicine in 2000 by Tazebay[75]. This suggested the intriguing prospect that the physiological pathways whereby iodide is taken up into thyroid cells and incorporated into thyroid hormones could be exploited for therapy in breast cancer. A major step in the process of iodide uptake is mediated by NIS – the sodium iodide symporter. This protein was determined to be the main transporter in iodide uptake into thyroid cells, in the 1990s, and Tazebay demonstrated the presence of NIS protein, by IHC using 2 polyclonal antibodies, and one monocolonal anti-NIS antibody, in 87% of human breast cancer samples examined. The possibility of endogenous expression in breast cancer was exciting, given the interest in research incorporating a range of different methods to artificially induce NIS expression in a variety of cancers. Radioisotope therapy has a long and safe record of utility in thyroid cancer, and would be a valuable addition to the armamentarium of therapies available in metastatic breast cancer, should endogenous NIS expression in breast cancer translate into clinical relevance.

However, a further clinical study by Wapnir in 2004[79] showed that the incidence of NIS positivity in breast cancer cells may not be as high as initial studies had suggested. In Wapnir's study, of the 23 samples analysed for NIS protein expression by immunohistochemistry, eight demonstrated NIS expression (34.8%), and only two of these patients demonstrated uptake on scintigraphy (7%).

Positive immunostaining was defined as being present if >20% of cells demonstrated brown immunostaining. The presence of plasma membrane staining was noted, but the incidence not reported in their paper. In nine of the 23 patients, metastatic tissue was available for analysis, in addition to the primary tumour. Of note 87% of the NIS positive cases in Wapnir's study were ER negative. Moon, however, demonstrated radio-isotope uptake of Tc99m Pertechnetate in four of 25 breast cancer patients[77]. It was also noted that these four patients had comparatively higher levels of NIS mRNA as compared with those patients whose tumours did not take up radio-isotope.

The above studies suggest that NIS positivity and uptake in breast cancers may not be as high as initially thought in the landmark Tazebay study. However, a level of 34.8 % NIS expression compares well with the level of Her2/neu over-expression or amplification seen in breast cancer of approximately 20%, a target which is in routine use for therapeutic manipulation.

11.2 – Current study

11.2.1 – Immunohistochemistry

Initial review of the available literature regarding immunohistochemical methods used to detect the presence of NIS protein in metastatic breast cancer and thyroid cancer, suggested the use of the mouse anti-NIS monoclonal antibody Chemicon, MAB3564[107]. This antibody was initially optimised by using a variety of staining conditions on samples of differentiated thyroid cancers. While this antibody was effective when used to stain differentiated thyroid samples, a panel of 25 random breast cancers and 20 study patients stained poorly, in terms of intensity, and number of cells demonstrating staining.

In view of the relatively poor staining seen with this monoclonal antibody, a literature search was performed to identify workers in this area. To this end, contact was made with Professor Jhiangs's group in Ohio, US. They kindly agreed to the loan of their rabbit anti-NIS polyclonal antibody. The suggested protocol was as described in section 6.2.8.2. It was found, however, that staining was superior using the DAKO Autostainer machine with this rabbit anti-NIS polyclonal antibody.

It has been previously reported that Graves' disease of the thyroid was the most effective positive control (Jhiang, personal communication). This, in fact stained very strongly and was used as a positive control and a reference for membrane staining of 3+ in 100% of cells (Histoscore 300) (see figure nine).

If patient X is included, 15 cases were defined as truly immunopositive, with the criteria for true positivity being a Histoscore of > 150, or demonstration of membrane staining. Seven cases were negative by the above criteria. See table four for immunocytochemistry results, and figures 11-12 for examples of immunostaining from study patients.

This represents a prevalence of NIS staining in study patients of 68%. In this study, of the 14 NIS positive cases where oestrogen receptor results were available, seven were ER negative (50%) and seven were ER positive (50%).

Interestingly none of the random breast cancer samples had positive IHC assessed by the polyclonal antibody (see table five). This may have been due to the relatively small sample size.

11.2.2 – Imaging

Tc99m Pertechnetate uptake was demonstrated in 11 of 24 patients who were scanned (46%).

Of those patients who demonstrated uptake of Tc99m Pertechnetate, characteristics were as follows: on conventional imaging, no patients had bone-only metastatic disease, five patients had visceral and bone metastatic disease, one patient had breast and possibly nodal disease, one patient had visceral and soft tissue disease, one patient had soft tissue disease only, one had visceral, bone and nodal disease, and two patients had nodal only disease. Uptake was seen in all known disease in only two patients and this was nodal disease in the supraclavicular fossa in one patient (patient 10) and a soft tissue mass near sternum in the second (patient 19).

Differential uptake, i.e., uptake in some of a patient's known metastatic lesions, but not

others, of Tc99m Pertechnetate was seen in the majority of patients who demonstrated uptake (nine patients). Of the five patients who had known metastases in bone and viscera, three (patients three, six and 20) demonstrated Tc99m Pertechnetate uptake in only some of their bone metastases, and not at all in their visceral metastases. Patient 23 demonstrated uptake in all known bone metastases in her spine, but not in the known visceral disease in her small bowel. Patient 16 had positive uptake in her pleural effusion only, not in bone or liver metastases.

The patient (patient 13) with breast and possible axillary nodes, had uptake only in the biopsy proven breast cancer, not axillary nodes, but it was unclear if these nodes were reactive or contained malignant deposits. Patient 14 had known disease in viscera and chest wall, but only demonstrated uptake in the large chest wall lesion, not small lung metastases.

Patient 22 had metastases in viscera, bone and nodes. Uptake was seen only in liver and lumbar vertebrae, not in nodes, thoracic spine, ribs or pelvis. Patient 24 had metastatic disease in two nodal areas, but demonstrated uptake in only one of these.

Overall, it seems that Tc99m Pertechnetate uptake is best seen in bone disease as opposed to visceral disease. Nodal and soft tissue disease is also fairly well visualised.

Subjectively, there did seem to be some difference between the appearance of the 4-hour and the 24-hour scans generally, in that the patients with bony disease (patients three and four), seemed to have more prominent uptake in this bony disease seen at 24 hours as compared with the 4 hour scan. Background blood pool activity appeared to have reduced at 24 hours and therefore there was better contrast of uptake in the spine compared with physiological uptake. At 24 hours, however, there is also increased activity within the bowel due to excretion which impedes image interpretation**.** In contrast, patients where nodal, soft tissue or visceral uptake was seen (patients 10, 13, 14, 16, 19 and 24) seemed to demonstrate this best at 4 hours (see appendix two). This would support the policy of scanning all patients at two separate time points.

Attempts were made to block physiological uptake using perchlorate and potassium iodate. Perchlorate and potassium iodate did seem to appreciably reduce the physiological uptake of Tc99m Pertechnetate by a number of organs, including thyroid and bowel. This was a preliminary study, where it was felt that it would be useful to look at a number of blocking methods, to find the most useful agent and dose. Following this study, this would be regarded as being potassium iodate, as there was no great temporal effect as seen with perchlorate. Also, physiological blocking was observed. Clearly, only small numbers have been scanned with this method, and further studies would be required.

Other workers have used a low iodine diet in combination with T3 and methimazole to suppress thyroidal uptake[79]. This was seen to be useful in suppressing thyroidal uptake in that dosimetric study. This may be a further useful approach in future work, but in this study, it was felt that examining perchlorate at escalating doses and potassium iodate, would be more valuable in terms of assessment of physiological blocking.

11.2.3 – RNA analysis

One of the stated aims of this project was to extract RNA from paraffin embedded tissue, and analyse this for NIS expression. A technique was developed for extracting RNA reliably from patient's archival samples (Ambion method). Although GAPDH signal could readily be detected, it was not possible to detect NIS signal from paraffin embedded breast tissue.

It was proven that the RNA quality was good, as GAPDH was consistently detected, and analysis by Nanodrop confirmed quality. It was, however, possible to detect a NIS signal from paraffin embedded cells extracted from a NIS expressing cell line. This suggests that it is not the formalin fixation and paraffin embedding process that renders NIS undetectable in these samples. It was also possible to detect NIS positivity in RNA which had been extracted from paraffin-embedded Graves thyroid tissue, suggesting that this method is sensitive, but not sufficiently so to detect NIS in paraffin-embedded breast tissue, where NIS is likely to be less abundant. It is clear from the literature[108] that RNA can be reliably extracted from fresh tissue, but extraction from paraffin embedded tissue is significantly

more challenging[101][109]. A number of factors have been shown to contribute to poor yield of RNA and may have been important in this study. These contributing factors are likely to have included the age of tissue, and therefore the length of time it has been stored. The median duration of storage of tissue used in this study was 5.3 years (range one to 19 years). The efficiency of amplifying mRNA in paraffin-embedded blocks has been shown to be greatly affected by time spent in paraffin[110].

It has been shown that abundance of quantifiable RNA fragments is lower in fixed tissue compared with fresh tissue, and this effect is magnified at larger amplicon sizes[111]. NIS primers and probe used in the majority of my study detected 137 base pairs amplicon size. GAPDH primers and probe were designed to detect an amplicon of 118 base pairs.

It seems likely that storage time in paraffin, and processing may cause large proportions of RNA in samples to be degraded. GAPDH, being a housekeeping gene, is likely to be present more abundantly than NIS; therefore it is likely that a small amount of GAPDH RNA will be detectable long after NIS RNA has completely degraded.

It also appears that different RNA species have different half lives in cells, with several factors contributing to RNA longevity including mRNA length, and more specific determinants such as stability/instability elements in coding regions, for example[112][113]. These may be contributory factors in why GAPDH is consistently detected, but NIS is not in the breast cancer tissue.

In conclusion, analysis of RNA extracted from paraffin embedded breast cancer tissue did not yield consistently reliable results. It was not reasonable or practical in my study to attempt to obtain fresh tissue from patients to allow analysis of RNA. It may be possible in the future, however, to obtain fresh tissue at the time of diagnosis of breast cancer, to assess for presence or absence of a panel of genes. NIS analysis at this stage may be useful for staging imaging with radio-isotope, to assess whether radio-isotope may be a useful therapy at time of relapse, or to assess its therapeutic use at an early stage. However, the sensitivity and specificity of the screening test would have to be vastly improved, to be

clinically applicable.

11.3 – Comparison Between Current Study and Wapnir's Study

The study by Wapnir et al evaluated 27 patients[79]. This present study assessed 24 subjects, and therefore represents the second largest study of radioisotope scanning in patients with breast cancer.

The mean age of patients in the Wapnir study was 50.4 years, as compared to 56 years in the current study. In the Wapnir study, seven of the eight patients (87.5%) who demonstrated NIS positivity on IHC were ER negative. In their paper, they comment that up-regulation of NIS in malignant cells may therefore be an oestrogen-independent event, and this is also seen in Tazebay's work[75], where transgenic mice carrying oestrogen-independent breast tumours take up iodide. In contrast, in this current study, seven of the 14 (50%) patients who were NIS positive by IHC demonstrated ER positivity. In this study, patients who were on hormonal therapy were excluded from recruitment; however, ongoing chemohormonal treatments were not interrupted in Wapnir's study. It is unclear how hormonal treatments may affect NIS expression. It seems from Tazebay's experiments, that oestrogen levels can affect NIS expression albeit in a complex fashion[75]. The higher numbers of patients with NIS positivity on IHC in the current study, who demonstrated ER positivity also, may be related to the lack of manipulation of hormonal status by therapeutic agents, but the numbers are too small to draw any conclusions.

The present study showed a greater number of patients with Tc99m Pertechnetate uptake than the Wapnir study (46% versus 14%). In Wapnir's study, only 1 patient demonstrated Tc99m Pertechnetate uptake, which was in an axillary metastasis (14% of patients had a positive scan therefore). However, in the Wapnir study, only seven patients received Tc99m Pertechnetate. These seven patients received a lower administered activity of Tc99m Pertechnetate than in the present study, (5-15mCi - equivalent to between 185 and 555 MBq versus 600 MBq in the present study). Scanning was performed at 15, 30, 60 and 120 minutes only (as compared with 4 and 24 hours in the present study). Therefore, although the number of patients scanned with Tc99m Pertechnetate was small

(seven) in the Wapnir study, the percentage of patients showing uptake were not as high as in the present study and the reasons may include lower administered activity of Tc99m Pertechnetate, and earlier timing of scans. The timescale of scans in the present study was agreed in the study protocol to allow detection of differential uptake in metastases between early and late images.

After these seven patients had been scanned, Wapnir's group changed their protocol to using the radio-isotope I^{123} to allow retention studies to be performed. Only one patient who was scanned in the latter part of the Wapnir study using I^{123} had positive uptake out of 20 patients scanned (5%).

In summary, in the present study, 24 patients received 600MBq of Tc^{99m} Pertechnetate and were scanned at 4 hours and 24 hours. Eleven, i.e. 46%, demonstrated uptake of Tc99m Pertechnetate in a range of bone and other lesions. This would suggest that the scanning protocol used in this study was superior to that in Wapnir's study, and should be explored in future studies.

11.4 – Summary

This data has shown that the prevalence of patients with metastatic breast cancer expressing NIS on immunohistochemistry is relatively high (15 of 22 samples: 68%), when compared with 1 other published study of similar patients[79]. The original Tazebay data demonstrated higher NIS expression by IHC, but this was in primary breast cancer tissue harvested at the time of IHC. Also, it has been demonstrated that a high proportion of NIS IHC positive patients who were scanned (eight of 14 – 57%) demonstrated uptake of Tc99m Pertechnetate in breast cancer primary tumour or metastases.

The question this study poses is "does immunohistochemistry as performed here provide a useful screening test to select patients who should go on to have Tc^{99m} Pertechnetate scanning performed?"

With a negative predictive value of 86%, and a sensitivity of 88%, the large majority of patients who would have a negative scan would be correctly detected, and not be

subjected to further tests. The positive predictive value of 57%, and specificity of 50% associated with this screening test would clearly not correctly detect all those patients who would be likely to benefit from Tc99m Pertechnetate therapy, but those patients who were destined to have a negative scan would later be excluded from therapy when they had their scan performed. This would suggest that it would be prudent to screen out those patients who demonstrate negative IHC, with a relatively straightforward and noninvasive examination of FFPE breast tissue available from the surgical specimen, and proceed to perform radio-isotope imaging**,** in those who demonstrated positive IHC i.e., that IHC does act as a useful screening test for those who may ultimately benefit from radioisotope treatment.

In this study, six of 12 cases which displayed no uptake by Tc99m Pertechnetate, where IHC was available, would have been deemed to have negative immunohistochemistry by the above criteria. The other six would have been deemed positive by IHC, but on subsequent scanning would not have demonstrated uptake in their metastases and therefore would have been considered unsuitable for therapeutic radioisotopes.

The question of why some (six of 14 IHC positive cases – 43%) of samples should demonstrate NIS immunoreactivity, but not take up Tc99m Pertechnetate scintigraphically is an interesting one. Of those patients with positive immunohistochemistry, who ultimately had negative scans, four of the six did not demonstrate membrane staining, perhaps suggesting a lack of functional NIS protein in these samples. It seems that simply demonstrating NIS positivity in the original breast cancer sample is not sufficient to assume NIS functional activity leading to Tc99m Pertechnetate uptake in known disease in every case.

In the present study, four patients (seven, 10, 15 and 19) were seen to have plasma membrane positivity on IHC. However, two of these (10 and 19) demonstrated isotope uptake and two did not (seven and 15). These are small numbers to be able to draw conclusions, but it may be that the discussed mechanisms that render metastases NIS negative by IHC over time are involved. This was also demonstrated in the Wapnir study, where eight cases

showed NIS expression, but 6 did not demonstrate uptake (75%). Wapnir's paper states that presence of plasma membrane NIS positivity was noted. However, the number of samples demonstrating this was not given in the paper.

There is recent evidence suggesting that NIS activity in thyroid cells requires not only TSH stimulation, but also cell polarisation and spatial organisation of thyrocytes into follicles[114]. There are also reports that some thyroid cancers overexpress NIS, but this does not always translate to increased iodide uptake, whether due to faulty targeting of NIS to the plasma membrane or insufficient retention of NIS in the plasma membrane[115][116][117]. It may be of relevance that only I^- and not I^2 uptake is affected by NIS expression, at least in breast cancer cells[82].

PI3K protein upregulation in breast cancer cells may be important here[83]. This protein seems to interfere with NIS cell surface trafficking leading to localization of NIS in the cell rather than at the cell surface, perhaps explaining why NIS positive breast cancer may not always take up radioiodide. Many oncogenes that are implicated in the development and progression of human breast cancer upregulate PI3K signalling, and there seems to be differential effects of PI3K in thyroid and breast cancers. This may be a future potential target for manipulation of improved radioisotope uptake in NIS positive breast cancers.

Disease progression has, by definition, occurred in all the patients between the time when their primary breast cancer was removed and when they were receiving treatment for metastatic disease. This may have led to altered expression of NIS function affecting scintigraphic uptake as can be seen in thyroid cancer[118]. Min demonstrated that seven of 11 lymph node metastatic differentiated thyroid cancer tissues showed loss of NIS expression by IHC, despite showing expression in the primary thyroid cancer[78]. This was also demonstrated in the Wapnir paper, where in two cases in which the primary breast cancer tissue and metastatic tissue were analysed together, it was demonstrated that the primary showed weak NIS positivity, but the metastases were NIS negative. This must be presumed to be the effect of interval treatments, or through the effects of disease progression on NIS expression. In the Wapnir study, there were in total

six cases showing NIS positivity, but no scintigraphic accumulation. Although primary and metastases were not available in every case, the same mechanisms may be assumed to be at work.

In the current study 17 of 24 patients were on some form of therapy at the time of their Tc^{99m} Pertechnetate scan, and this may alter NIS expression over time (see table 10). In only one case in the present study was the sample harvested contemporaneously – patient 13, a patient having neoadjuvant chemotherapy. Unfortunately, her sample was a core biopsy only and not adequate in terms of size for analysis of NIS expression. It was not felt ethical, generally, to subject patients to additional biopsies for the purpose of the study, and therefore original tumour samples were analysed rather than metastatic samples.

Of note, one patient (patient 14) demonstrated uptake scintigraphically, but the operative sample did not stain positively for NIS. This may have been because the sample had degenerated, although this case was only stored for two years prior to analysis.

11.5 – Future Work

The polyclonal antibody produced reliable staining, but RNA analysis of paraffin embedded tissue for expression of NIS was not reliable. The RNA longevity/degradation that has been discussed may have been important here. An experiment could be performed on paraffin fixed samples analysed at 0 hours, 24 hours, one week and one month after biopsy to assess copy number of NIS and GAPDH by Taqman analysis. This could be correlated with NIS positivity on IHC.

Whilst uptake was demonstrated in 57% of cases with positive IHC, there is scope to improve upon this. Akin to the situation with thyroid cancer and TSH stimulation by withdrawal of Thyroxine or use of recombinant TSH, which leads to improved uptake on thyroid scans, there may be ways to maximise Tc^{99m} Pertechnetate uptake in breast cancer patients. It has been demonstrated in the ER positive breast cancer cell line MCF-7 that all-trans Retinoic Acid (ATRA) could stimulate iodide uptake up to 9.4 times baseline levels[119]. Retinoids are known to be involved in cell differentiation[120], and there is

evidence for their effect on thyroid NIS expression. Encouraging results have been seen using ATRA in dedifferentiated thyroid cancers[121]. It has also been demonstrated that dexamethasone potentiates the effects of ATRA[122][123].

There is some evidence that ATRA induction of NIS expression may be limited to ER positive cells only[119]. It was postulated by these authors that ER positivity may lead to increased levels of Retinoic Acid Receptor (RAR) in the presence of 17-β-estradiol (E2), which may provide cellular conditions favorable for NIS expression. It is interesting to note that in the current study 50 % of patients who expressed NIS by IHC, were also seen to have ER positive tumours by IHC.

A novel ERE (oestrogen responsive element) has been identified in the NIS gene promoter. It has been shown by these authors that ER negative cell lines can be induced to express ER, and thereafter demonstrate ATRA induction of NIS expression[124]. In summary, future experiments could look at improving NIS expression and hence uptake in breast cancer patients using agents such as ATRA, or dexamethasone.

A further step, may be to look at the use of radio- isotopes with more potent cell kill effect such as Astatine (^{211}At). This is a radionuclide with many similar biological qualities to iodide, which decays by emission of high linear energy transfer alpha particles with short tissue range (60 μm) and greater cytotoxicity, compared to β-particles derived from the decay of ^{131}I. Carlin demonstrated ^{211}At distribution similar to that of ^{131}I in a NIS cell line[125], and Brown showed similar distributions in murine xenograft models of thyroid carcinoma[126]. However, concerns over normal tissue uptake, particularly in lung and spleen, have prevented clinical trials of ^{211}At, therefore minimisation of normal tissue uptake of astatine is now a major priority in the development this radionuclide. Carlin has suggested the development of cultured cell models to allow the study of the molecular mechanisms involved in astatine uptake.

A further recent study has demonstrated acceptable normal tissue effects in prostate cancer mouse models treated with astatine, but suggested due to short path length, this therapy

may be best reserved for treatment of small tumours or micrometastases only[127]. However, the short half-life of ^{211}At at 7.2 hours, provides difficulties in terms of production for a nuclear medicine department.

Other investigators have looked at the radioisotope $^{188}ReO_4^-$. For maximal radiobiological effect of a radioisotope and thus increased dose to tumour, biological $T_{1/2}$ should match the radiological $T_{1/2}$ of the isotope administered (in the case of ^{131}I this is eight days). $^{188}ReO_4^-$ (perrhenate), a beta-emitting chemical analogue of technetium, with similar characteristics is concentrated in the thyroid and stomach by endogenous NIS[128]. A report[129] of the biodistribution of perrhenate (radiological $T_{1/2}$ = 16.7 hours) in mouse mammary tumours expressing NIS, estimated an increase in tumor dose compared with ^{125}I, due in part to the comparatively shorter radiological $T_{1/2}$. Perrhenate is an attractive radioisotope, as it can be conveniently used on site in nuclear medicine departments, due to the long half life of its parent compound (69 days) and it has higher energy beta particles than ^{131}I (0.764 MeV), leading to a greater range than ^{131}I. Its gamma photon emissions are easier to shield than those of ^{131}I, and produce good quality images.

Improved retention of radio-isotope may be another potential target. This has been examined by a number of investigators and one method is coupling NIS gene transfer with Thyroid peroxidase (TPO) gene transfer as mentioned in section 4.5. TPO catalyses the organification of iodide i.e., its conversion from inorganic to organic form, allowing retention in the thyroid gland for several days. Boland postulated that the organification process in which TPO is involved could cause longer radioisotope retention time and significantly higher radiation dose to be delivered to tumour, although this has proved difficult to achieve in cervix cell lines[90]. However, Huang showed that the transfection of non-small cell lung cancer (NSCLC) cells with both NIS and TPO genes did lead to increased radioiodide uptake and retention, as well as to enhanced tumour cell kill[91]. A future direction could be to transfect NIS and TPO into breast cancer cell lines.

As described in section 11.4, PI3K may be a future potential target for manipulation of improved radioisotope uptake in NIS positive breast cancers.

The next logical step in development of the clinical use of NIS expression in breast cancer would be to run a further clinical study, where patients are screened by IHC analysis of NIS expression in breast tumour samples, and those with a Histoscore above 150 would proceed to a Tc^{99m} Pertechnetate scan, using potassium iodate blocking, in an attempt to avoid the temporal effects seen with perchlorate. It may also be worth examining the use of ^{123}I as an imaging agent, and investigating administering perchlorate and potassium iodate as blocking agents to the same patient at different time points.

A therapy dose of ^{131}I could be administered to those patients with positive uptake of Tc^{99m} Pertechnetate. Tc^{99m} Pertechnetate is not a suitable therapy agent as it has too short a half life and low energy gamma emissions. It would also be interesting to perform a dosimetric study of ^{131}I to review whether treatment doses are likely to be achieved in vivo.

Finally, it would be interesting to examine the uptake seen in primary breast cancers, and examine IHC from relatively fresh tissue, to see if yield would be higher. This early stage of disease may be a more appropriate clinical scenario for NIS therapy, before NIS expression may have been altered due to passage of time and therapeutic interventions. Recent data have been presented at ASCO 2008 which suggest early intervention with bisphosphonates, may prevent recurrence of breast cancer in patients at high risk of relapse following primary surgery[130].

Section 12 – References

1) www.isdscotland.org

2) Stiller CA. Thyroid cancer following Chernobyl. Eur J Cancer 2001; 37(8): 945-7.

3) Ron E, Lubin JH, Shore RE, et al. Thyroid cancer after exposure to external radiation: a pooled analysis of seven studies. Radiat Res 1995; 141(3): 259-77.

4) Suarez H, Daya-Grosjean L, Varlet I, Sarasin A. Susceptibility of Xeroderma pigmentosum cells to transformation with oncogenes. Biochimie 1988; 70(7): 969-73.

5) Tallini G. Molecular pathobiology of thyroid neoplasms. Endocr Pathol 2002; 13(4): 271–288.

6) Kondo T, Ezzat S, Asa SL. Pathogenetic mechanisms in thyroid follicular-cell neoplasia. Nat Rev Cancer 2006; 6:292–306.

7) Ohmori M, Endo T, Harii N, Onaya T. A novel thyroid transcription factor is essential for thyrotropin-induced up-regulation of Na+/I- symporter gene expression. Mol Endocrinol 1998; 12(5): 727-36.

8) Riedel C, Dohan O, De la Vieja A, Ginter CS, Carrasco N. Journey of the iodide transporter NIS: from its molecular identification to its clinical role in cancer. Trends Biochem Sci 2001; 26(8): 490-6.

9) Scott DA, Wang R, Kreman TM, Sheffield VC, Karniski LP. The Pendred syndrome gene encodes a chloride-iodide transport protein. Nat Genet 1999; 21(4): 440-3.

10) NCCN Thyroid Carcinoma Guidelines 2007, www.nccn.org.

11) Schlumberger M, Pacini F, Wiersinga WM, et al. Follow-up and management of differentiated thyroid carcinoma: a European perspective in clinical practice. Eur J Endocrinol 2004; 151(5): 539-48.

12) Hoefnagel CA, Clarke SE, Fischer M, et al. Radionuclide therapy practice and facilities in Europe. EANM Radionuclide Therapy Committee. Eur J Nucl Med 1999; 26(3): 277-82.

13) Mazzaferri EL, Jhiang SM. Long-term impact of initial surgical and medical therapy on papillary and follicular thyroid cancer. Am J Med 1994; 97(5): 418-28.

14) Mazzaferri E, 2001, Kloos RT. Clinical review 128: Current approaches to primary therapy for papillary and follicular thyroid cancer. J Clin Endocrinol Metab 2001; 86(4): 1447-63.

15) Goldman JM, Line BR, Aamodt RL, Robbins J. Influence of triiodothyronine withdrawal time on ^{131}I uptake post-thyroidectomy for thyroid cancer. J Clin Endocrinol Metab 1980; 50: 734-9.

16) Edmonds CJ, Hayes S, Kermode JC, Thompson BD. Measurement of serum TSH and thyroid hormones in the management and treatment of thyroid carcinoma with radioiodine. Br J Radiol 1977; 50: 799.

17) Jeevanram RK, Shah DH, Sharma SM, Ganatra RD. Influence of initial large dose on subsequent uptake of therapeutic radioiodine in thyroid cancer patients. International Journal of Radiation Applications & Instrumentation - Part B, Nucl Med Biol 1986; 13(3): 277-9.

18) Medvedec M. Thyroid stunning in vivo and in vitro. Nucl Med Commun 2005; 26(8): 731-5.

19) Ferlay F, Autier P, Boniol M, Heanue M, Colombet M, Boyle P. Estimates of the cancer incidence and mortality in Europe in 2006. Ann Oncol 2007; 18(3): 581-92.

20) Berger MS, Locher GW, Saurer S, et al. Correlation of c-erbB-2 gene amplification and protein expression in human breast carcinoma with nodal status and nuclear grading. Cancer Res 1988; 48:1238- 43.

21) Slamon DJ, Human breast cancer: correlation of relapse and survival with amplification of the HER-2/neu oncogene. Science 1987; 235: 177-182.

22) Varley JM, Swallow JE, Brammar WJ, et al. Alterations to either c-erbB-2 (neu) or c-myc proto-oncogenes in breast carcinomas correlate with poor short- term prognosis. Oncogene 1987; 1: 423-430.

23) Elwood JM, Godolphin W. Oestrogen receptors in breast tumours: Associations with age, menopausal status and epidemiological and clinical features in 735 patients. Br J Cancer 1980; 42: 635-44.

24) Knight WA. Hormonal receptors in primary and advanced breast cancer. Clin Endocrinol Metab 1980; 9: 361-68.

25) Lakhani SR. Molecular genetics of solid tumours: translating research into clinical practice. What we could do now: breast cancer. Mol Pathol 2001; 54: 281-284.

26) Wilcken N, Hornbuckle J, Ghersi D. Chemotherapy alone versus endocrine therapy alone for metastatic breast cancer. Cochrane database of systematic reviews (2) CD002747, 2003.

27) Hortobagyi GN, Piccart-Gebhart MJ. Current management of advanced breast cancer. Semin Oncol 1996; 23(5 Suppl 11):1-5.

28) Fossatti R, Confaloniere C, Torri V, et al. Cytotoxic and hormonal treatment for metastatic breast cancer: a systematic review of published randomised trials involving 31, 510 women. J Clin Oncol 1998; 16(10): 3439-60.

29) Lister–Sharp D, Mcdonagh MS, Khan KS, Kleijnen J. A rapid and systematic review of the effectiveness and cost-effectiveness of the taxanes used in the treatment of advanced breast and ovarian cancer. Health Technol Assess 2000; 4(17): 1-113

30) O'Shaugnessy J, Miles D, Vukelja S, et al. Superior survival with capecitabine plus docetaxel chemotherapy in anthracycline-pre treated patients with advanced breast cancer: phase III trial results. J Clin Oncol, 2002; 20: 2812-23.

31) Jones S, Winer E, Vogel C, et al. Randomised comparison of vinorelbine and melphalan in anthracycline-refractory advanced breast cancer. J Clin Oncol 1995; 13: 2567-74.

32) Cancer Care Ontario. Breast Cancer Disease Site Group. Use of bisphosphonates in women with breast cancer. Toronto; Cancer Care Ontario: 2004. Available from

URL: http//www.cancercare.on.ca/pdf/pebc1-11f.pdf/

33) Pavlakis N, Stockler M. Bisphosphonates for breast cancer. In the Cochrane library, Issue 2, 2002. Oxford: Update Software.2002.

34) Bloomfield DJ. Should bisphosphonates be part of the standard therapy of patients with multiple myeloma or bone metastases from other cancers? An evidence based review. J Clin Oncol 1998; 16(3):1218-25.

35) Wu JS-Y, Wong R, Johnston M, Bezjak A, Whelan T. Meta-analysis of dose fractionation radiotherapy trials for the palliation of painful bone metastases. Int J Radiat Biol 2003; 55: 594-605.

36) Druker BJ. Imatinib as a paradigm of targeted therapies. J Clin Oncol 2003; 21(23 Suppl): 239s-245s.

37) Kantarjian H, Sawyers C, Hochhaus A, et al: Hematologic and cytogenetic responses to imatinib mesylate in chronic myelogenous leukemia. N Engl J Med 346: 645–652, 2002.

38) Klijn JG, Blamey RW, Boccardo F, Tominaga T, Duchateau L, Sylvester R; Combined Hormone Agents Trialists' Group and the European Organization for Research and Treatment of Cancer. Combined tamoxifen and luteinising hormone-releasing hormone (LHRH) agonist versus LHRH agonist alone in premenopausal advanced breast cancer: a meta-analysis of 4 randomised trials. J Clin Oncol 2001; 19(2): 343-53.

39) Early Breast Cancer Trialists' Collaborative Group. Tamoxifen for early breast cancer: an overview of the randomised trials. Lancet, 1998; 351(9114): 1451-67.

40) Goss PE, Ingle JN, Martino S, et al. Randomised trial of letrozole following tamoxifen as extended adjuvant therapy in receptor-positive breast cancer: updated findings from NCIC CTG MA.17. J Natl Cancer Inst 2005; 97(17): 1262-71.

41) Osborne C, Wilson P, Tripathy D. Oncogenes and tumor suppressor genes in breast cancer: potential diagnostic and therapeutic applications. Oncologist 2004; 9(4):

361-77.

42) Witton CJ, Reeves JR, Going JJ, Cooke TG, Bartlett JM. Expression of the HER1-4 family of receptor tyrosine kinases in breast cancer. J Pathol 2003; 200(3): 290-7.

43) Mita MM, Mita A, Rowinsky EK. The molecular target of rapamycin (mTOR) as a therapeutic target against cancer. Cancer Biol Ther 2003; 2(4 Suppl 1): S169-77.

44) Chan S, Scheulen ME, Johnson S et al. Phase 2 study of two dose levels of CCI-779 in locally advanced or metastatic breast cancer failing prior anthracycline and/ or taxane. Proc Am Soc Clin Oncol 2003; 22: 193.

45) Nass SJ. Dickson RB. Defining a role for c-Myc in breast tumorigenesis. Breast Cancer Res Treat 1997; 44(1): 1-22.

46) Varley JM, Brammar WJ, Walker RA. Oncogene organisation and expression: prediction in breast cancer. Horm Res 1989; 32 Suppl 1:250-3.

47) Carroll JS, Swarbrick A, Musgrove EA, Sutherland R. Mechanisms of growth arrest by c-myc antisense oligonucleotides in MCF-7 breast cancer cells: implications for the antiproliferative effects of antiestrogens. Cancer Res 2002; 2: 3126–3131.

48) Vogel LC, Cobleigh MA, Tripathy D, et al. Efficacy and safety of Trastuzumab as a single agent in first-line treatment of HER-2-overexpressing metastatic breast cancer. J Clin Oncol 2002; 20(3): 719-26.

49) Slamon DJ, Leyland-Jones B, Shak S, et al. Use of chemotherapy plus a monoclonal antibody against HER2 for metastatic breast cancer that overexpresses HER2. New Engl J Med 2001; 344(11): 783-92.

50) Piccart- Gebhart MJ, Procter M, Leyland-Jones B, et al. Trastuzumab after adjuvant chemotherapy in HER2-positive breast cancer. N Engl J Med 2005; 353: 1659-72.

51) Ljunggren J-G, Torring O, Wallin G, et al. Quality of life aspects and costs

in treatment of Graves' hyperthyroidism with anti thyroid drugs, surgery, or radioiodine: results from a prospective, randomized study. Thyroid 1998; 8: 653-659.

52) Chatal J-F, Hoefnagel CA. Radionuclide therapy. Lancet 1999; 354: 931-5.

53) Heuft-Dorenbosch LLJ, de Vet HCW, van der Linden S. Yttrium radiosynoviorthesis in the treatment of knee arthritis in rheumatoid arthritis: a systematic review. Ann Rheum Dis 2000; 59: 583-586.

54) Palmedo H, Rockstroh JK, Bangard M, et al. Painful Multifocal arthritis: Therapy with Rhenium 186 Hydroxyethylidenediphosphate (186 ^{Re} HEDP) after failed treatment with medication-Initial results of a prospective study. Radiology 2001; 221: 256-260.

55) Streiff MB, Smith B, Spivak JL. The diagnosis and management of polycythemia vera in the era since the Polycythemia Vera Study Group: a survey of American Society of Hematology members' practice patterns. Blood 2002; 99(4): 1144-9.

56) Pandit-Taskar N, Batraki M, Divgi CR. Radiopharmaceutical therapy for palliation of bone pain from osseous metastases. J Nucl Med 2004; 45(8): 1358-1366.

57) Robinson RG, Preston DF, Schiefelbein M, Baxter KG. Strontium 89 therapy for the palliation of pain due to osseous metastases. JAMA 1995; 274(5): 420-4.

58) Sciuto R, Festa A, Pasqualoni R, et al. Metastatic bone pain palliation with 89-Sr and 186-Re-HEDP in breast cancer patients. Breast Cancer Res Treat 2001; 66: 101-9.

59) De Clerk JM, van hel Schip AD, Zonnenberg BA, et al. Phase 1 study of rhenium-186-HEDP in patients with bone metastases originating from breast cancer. J Nucl Med 1996; 37: 244-249.

60) Maxon HR 3rd, Schroder LE, Washburn LC, et al. Rhenium-188(Sn)HEDP for treatment of osseous metastases. J Nucl Med 1998; 39: 659-663.

61) Blitzer PH. Re-analysis of the RTOG study of the palliation of symptomatic

osseous metastasis. Cancer 1985; 55: 1468-72.

62) Friedland J. Local and systemic radiation for palliation of metastatic disease. Urol Clin North Am 1999; 26(2): 391-402.

63) Hoskin, PJ. Radiotherapy for bone pain. Pain 1995; 63:137-139.

64) McQuay HJ. Collins SL. Carroll D. Moore RA. Radiotherapy for the palliation of painful bone metastases. Cochrane Database of Systematic Reviews 2000; (2):CD001793.

65) Mcewan AJ, Amyotte GA, McGowan DG, et al. A retrospective analysis of the cost effectiveness of treatment with Metastron in patients with prostate cancer metastatic to bone. Eur Urol 1994; 26(Suppl 1): 26-31.

66) Malmberg I, Persson U, Ask A, Tenvall J, Abrahamsson P-E. Painful bone metastases in hormone-refractory prostate cancer: economic costs of strontium-89 and/or external radiotherapy. Urology 1997; 50: 747-753.

67) Burnet NG, Williams G, and Howard N. Phosphorus-32 for intractable bony pain from carcinoma of the prostate. Clin Oncol 1990; 2: 220-223.

68) Carrasco N. Iodide transport in the thyroid gland. Biochim Biophys Acta 1993; 1154:65–82.

69) De la Vieja A, Dohan O, Levy O, Carrasco N. Molecular analysis of the sodium/ iodide symporter: impact on thyroid and extrathyroid pathophysiology. Physiol Rev 2000; 80:1083–1105.

70) Dohan O. Carrasco N. Advances in Na (+)/I(-) symporter (NIS) research in the thyroid and beyond. Mol Cell Endocrinol 2003; 213(1): 59-70.

71) Dai G, Levy O, Carrasco N. Cloning and characterization of the thyroid iodide transporter. Nature 1996; 379: 458–460.

72) Smanik PA, Liu Q, Furminger TL, et al. Cloning of the human sodium iodide symporter. Biochem Biophys Res Commun 1996; 226:339–345.

73) Smanik PA, Ryu KY, Theil KS, Mazzaferri EL, Jhiang SM. Expression, exon-

intron organization, and chromosome mapping of the human sodium iodide symporter. Endocrinology 1997; 138: 3555–3558.

74) Levy O, Carrasco N. Structure and function of the thyroid iodide transporter and its implications for thyroid disease. Curr Opin Endocrinol Diabetes Obes 1997; 4: 364–370.

75) Tazebay UH, Wapnir IL, Levy O, et al. The mammary gland iodide transporter is expressed during lactation and in breast cancer. Nat Med 2000; 6:871–878.

76) Wapnir IL, van de Rijn M, Nowels K et al. Immunohistochemical profile of the sodium/iodide symporter in thyroid, breast and other carcinomas using high density tissue microarrays and conventional sections. J Clin Endocrinol Metab 2003; 88: 1880-8.

77) Moon DH, Lee SJ, Park KY, et al. Correlation between 99mTc-pertechnetate uptakes and expression of human sodium iodide symporter gene in breast tumour tissues. Nucl Med Biol 2001; 28: 829-834.

78) Min J-J, Chung J-K, Lee YJ, et al. Relationship between expression of the sodium/ iodide symporter and 131I uptake in recurrent lesions of differentiated thyroid carcinoma. Eur J Nucl Med 2001; 28: 639-645.

79) Wapnir I, Goris M, Yudd A, et al. The Na/I symporter mediates iodide uptake in breast cancer metastases and can be selectively down-regulated in the thyroid. Clin Cancer Res 2004; 10: 4294-4302.

80) Arturi F, Ferretti E, Presta I, et al. Regulation of iodide uptake and sodium/ iodide symporter expression in the MCF-7 human breast cancer cell line. J Clin Endocrinol Metab 2005; 90(4): 2321-2326.

81) Kogai T, Schultz JJ, Johnson LS, Huang M, Brent GA. Retinoic acid induces sodium/iodide symporter gene expression and radioiodide uptake in the MCF-7 breast cancer cell line. Proc Natl Acad Sci USA 2000; 97(15): 8519-24.

82) Helguera O A, Anguiano B, Delgado G, Aceves C. Uptake and antiproliferative

effect of molecular iodine in the MCF-7 breast cancer cell line. Endocr Relat Cancer 2006; 13: 1147-1158.

83) Knostman K, McCubrey J, Morrison C, Zhang Z, Capen C, Jhiang S. PI3K activation is associated with intracellular sodium/iodide symporter protein expression in breast cancer. BMC Cancer 2007;7: 137-147.

84) Shimura H, Haraguchi K, Myazaki A, Endo T, Onaya T. Iodide uptake and experimental 131 I therapy in transplanted undifferentiated thyroid cancer cells expressing the Na^+/I^- symporter gene. Endocrinology 1997; 138:4493–4496.

85) Mandell RB, Mandell LZ, Link Jr CJ. Radioisotope concentrator gene therapy using the sodium/iodide symporter gene. Cancer Res 1999; 59:661–668.

86) Kang JH, Chung J-K, Lee YJ et al. Establishment of a human hepatocellular carcinoma cell line highly expressing sodium iodide symporter for radionuclide gene therapy. J Nucl Med 2004; 45: 1571-1576.

87) Haberkorn U, Kinscherf R, Kissel M et al. Enhanced iodide transport after transfer of the human sodium iodide symporter gene is associated with lack of retention and low absorbed dose. Gene Ther 2003; 10: 774-780.

88) Boland A, Ricard M, Opolon P, et al. Adenovirus-mediated transfer of the thyroid sodium/iodide symporter gene into tumours for targeted radiotherapy. Cancer Res 2000; 60: 3484-3492.

89) Nakamoto Y, Saga T, Misaki T, et al. Establishment and characterisation of a breast cancer cell line expressing Na/I symporters for radioiodide concentrator gene therapy. J Nucl Med 2000; 41: 1898- 1904.

90) Boland A, Magnon C, Filetti S, et al. Transposition of the thyroid iodide uptake and organification system in nonthyroid tumor cells by adenoviral vector-mediated gene transfers. Thyroid 2002; 12: 19–26.

91) Huang M, Batra RK, Kogai T, et al. Ectopic expression of the thyroperoxidase gene augments radioiodide uptake and retention mediated by the sodium iodide

symporter in non-small cell lung cancer. Cancer Gene Ther 2001; 8: 612–618.

92) Spitzweg C, O'Connor MK, Bergert ER, Tindall DJ, Young YF, Morris JC. Treatment of prostate cancer by radioiodine therapy after tissue-specific expression of the sodium-iodide symporter. Cancer Res 2000; 60: 6526-6530.

93) Dingli D, Russell SJ, Morris JC. In vivo imaging and tumour therapy with the sodium iodide symporter. J Cell Biochem 2003; 90: 1079-1086.

94) Carlin S, Cunningham SH, Boyd M, McCluskey AM, Mairs RJ. Experimental targeted radioiodide therapy following transfection of the sodium iodide symporter gene: effect on clonogenicity in both two- and three-dimensional models. Cancer Gene Ther 2000; 7: 1529–1536.

95) Warburg O, Christian W. Isolation and crystallisation of enolase. Biochem 1942; 310: 384-421.

96) Upadhyay G, Singh R, Agarwal G, et al. Functional expression of sodium iodide symporter (NIS) in human breast cancer tissue. Breast Cancer Res Treat 2003; 77: 157-165.

97) WHO guidelines for Iodine prophylaxis following Nuclear Accidents, update 1999.

98) "Notes for guidance on the clinical administration of Radiopharmaceuticals and use of sealed radioactive sources". Administration of Radioactive Substances Advisory Committee, March 2006.

99) Benitez-Bribiesca L, Guevara R, Ruiz MT, Martinez G and Rodriguez-Cuevas S. A simplified Histoscore for the Estrogen receptor assay in breast cancer. Pathol Res Pract 1992; 188: 461-165.

100) Zlobec I, Steele R, Michel R, Compton C, Lugli A, and Jass J. Scoring of p53, VEGF, Bcl-2 and APAF-1 immunohistochemistry and interobserver reliability in colorectal cancer. Modern Path 2006; 19: 1236–1242.

101) Masuda N, Ohnishi T, Kawamoto S, et al. Analysis of chemical modification of RNA from formalin-fixed samples and optimization of molecular biology

applications for such samples. Nucleic Acids Res 1999; 27: 4436-4443.

102) Mies C. Molecular biological analysis of paraffin-embedded tissues. Human Pathology 1994; 25(6): 555-60.

103) Korbler T, Grskovic M, Dominis M, Antica M. A simple method for RNA isolation from formalin-fixed and paraffin-embedded lymphatic tissues. Exp Mol Pathol 2003: 74(3): 336-40.

104) Vincek V, Nassiri M, Block N, Welsh C, Nadji M, Morales AR. Methodology for preservation of high molecular-weight RNA in paraffin-embedded tissue: application for laser-capture microdissection. Diagn Mol Pathol 2005; 14(3): 127-33.

105) Penland SK, Temitope OK, Torrice C, et al. RNA expression analysis of formalin-fixed paraffin-embedded tumours. Lab Invest 2007; 87: 383- 391.

106) http://info.cancerresearchuk.org/cancerstats/types/breast/mortality

107) Castro MR, Bergert ER, Beito TG, et al. Monoclonal antibodies against the human sodium iodide symporter: utility for immunocytochemistry of thyroid cancer. J Endocrinol 1999; 163: 495-504.

108) Micke P, Ohshima M, Tahmasebpoor S, et al. Biobanking of fresh frozen tissue: RNA is stable in nonfixed surgical specimens. Lab Invest 2006; 86: 202–211.

109) Cronin M, Pho M, Dutta D, et al. Measurement of gene expression in archival paraffin-embedded tissues: development and performance of a 92-gene reverse transcriptase-polymerase chain reaction assay. Am J Pathol 2004; 164: 35-42.

110) Mizuno, T, Nagamura H, Iwamoto KS, et al., RNA from decades-old archival tissue blocks for retrospective studies. Diagn Mol Pathol 1998; 7(4): 202-208.

111) Godfrey TE, Kim S-H, Chavira M, et al. Quantitative mRNA expression analysis from formalin-fixed, paraffin-embedded tissues using 5‘ nuclease quantitative reverse transcription-polymerase chain reaction. J Mol Diagn 2000; 2(2): 84-91.

112) Caponigro G, Muhlrad D, and Parker R. A small segment of the MATa1 transcript

promotes mRNA decay in Saccharomyces cerevisiae: a stimulatory role for rare codons. Mol Cell Biol 1993; 13: 5141-5148.

113) Sachs AB. Messenger RNA degradation in eukaryotes. Cell 1993; 74: 413-421.

114) Kogai T, Curcio F, Hyman S, Cornford EM, Brent GA, Hershman JM. Induction of follicle formation in long-term cultured normal human thyroid cells treated with thyrotrophin stimulates iodide uptake but not sodium/iodide symporter messenger RNA and protein expression. J Endocrinol 2000; 167: 125-135.

115) Saito T, Endo T, Kawagachi A et al. Increased expression of the sodium/iodide symporter in papillary thyroid carcinomas. J Clin Invest 1998; 101: 1296-1300.

116) Arturi F, Russo D, Giuffrida D, Schlumberger M, Filetti S. Sodium-iodide symporter (NIS) gene expression in lymph-node metastases of papillary thyroid carcinomas. Eur J Endocrinol 2000;143: 623-627.

117) Dohan O, Baloch Z, Banrevi Z, Livolsi V, Carrasco N. Predominant intracellular overexpression of the Na+/I symporter (NIS) in a large sampling of thyroid cancer cases. J Clin Endocrinol Metab 2001; 86: 2697-2700.

118) Park HJ, Kim JY, Park KY, Gong G, Hong SJ, Ahn IM. Expressions of human sodium iodide symporter mRNA in primary and metastatic papillary thyroid carcinomas. Thyroid 2000; 10: 211- 217.

119) Kogai T, Schultz J, Johnson L, Huang M, Brent G. Retinoic acid induces sodium/ iodide symporter gene expression and radioiodide uptake in the MCF-7 breast cancer cell line. Proc Natl Acad Sci USA 2000; 97(15): 8519- 8524.

120) Evans TR, Kaye SB. Retinoids, present role and future potential. Br J Cancer, 1999; 80: 1-8.

121) Simon D, Korber C, Krausch M et al. Clinical impact of retinoids in redifferentiation therapy of advanced thyroid cancer: final results of a pilot study. Eur J Nucl Med Mol Imaging 2002; 29: 775–782.

122) Kogai T, Kanamoto Y, Li AI et al. Differential regulation of sodium/iodide

syporter gene expression by nuclear receptor ligands in MCF-7 breast cancer cells. Endocrinology 2005; 146: 3059- 3069.

123) Unterholzner S, Willhauck MJ, Cengic N, et al. Dexamethasone stimulation of Retinoic acid induced sodium iodide symporter expression and cytotoxicity of 131-I in breast cancer cells. J Clin Oncol Metab 2006; 91(1): 69-78.

124) Alotaibi H, Yaman E C, Demirpence E, Tazebay U. Unliganded oestrogen receptor activates transcription of the mammary gland Na/I symporter gene. Biochem Biophys Res Commun 2006; 345(4): 1487-1496**.**

125) Carlin S, Mairs R, Welsh P, Zalutsky M. Sodium-iodide symporter (NIS) mediated accumulation of ^{211}At in NIS-transfected human cancer cells. Nucl Med Biol 2002; 29(7): 729-739.

126) Brown I, Carpenter R. Endogenous ^{211}At α-particle radiotherapy for undifferentiated thyroid cancer. Acta Radiologica 1991: 376: 174–175.

127) Willhauck MJ, Samani B-R, Wolf I et al. The potential of ^{211}Astatine for NIS-mediated radionuclide therapy in prostate cancer. Eur J Nucl Mod Imaging 2008; 35: 1272-1281.

128) Lin W, Hsieh J, Tsai S, Yen T, Wang S, Knapp F. A comprehensive study on the blockage of thyroid and gastric uptakes of 188Re-perrhenate in endovascular irradiation using liquid-filled balloon to prevent restenosis. Nucl. Med. Biol 2000; 27**:** 83–87.

129) Dadachova E, Bouzahzah B, Zuckier L, Pestell R. Rhenium-188 as an alternative to Iodine-131 for treatment of breast tumors expressing the sodium/iodide symporter (NIS). Nucl. Med. Biol 2002; 29**:** 13–18.

130) www.**asco**.org/

Section 13 – Tables

Table One – Nanodrop results

Sample	Nanodrop purity A260/280	Nanodrop concentration (ng/ul)
1	1.92	53.34
2	1.78	19.44
3	Not done	Not done
4	1.99	145.55
5	2.02	88.8
6	2.06	168.4
7	1.98	60.1
8	2.01	321.36
10	2.0	680.8
11	0.8	9.55
12	1.99	468
13	Not done	Not done
14	1.93	390.6
15a4- nodal	1.98	31.55
15a7- lymphatics	1.98	201.59
16	1.88	1046
17	1.9	1.9
18	1.96	56.64
19	1.98	444.27
20	1.94	125.24
21	2.06	278.9

Table 2: RNA extraction techniques used

Technique	Tissue used	Deparaffination	Digestion	Purification	RT-PCR
Quiagen Minikit	FFPE thyroid 1 year old	Xylene and 100,70,50 and 20% ethanol.	Buffer RLT	Spin column	2 step kit. NIS 137bp, GAP 432bp primers.
ZYMO	As above	As above	Buffer and prt K 4 hours 55°C	Spin column	As above
Trizol	FFPE thyroid, fresh breast, thyroid and NIS cell pellet	Xylene and 100% ethanol. Vaccum dessicate dry 5 mins	Tris HCL, 10% SDS and prt K o/n at 37°C in water bath	Trizol, chloroform and isopropanol	1 step kit. Used PBG 65 and 265bp primers.
Purescript	As above	As above, but air dried.	Prt K and glycogen o/n at 55°C in rotary oven	Prt-DNA precipitation solution, isopropanol and RNA hydration solution.	2 step kit. Used PBG 65bp primers.
Ambion	FFPE breast	Xylene and 100% ethanol	Proteinase and Buffer	Filter cartridge	2 step kit and Taqman

Table 3: IHC methods used by other groups

Group	Antibody	Tissue used	Dilution	Antigen retrieval	Peroxidase blocking	Ab incu-bation
Wapnir (*76*)	Rabbit polyclonal antibody against C terminus peptide of human NIS	Human breast cancer, primary or meta-stases.	1 in 10,000	10% citrate buffer 45 minutes	3% hydrogen peroxide/ methanol 15 minutes pre Antigen retrieval	15 mins
Castro (*103*)	Mouse monoclonal antibody against C terminus of human NIS	Human normal thyroid gland, Graves disease, and differ-entiated thyroid cancers	1 in 1500	10% citrate 30 minutes	As above 10 minutes	1 hour
Jhiang (personal comm-unication)	Rabbit polyclonal against human NIS	Human breast	1 in 500 to 1000	Citric acid 30 minutes	As above	1 hour
Tazebay (*75*)	Rat polyclonal antibody against C terminus of human NIS and, rat monoclonal antibody against C terminus of human NIS	Human normal breast and breast cancer	1 in 750 to 100	10% citrate buffer	DAKO system	15 minutes
Spitzweg (92)	Mouse monoclonal antibody against C terminus of human NIS	Mouse prostate cancer	1 in 1600	Citrate 30 mins	Not specified	90 minutes

Table 4: Immunohistochemistry results

Patient	Histoscore	Intensity (0-3)	% Cells Staining	Cytoplasmic or Membranous Staining	Overall positive or negative result
1	200	2+	100%	Cyto only	positive
2	100	1+	100%	Cyto only	negative
3	160	2+	80%	Cyto only	positive
4	160	2+	80%	Cyto only	positive
5	160	2+	80%	Cyto only	positive
6	300	3+	100%	Cyto only	positive
7	160	2+	80%	Cyto/mem	positive
8	80	1+	80%	Cyto only	negative
9	Sample not available				
10	160	2+	80%	Cyto/ patchy mem staining	positive
11	100	1+	100%	Cyto only	negative
12	80	1+	80%	Cyto only	negative
13	NA – poor sample				
14	20	1+	<20%	Cyto only	negative
15 a4-nodal tissue	200	2+	100%	Strong mem and cyto	positive
15 a7-lymphatics	300	3+	100%	Strong mem and cyto	positive
16	180	2+	90%	Cyto only	positive
17-nodal tissue	80	1+	80%	Cyto only	negative
18	160	2+	80%	Cyto only	positive
19	100	1+	100%	Some mem staining and 100% cyto	positive
20	160	2+	80%	Cyto only	positive
21	80	1+	80%	Cyto only	negative
22	160	2+	80%	Cyto only	positive
23	300	3+	100%	Cyto only	positive
24	Sample not available				
X (not scanned)	160	2+	80%	Cyto only	positive

Table 5: Random breast samples immunostaining results

Patient number	Intensity staining (0-3)	% Cells staining	Histoscore	Cytoplasmic or membrane staining
1	1+	40	40	Cytoplasmic
2	2+	60	120	Cytoplasmic
3	1+	10	10	Cytoplasmic
4	1+	50	50	Cytoplasmic
5	1+	80	80	Cytoplasmic
6	0	0	0	Cytoplasmic
7	1+	70	70	Cytoplasmic
8	2+	10	20	Cytoplasmic
9	0	0	0	Cytoplasmic
10	1+	30	30	Cytoplasmic
11	0	0	0	Cytoplasmic

Table 6: details of sites of disease on conventional imaging

Patient number	Site of disease on conventional imaging	Visceral/ bone / soft tissue	Type of imaging/ assessment	Proximity to NIS scan	Differential uptake on pertechnetate scan?
1	Liver/lung/ bone/ axillary and mediastinal nodes	Visceral/ bone/ nodal	CT	1 month	No Uptake
2	Liver/bone/ovary	Visceral/ bone	CT	2 months	No Uptake
3	Liver/lung/ bone	Visceral/ bone	Bone scan, USS liver, MRI spine, cxr	3-4 months	Yes
4	Lung/Bone/ brachial plexus	Visceral/ bone/ nodal	CT	1 week	No Uptake
5	Lung/chest wall	Visceral/ soft tissue	CT and clinical assessment (CA)	CT 6 months, regular CA	No Uptake
6	Lung/bone	Visceral/ bone	CT and bone scan	7 months	Yes
7	Lung/chest wall	Visceral/ soft tissue	CT and CA	4 months, regular CA	No Uptake
8	Lung/ mediastinal nodes	Visceral/ nodal	CT	1 month	No Uptake
9	Liver/bone	Visceral/ bone	CT	1 month	No Uptake
10	Supraclavicular nodes	Nodal	CT	2 months	No
11	Bone	Bone	CT	1 month	No Uptake
12	Bone	Bone	CT and bone scan	1 month	No Uptake
13	Primary breast lesion/ axillary nodes	Breast and local nodes	CT and CA	2 months, regular CA	Yes
14	Lung/chest wall	Visceral/ soft tissue	CT	2 weeks	Yes
15	Pleural effusion, sphenoid and pelvic masses mediastinal and neck nodes.	Visceral/ nodal	CT	1 month	No Uptake
16	Liver/ lung/bone	Visceral/ bone	CT	1 month	Yes

Continued on next page

Table Six continued

Patient number	Site of disease on conventional imaging	Visceral/ bone / soft tissue	Type of imaging/ assessment	Proximity to NIS scan	Differential uptake on pertechnetate scan?
17	Neck and axillary nodes	Nodal	CT	2 weeks	No uptake
18	Liver/bone/para-aortic nodes/	Visceral/ bone / nodal	CT and bone scan	3-5 months	No Uptake
19	Chest wall	Soft tissue	CT	3 months	No
20	Liver/ lung/bone	Visceral/ bone	CT	3 months	Yes
21	Liver/ lung/ bone/axillary and mediastinal nodes	Visceral/ bone/ nodal	CT	1 month	No Uptake
22	Liver/ lung/bone/ neck and axillary nodes	Visceral/ bone/ nodal	MRI spine, CT and bone scan	3 months	Yes
23	Small bowel/ bone	Visceral/ bone	CT and MRI	1-7 months	Yes
24	Supraclavicular/ axillary nodes	Nodal	CT	3 months	Yes

Table 7: Taqman results

Pt number	GAP ct mean	GAP qty mean	NIS ct mean	NIS qty mean
1	33.547439	2.81E+05	0	0
2	37.995	1.22E+04	0	0
3	33.40664	144995.92	0	0
4	32.9165	251093	0	0
5	30.883781	641624.1	0	0
6	27.9985	8927596	0	0
7	32.499626	196727.25	0	0
8	30.229	1.40E+06	0	0
10	26.249401	1.36E+07	0	0
11	30.117	2.06E+06	0	0
12	24.603	4.67E+07	0	0
13	28.833942	2695088.2	0	0
14	31.737778	326226.8	0	0
15(nodal)	35.81555	307206.3	0	0
15(lymphatics)	32.168304	146451.14	0	0
16	37.988487	4714.8643	0	0
17	32.111298	252121.31	0	0
18	30.74	1.37E+06	0	0
19	39.719	7.17E+03	0	0
20	38.582405	3130.5415	0	0
21	26.88	1.12E+07	0	0
Positivecontrol 1 (Graves)	35.50981	26319.035	36.359074	81.607025
Positivecontrol 2 (NIS pellet)	24.92593	3.33E+07	33.474136	543.1411

Note: patient 9 ommitted.

Table 8: Effects of blocking agents

Patient number	Method of physiological blocking	Uptake evident
1	None	Minimal thyroid uptake
2	None	Thyroid uptake
3	None	Thyroid uptake
4	None	Thyroid uptake
5	None	Thyroid uptake
6	None	Thyroid uptake
7	None	Thyroid uptake
8	None	Thyroid uptake
9	100mg perchlorate	Thyroid blocking
10	100mg perchlorate	Thyroid blocking
11	200mg perchlorate	Thyroid blocking
12	200mg perchlorate	Thyroid blocking at 4 hours
13	200mg perchlorate	Thyroid blocking
14	300mg perchlorate	Thyroid blocking at 4 hours
15	300mg perchlorate	Thyroid blocking
16	300mg perchlorate	Thyroid blocking at 4 hours
17	300mg perchlorate	Thyroid blocking
18	None	Thyroid uptake
19	Potassium iodate	Thyroid blocking
20	Potassium iodate	Thyroid uptake
21	Potassium iodate	Minimal thyroid uptake
22	Potassium iodate	Thyroid blocking
23	300mg perchlorate	Thyroid blocking
24	Potassium iodate	Thyroid uptake

Table 9: Pathological status and uptake

Patient number	Sample analysed	ER status	PR status	Her 2 status	Grade	Nodal status	Nis positive on IHC?	Pertechnetate uptake?
1	Breast-ductal	Positive	Not available (NA)	1+	3	N+	Yes	No
2	Breast-ductal	Positive	NA	Negative	2	N-	No	No
3	Breast-ductal	Positive	NA	Negative	2	N-	Yes	Yes
4	Breast-ductal	Positive	Positive	Negative	NA	N+	Yes	No
5	Breast-ductal	Negative	NA	Negative	NA	N+	Yes	No
6	Breast-ductal	Negative	Negative	NA	3	N+	Yes	Yes
7	Breast-ductal	Negative	Negative	3+	3	N+	Yes	No
8	Breast-ductal	Weakly positive	Negative	NA	3	N+	No	No
9	Breast-ductal	Negative	NA	3+	NA	N+	NA	No
10	Breast-ductal	Negative	NA	NA	3	N+	Yes	Yes
11	Breast-ductal	Positive	NA	Negative	NA	N-	No	No
12	Breast-ductal	Negative	Negative	Negative	3	N+	No	No
13	Breast core	Weakly positive	Weakly positive	NA	NA	N-	Poor sample	Yes
14	Breast-ductal	Negative	Negative	NA	3	N-	No	Yes
15 a4	Nodal tissue	Negative	NA	NA	NA	N+	Yes	No
15 a7	lymphatics	Negative	NA	NA	NA	N+	Yes	No
16	Breast-ductal	NA	NA	Negative	NA	N-	Yes	Yes
17	Jugular node-ductal on original path	Negative	NA	3+	3	N-	No	No

Continued on next page

Table 9 continued

Patient number	Sample analysed	ER status	PR status	Her 2 status	Grade	Nodal status	Nis positive on IHC?	Pertechnetate uptake?
18	Breast-lobular	Positive	NA	0	2	N-	Yes	No
19	Breast-ductal	Positive	Weakly positive	0	NA	N+	Yes	Yes
20	Breast-lobular	NA	NA	NA	NA	N-	Yes	Yes
21	Breast-ductal	Positive	NA	Negative	1	N+	No	No
22	Breast-ductal	Positive	NA	3+	3	N+	Yes	Yes
23	Breast-lobular	Positive	Positive	Negative	2	N+	Yes	Yes
24	NA	Negative	Negative	Negative	3	N+	NA	Yes

Patient X not included, as no pathology details and not scanned.

Table 10: Type of current therapy

Therapy type	Number of patients
Chemotherapy	8
Bisphosphonate	7
Both	2
Nil	7

Section 14 – List of Figures

Figure One: Current NIS structure model. The model contains 13 putative transmembrane segments. Obtained from review : Dohan O, De la Vieja A, Paroder V et al. The sodium iodide symporter (NIS): characterisation, regulation and medical significance. Endocrine Reviews, 2003; 24(1): 48-77.

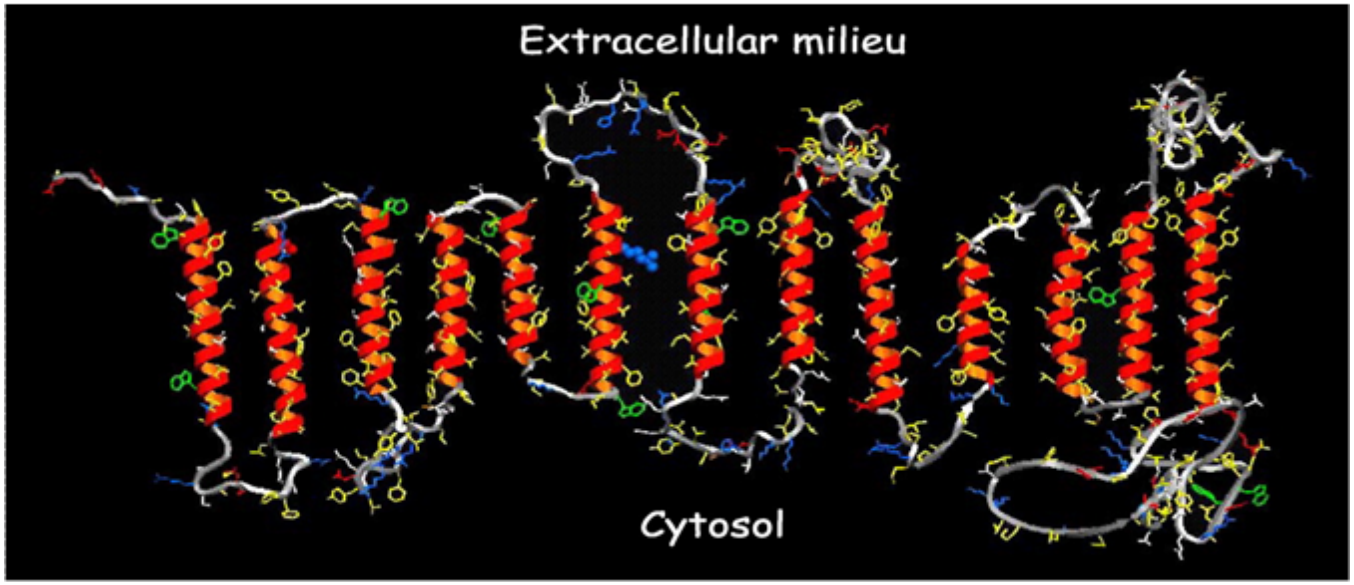

Dohan, O. et al. Endocr Rev 2003;24:48-77

ENDOCRIN REVIEWS

Figure Two: Schematic illlustration of a thyroid follicular cell showing aspectsof Iodide transport and thyroid hormone synthesis, obtained from review : Spitzweg C, Morris J. The Sodium Iodide Symporter: its pathophysiological and therapeutic implications. Clin Endo, 2002;57:559-574.

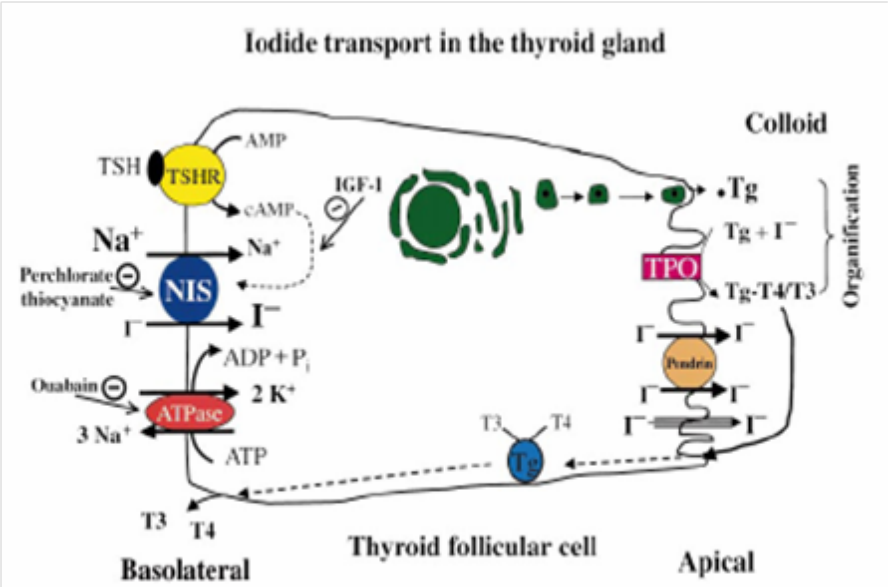

Fig. 1 Schematic illustration of a thyroid follicular cell showing the key aspects of thyroid iodine transport and thyroid hormone synthesis. TSHR, TSH-receptor; NIS, sodium iodide symporter; TPO, thyroid peroxidase; Tg, thyroglobulin.

Figure Three: Marsden hospital flowchart for management of differentiated thyroid cancer

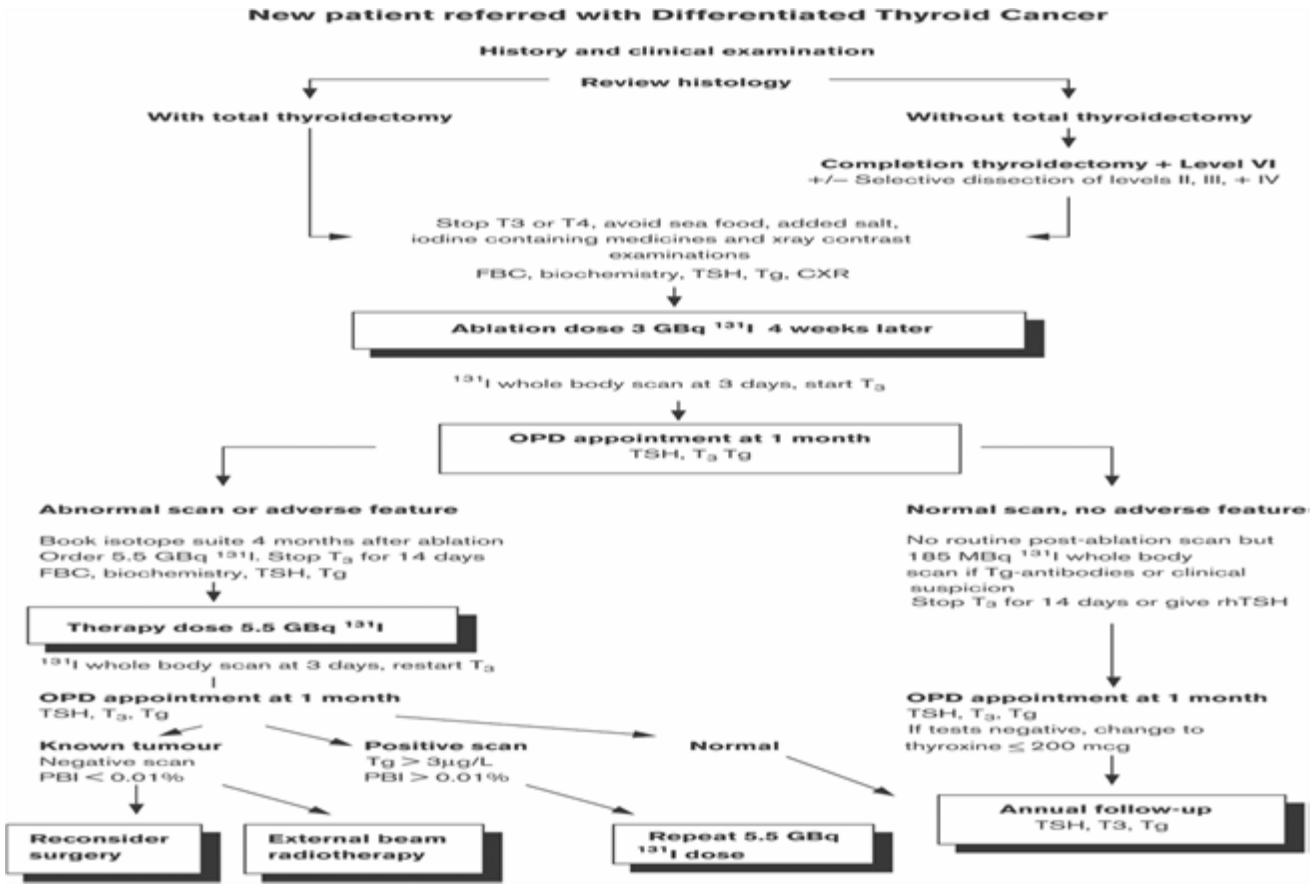

Figure Four: Inclusion criteria

- Female patients with histologically- or cytologically-proven metastatic breast
- cancer.
- Written, informed consent (appendix III).
- Age $\geq$ 18 years.
- Performance status $\leq$ 2 (ECOG – Appendix I).
- Estimated life expectancy $\geq$ 3 months.
- Adequate haematological function: Haemoglobin $\geq$ 9.0 g/dl;
- absolute neutrophil count $\geq$ 1.5 x 109/L; platelets $\geq$ 100 x 109/L.
- Able to comply with study procedures.
- Female patients with reproductive potential must have a negative serum
- pregnancy test within 7 days of radio-isotope imaging.

Figure Five: Exclusion criteria

- Anticancer therapy including chemotherapy, radiotherapy, endocrine therapy, immunotherapy or use of other investigational agents within previous 4 weeks.
- Patients with known brain metastases.
- Pregnant or lactating women.
- Patients with inadequate renal function: serum creatinine > 1.5 x upper limit of the reference range of the laboratory.
- Deranged liver function tests: serum bilirubin > 1.5 x upper limit of normal reference range for laboratory; transaminases (AST, ALT) > 5 x upper limit of normal reference range of the laboratory.
- Any evidence of uncontrolled cardiac disease or any other serious medical or psychiatric disorder that would be a contra-indication to the study procedures.
- Any history of clinically significant thyroid disease.
- History of allergies to any of the compounds administered during the imaging procedures.

Figure Six: NIS immunohistochemistry of a human breast cancer. NIS staining is observed only in breast tumoral tissue (intense plasma membrane and intracellular NIS staining is observed. Obtained from: Dohan O, Carrasco N. Advances in Na^+/I^- symporter (NIS) research in the thyroid and beyond. Mol and cell endo, 2003; 213(1): 59-70

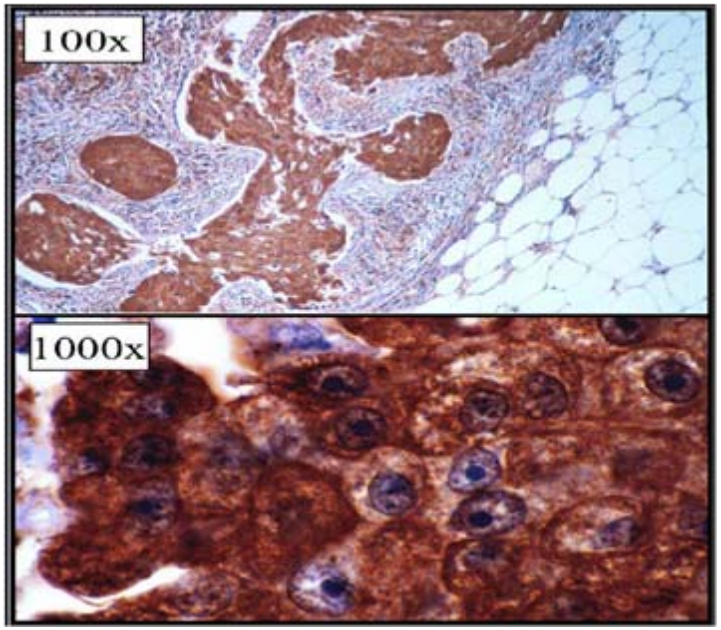

Figure Seven: NIS immunohistochemistry. A thyroid follicular carcinoma is shown overexpressing NIS protein relative to the surrounding normal tissue. Obtained from: Dohan O, Carrasco N. Advances in Na^+/I^- symporter (NIS) research in the thyroid and beyond. Mol and cell endo, 2003; 213(1): 59-70.

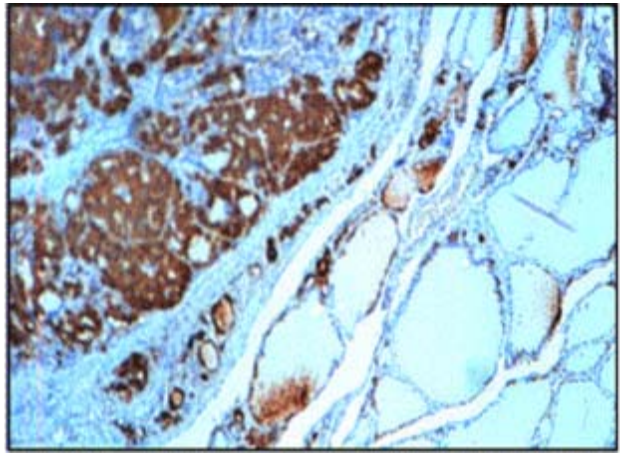

Figure Eight: NIS Immunohistochemistry. Examples of staining of Graves thyroid tissue X200, demonstrating intense staining(A), and increasing intensity of staining (B-F), obtained from Patel A, Jhiang S, Dogra S et al. Differentiated thyroid carcinoma that express sodium iodide symporter have a lower risk of recurrence for children and adolescents. Pediatric Research, 2002; 52: 737-744.

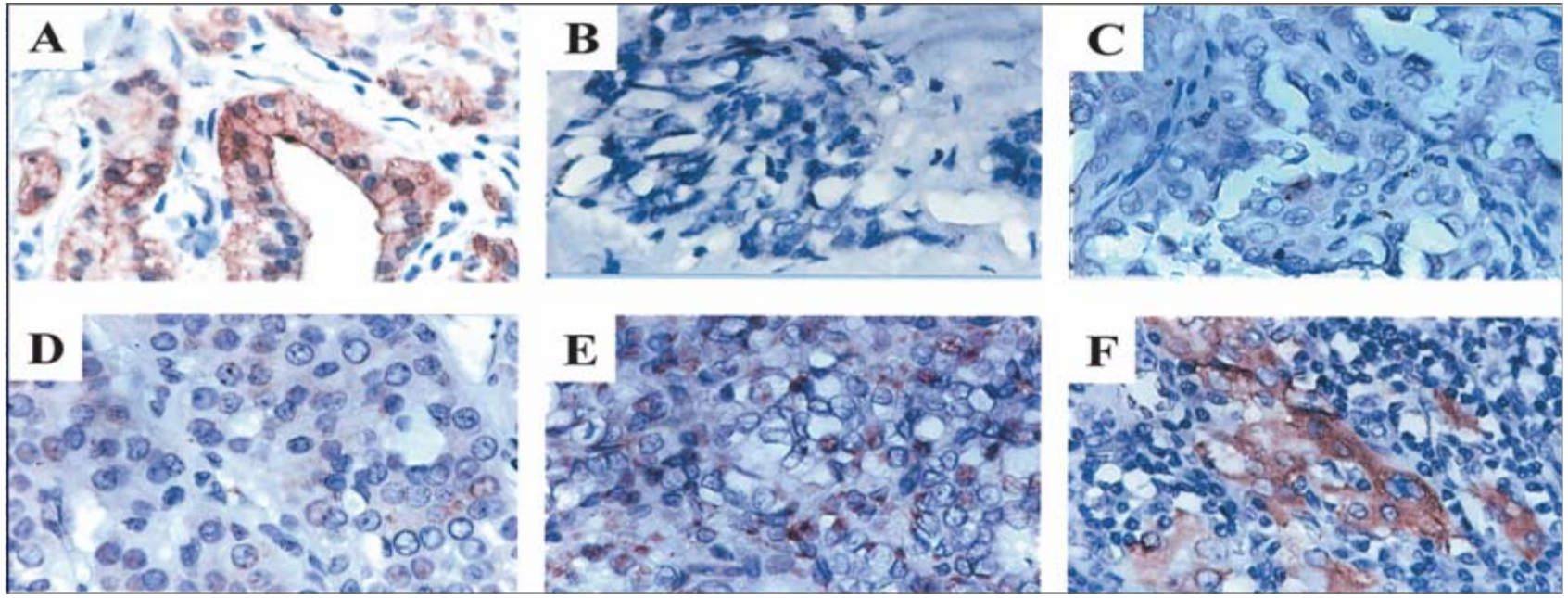

Figure nine: NIS Immunohistochemistry. Graves control x 40, from my study demonstrating intense (3+) cytoplasmic and membranous staining of NIS protein in 100% of cells.

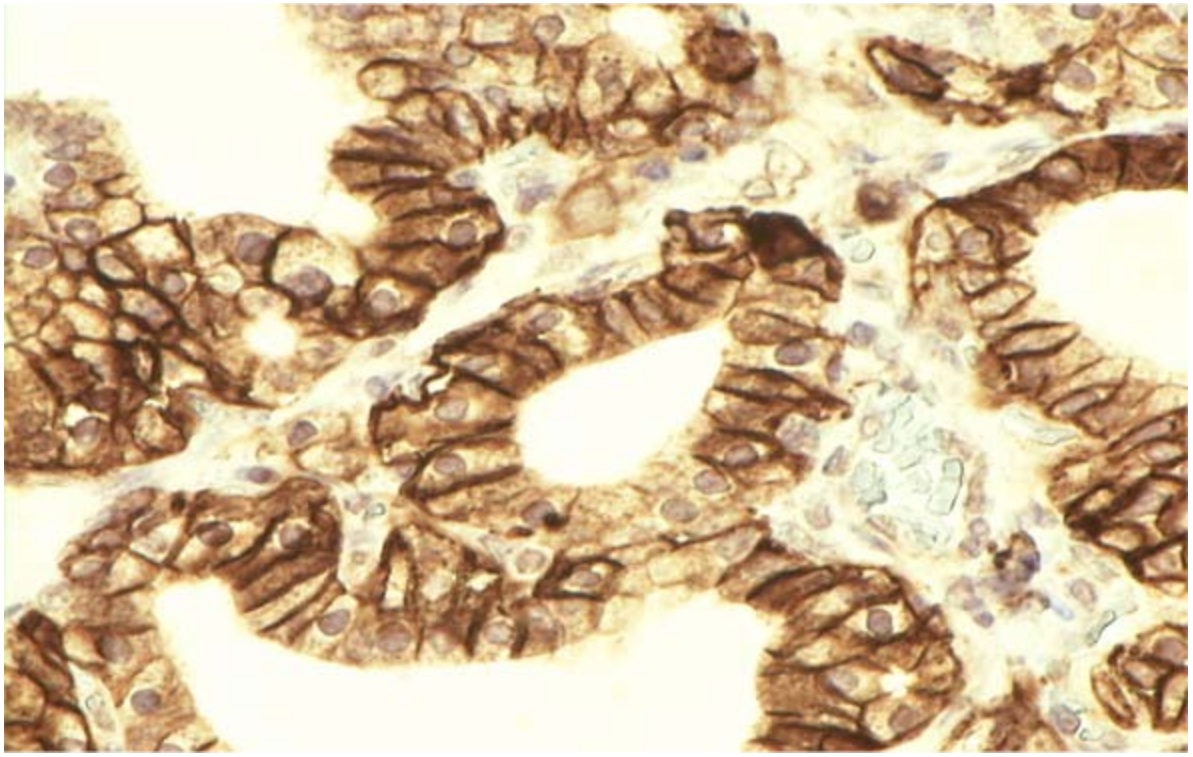

Figure 10: NIS Immunohistochemistry. Thyroid control x 20 from my study demonstrating diffuse, patchy staining of NIS protein.

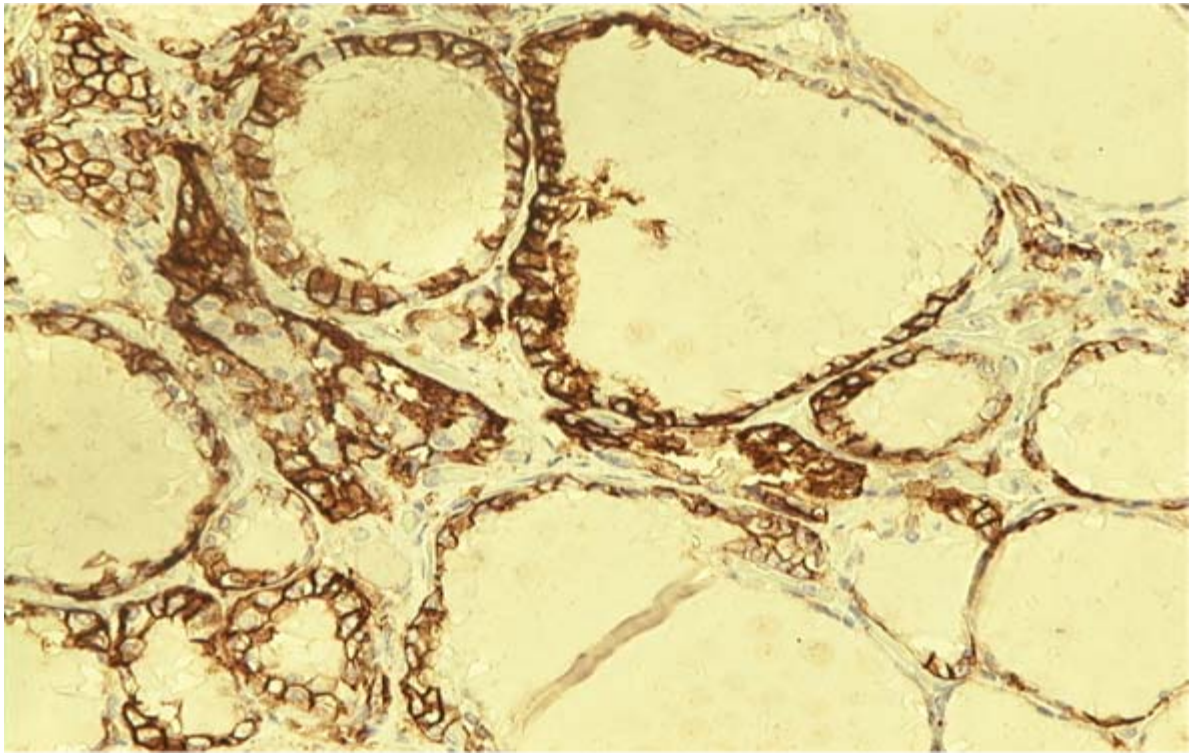

Figure 11: NIS Immunohistochemistry. Breast cancer sample x 20, demonstrating no staining of NIS protein.

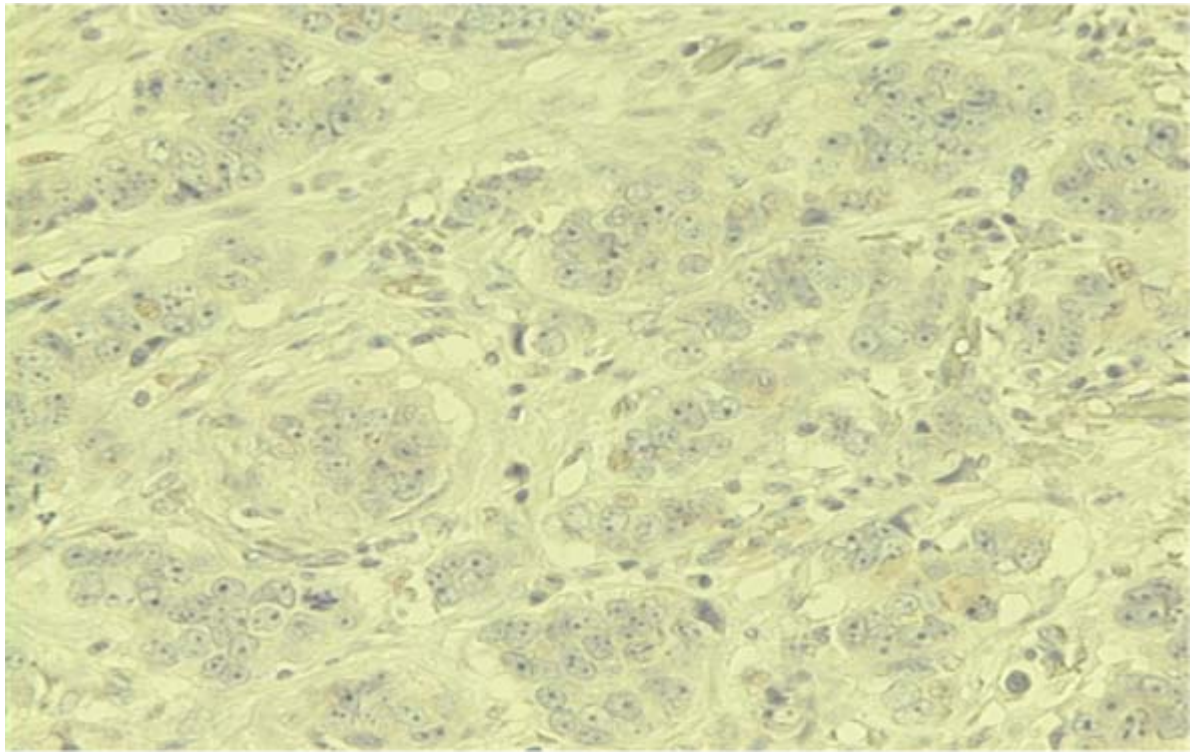

Figure 12: NIS Immunohistochemistry. Breast cancer sample x 20, demonstrating staining of NIS protein.

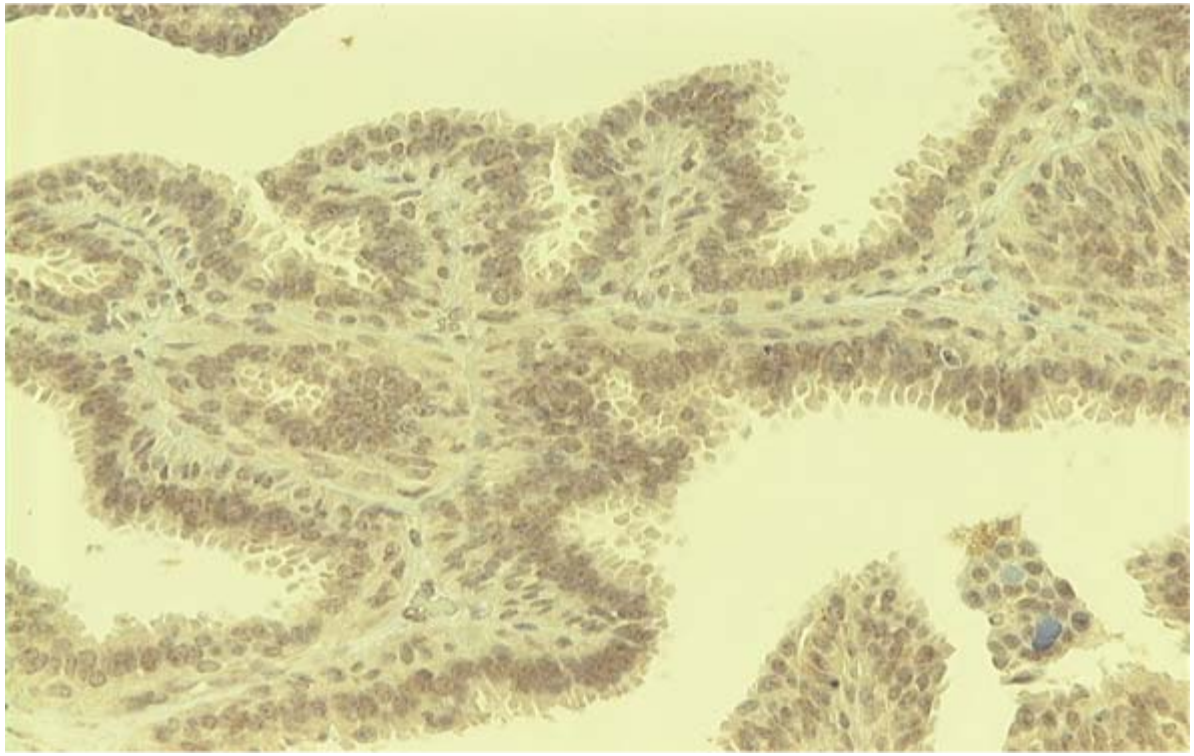

Figure 13: gel electrophoresis scan by Gene Genius image capture system, demonstrating GAPDH and NIS bands in RNA from positive control cell line, but no NIS band in T47D or MCF7 breast cell lines.

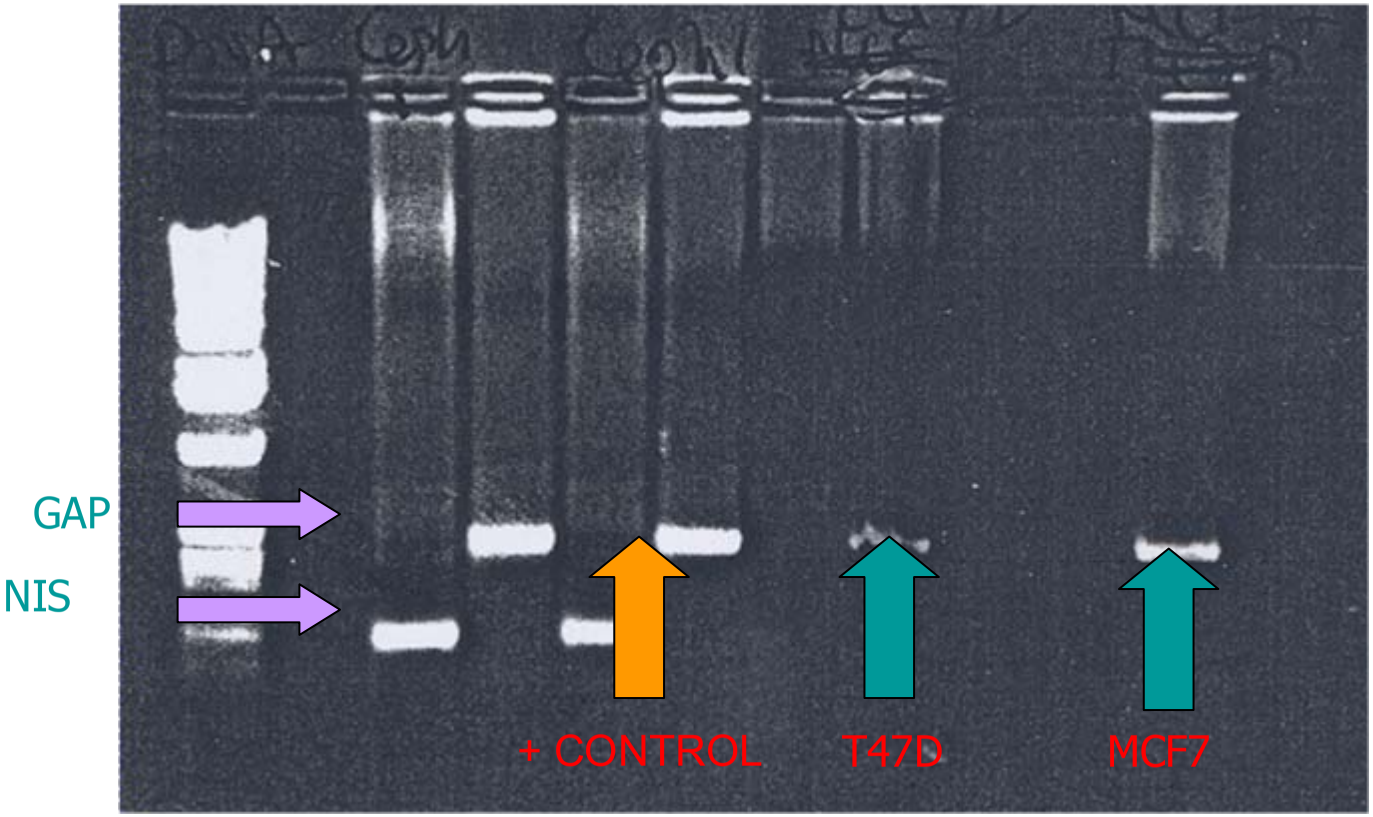

Figure 14: gel electrophoresis scan by Gene Genius image capture system, demonstrating GAPDH and NIS bands in RNA from UVW-NIS positive control cell line, but no NIS band in RNA extracted from FFPE differentiated thyroid cancer sample.

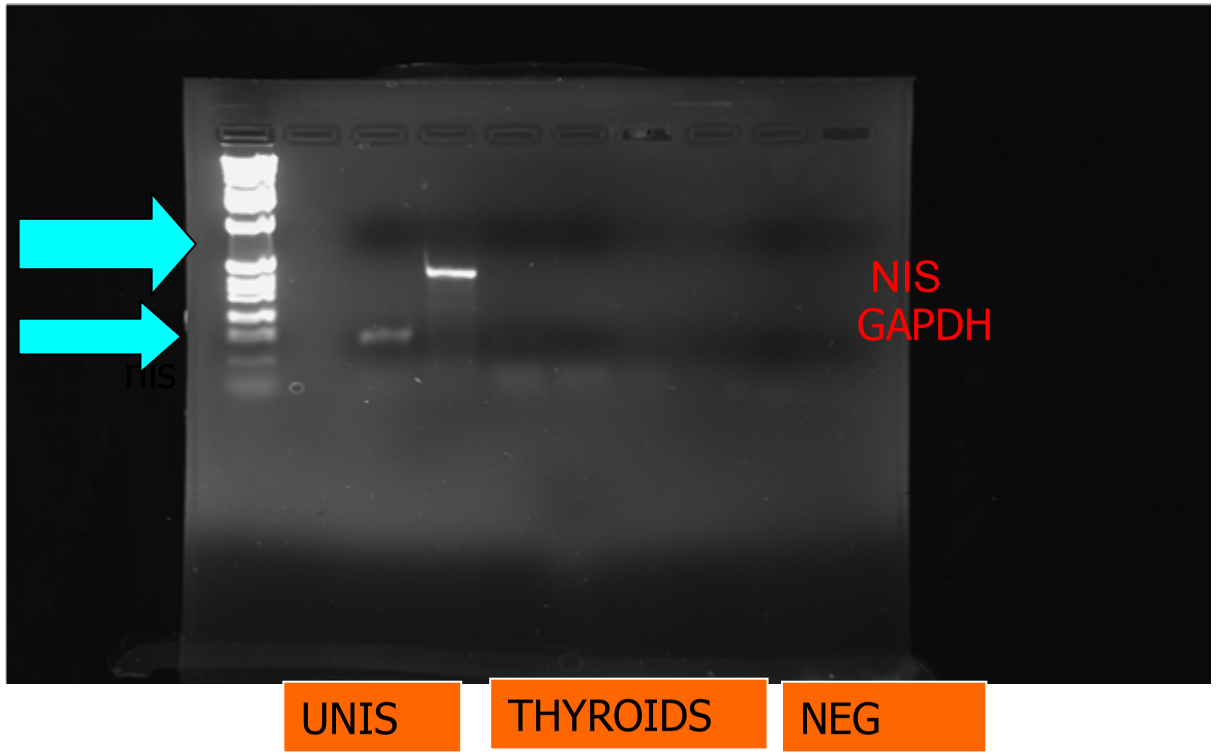

Section 15 – Appendices

Appendix One

Taqman graphs

Amplification plot of NIS standards with 5µM probe and 10µm primer concentration, 40 PCR cycles 14/8/6
Slide 1

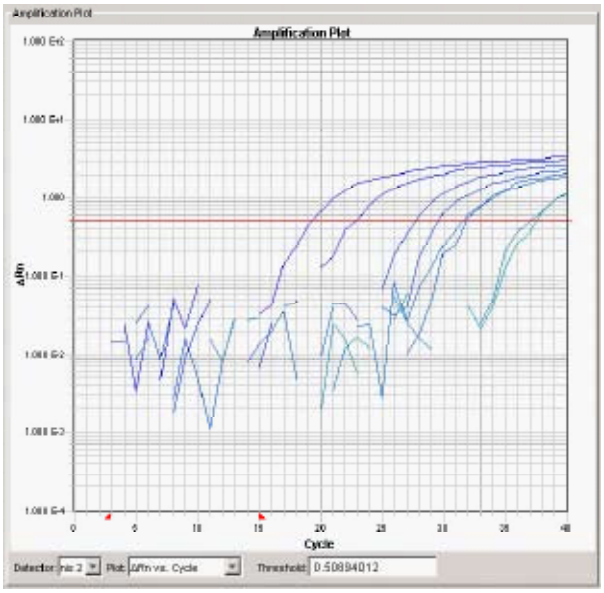

Standard curve plot of NIS standards with 5µM probe and 10µm primer concentration, 40 PCR cycles 14/8/6
Slide 2

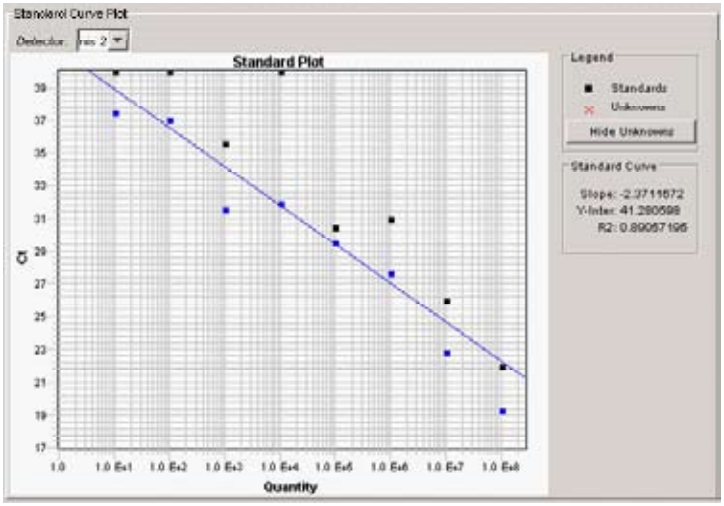

Amplification plot of NIS standards with 20µM probe and 10µm primer concentration, 40 PCR cycles 14/8/6
Slide 3

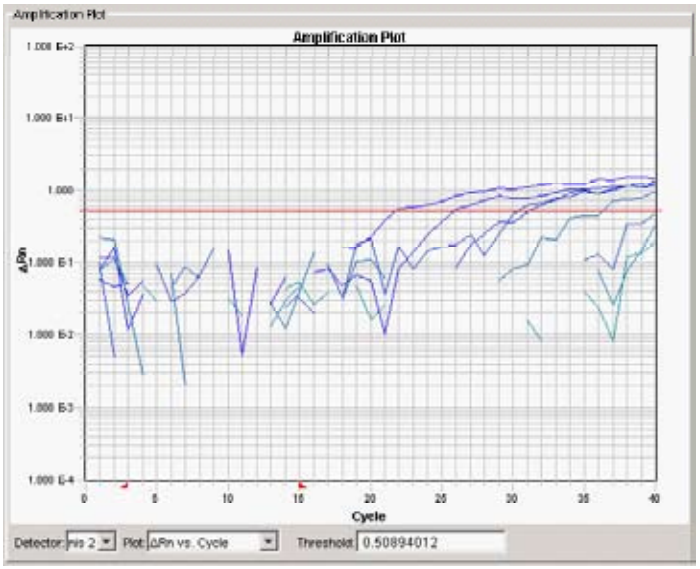

Standard curve plot of NIS standards with 20µM probe and 10µm primer concentration, 40 PCR cycles 14/8/6
Slide 4

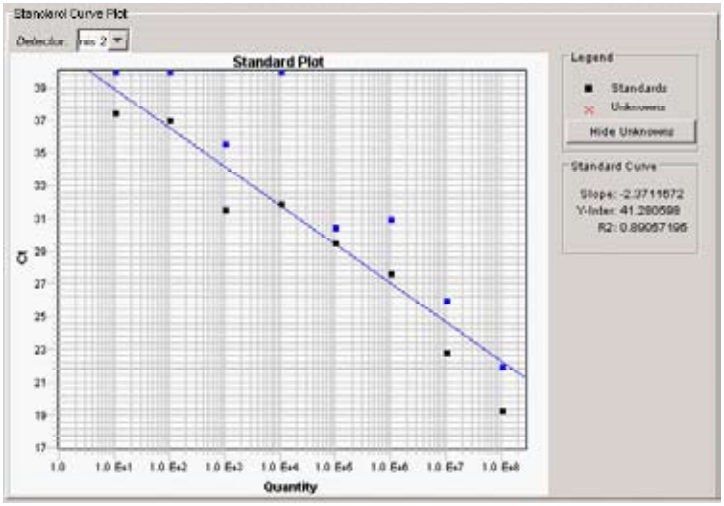

Amplification plot of NIS samples and standards 23/8/6
Slide 5

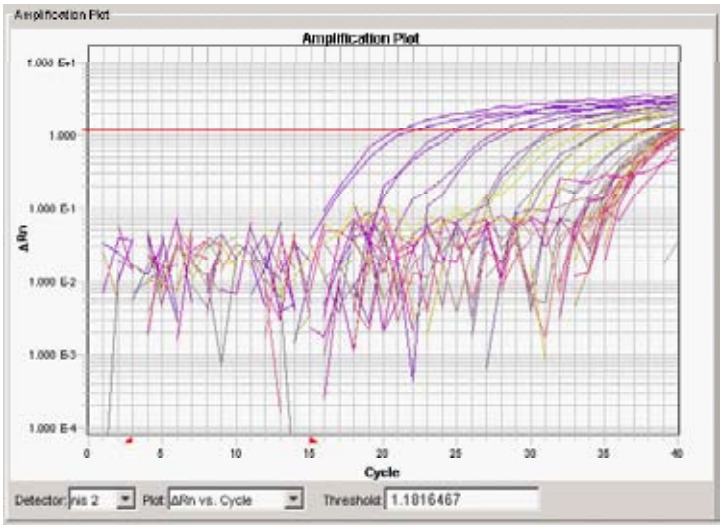

Standard curve plot of NIS standards 23/8/6
Slide 6

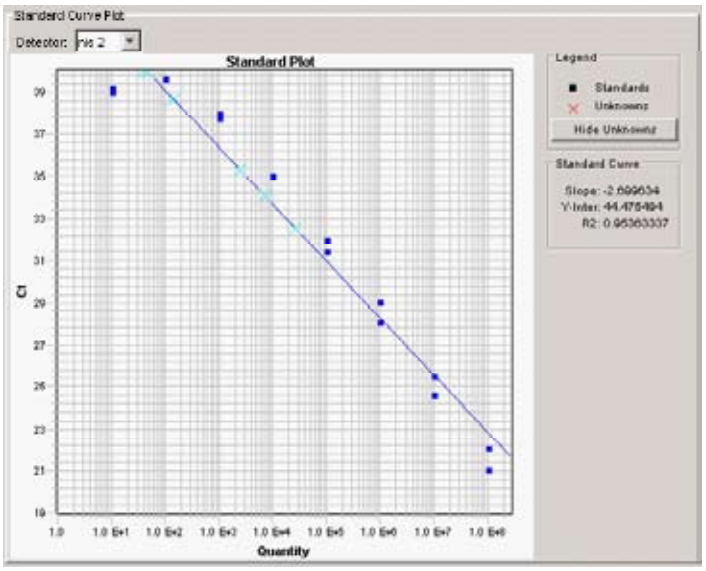

Amplification plot of GAPDH samples and standards 23/8/6
Slide 7

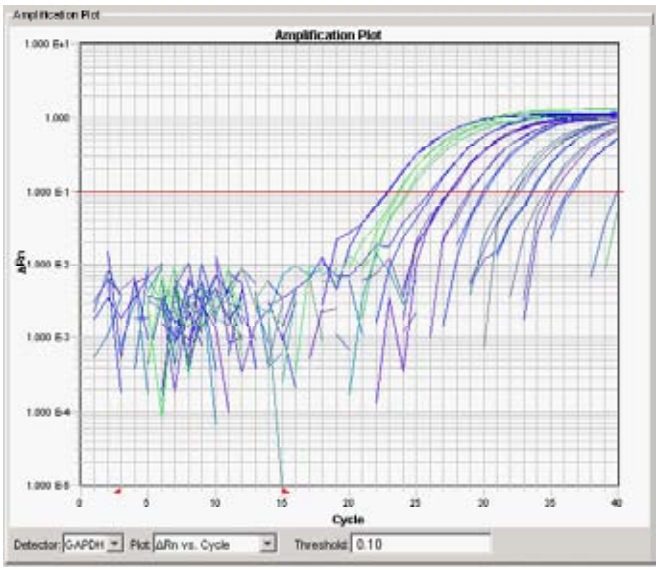

Standard curve plot of GAPDH standards 23/8/6
Slide 8

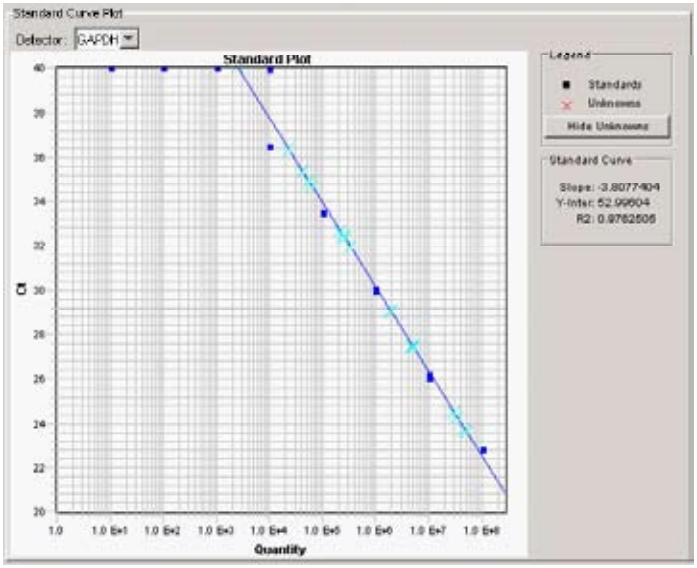

Appendix Two

Pertechetate images

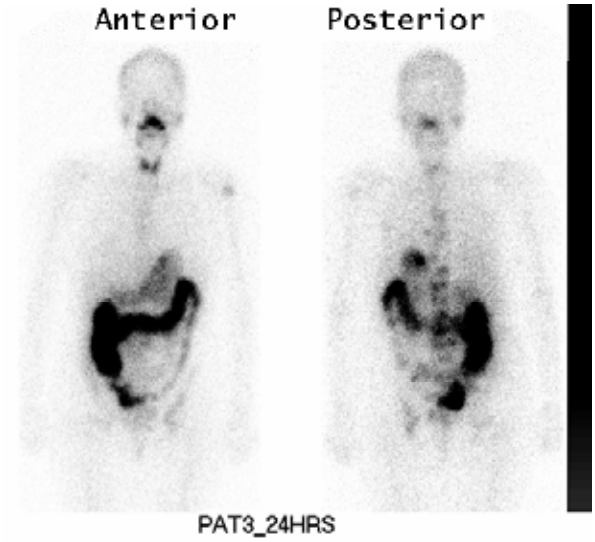

Figure 1: Uptake in spine, shoulders and pelvis

Figure 2: Uptake in Left femoral head and mediastinum

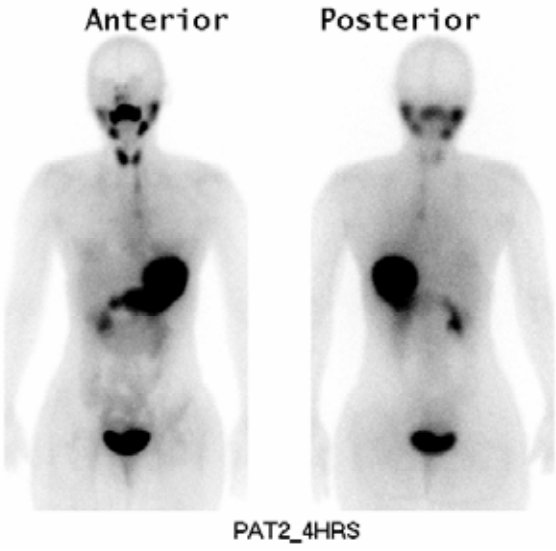

Figure 3 : typical 4 hours scan - salivary gland, thyroid gland, and stomach uptake.

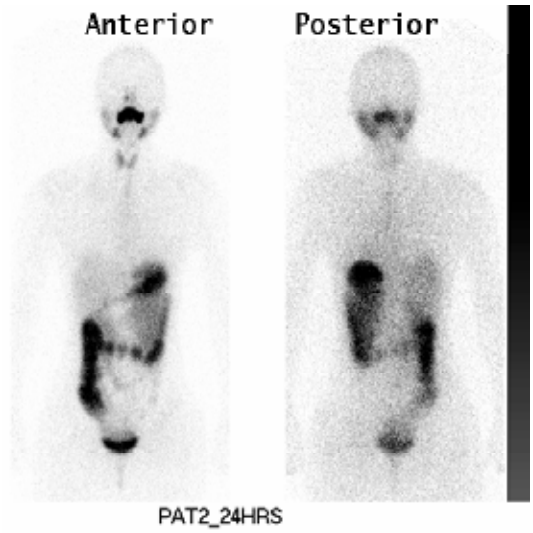

Figure 4: typical 24 hours scan – bowel uptake

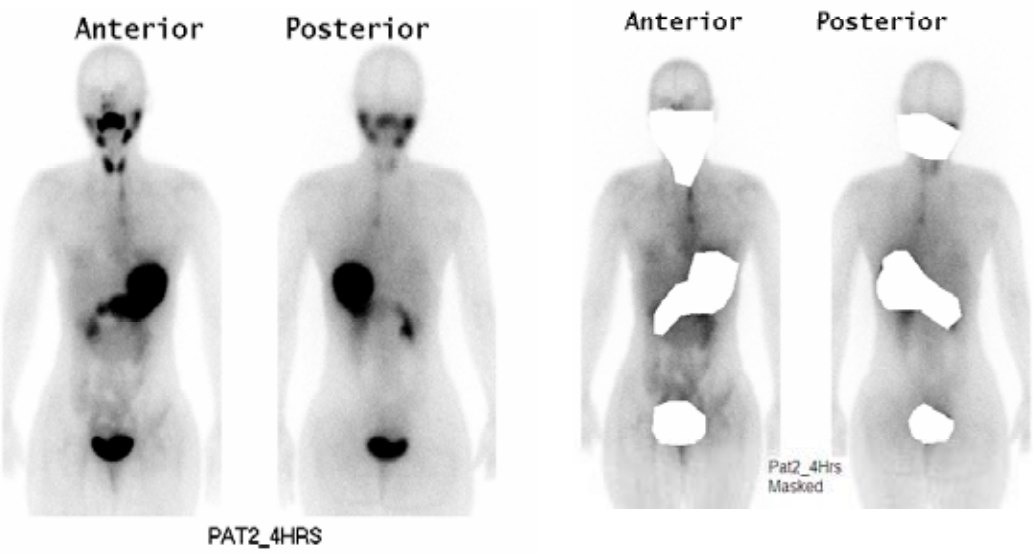

Figure 5 : example of software masking

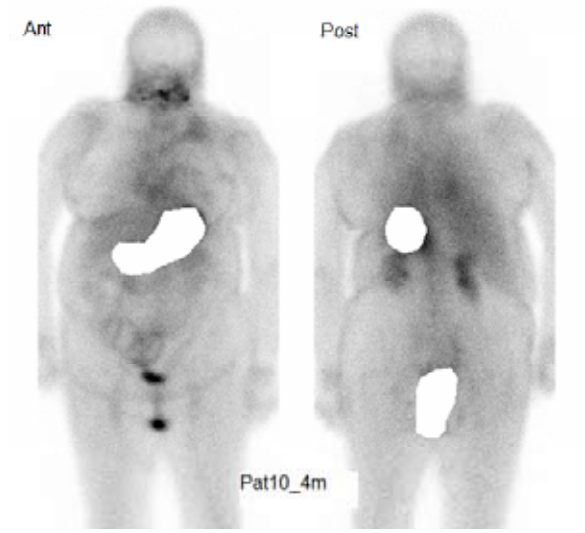

Figure 6: Uptake in Left supraclavicular fossa mass

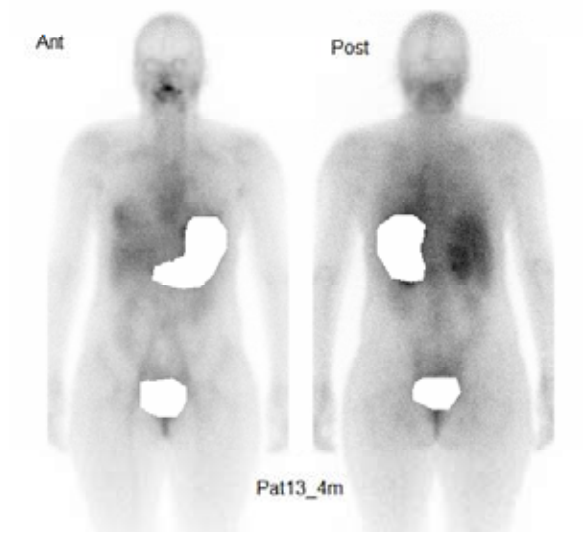

Figure 7: Uptake in Right breast

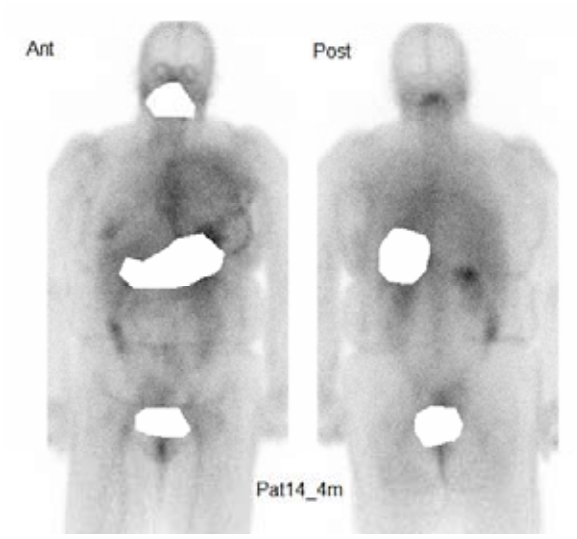

Figure 8: Uptake in Left pectoral area

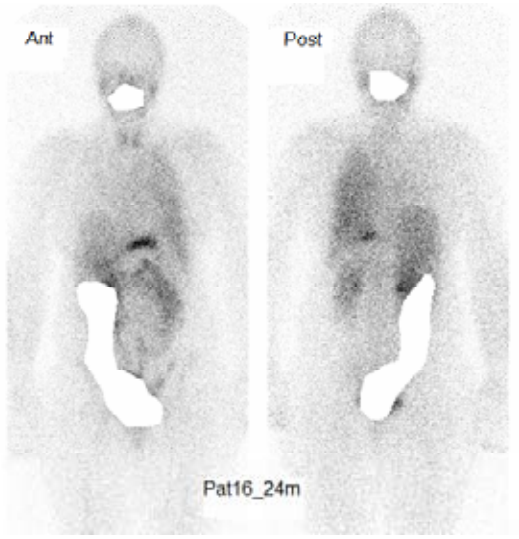

Figure 9: uptake in left pleural effusion

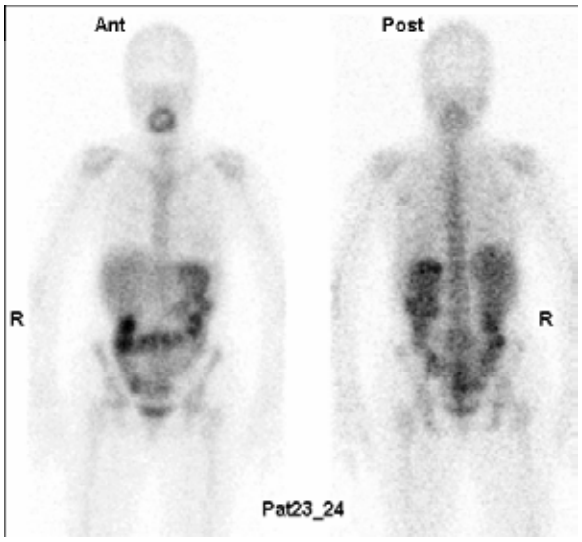

Figure 10: Uptake in vertebral column

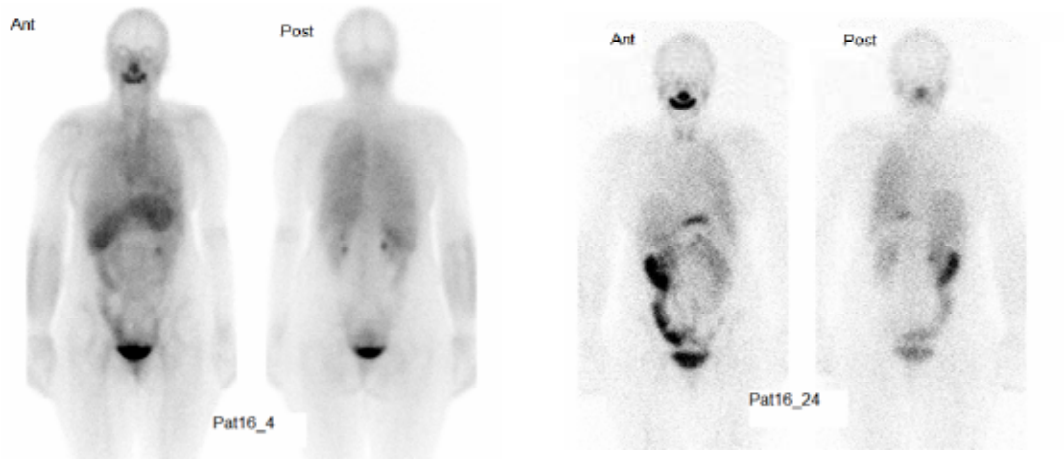

Figure 11 : 4 Hours and 24 hours - 300mg perchlorate

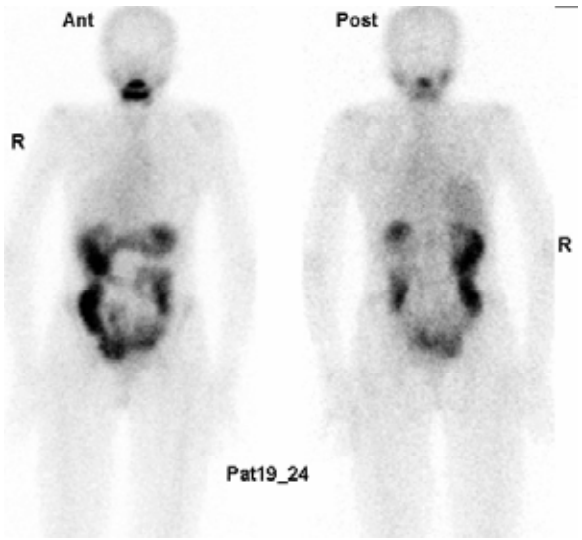

Figure 12: Uptake medial to Right breast

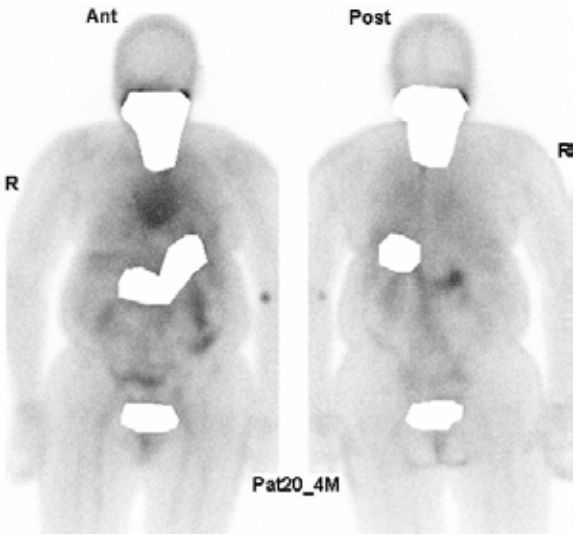

Figure 13 : Uptake in sternum

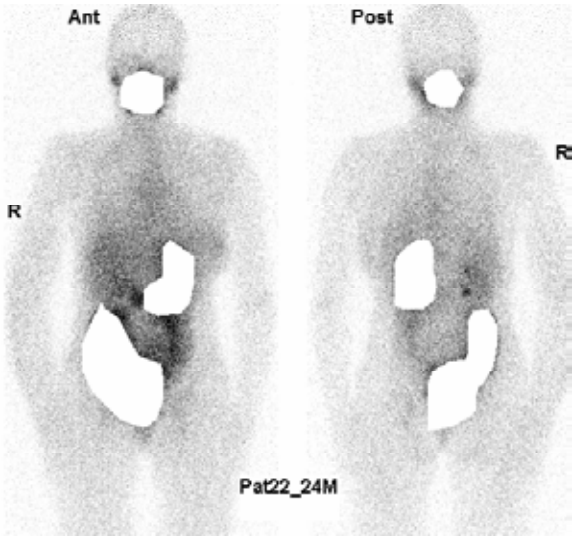

Figure 14: Uptake in liver and lower lumbar vertebrae

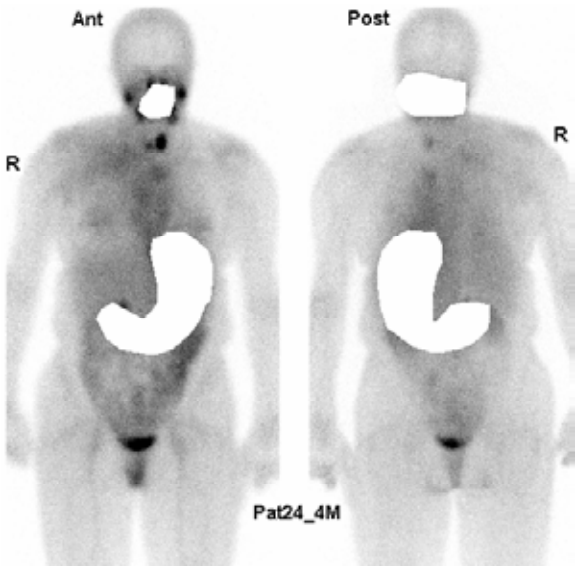

Figure 15: Uptake in Right sided neck nodes

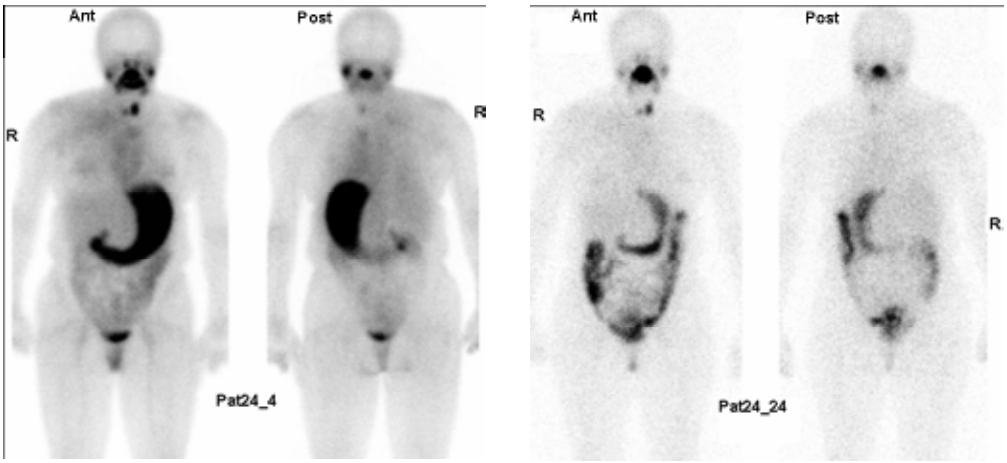

Figure 16: 4 hours and 24 hours –potassium iodate

Acknowledgements

First, I must thank Professor Evans, Rob Mairs, Marie Boyd and their team of scientists who supervised my work on NIS. Their enthusiasm and scientific endeavours created the opportunity to be involved in a thoroughly fascinating and exciting research project. Special thanks goes to Tony McLuskey, who was always on hand for advice.

I must thank Karin Oien for her invaluable advice during my project as my adviser.

At GRI, I thank Dr McNicol for her support with respect to the IHC interpretation. I would like to thank Jim, Ian and Brian for great help in the IHC laboratory.

I would like to thank Professor Mckillop, Jo Prosser and Gerry Gillen in nuclear medicine for their support with the imaging project.

Kathryn Knostman in Professor Jhiang's group in Ohio was very prompt in helping me with the supply and use of the polyclonal antibody.

Orla Sheil's group in Ireland were very helpful in ironing out some RNA extraction problems.

I would like to thank Peter Canney for allowing me access to his metastatic breast clinic.

Colin Campbell provided much needed help with the final preparation of the formatting, and his input was of immense value.

Finally, I would like to thank Maura Farquharson and David from the GRI pathology laboratory. Maura was inspirational to me in her meticulous methods, her endless patience, and continuing friendship.